

PULSATING MICROFLUIDICS FLOW THROUGH THE HEATED PIPE

A thesis submitted by

DURGA PRIYADARSINI GAMPALA

(2BL19PMA03)

Under the Guidance of

Dr. Gurunath C. Sankad

Professor

Department of Mathematics

**B.L.D.E. A's V. P. Dr. P. G. Halakatti College of Engineering and
Technology, Vijayapur – 586101**

For the award of the degree of

Doctor of Philosophy

In Mathematics



VISVESVARAYA TECHNOLOGICAL UNIVERSITY

BELAGAVI, KARNATAKA, INDIA

Research Centre

**Department of Mathematics, B.L.D.E. A's V.P. Dr. P.G. Halakatti College
of Engineering and Technology, Vijayapur -586103, Karnataka, India**

May - 2024



DEPARTMENT OF MATHEMATICS
B.L.D.E. A's V.P. Dr. P.G. Halakatti College of
Engineering and Technology, Vijayapur -586101,
Karnataka, India



CERTIFICATE

I hereby confirm that Mrs. Durga Priyadarsini Gampala has conducted research under my guidance for her PhD thesis entitled “PULSATING MICROFLUIDICS FLOW THROUGH THE HEATED PIPE”. I hereby affirm that the present work is authentic and has not been previously submitted, either in its entirety or partially, to any other college or university to obtain any other degree.


Dr. Gurunath C. Sankar
Research Supervisor
Research Centre Mathematics
B.L.D.E.A's VP Dr PGH
Professor, Dept. of Mathematics
College of Engg. & Tech. Vijapur

B.L.D.E. A's V. P. Dr. P. G. Halakatti College of Engineering and Technology,
VIJAYAPUR – 586101

Date: 30/05/2024

Place: VIJAYAPUR

DECLARATION

I hereby affirm that the research thesis titled " **PULSATING MICROFLUIDICS FLOW THROUGH THE HEATED PIPE**" is being submitted to Visvesvaraya Technological University, Belagavi, as a partial fulfillment of the requirements for the degree of **Doctor of Philosophy in Mathematics**. This thesis represents an authentic account of the research conducted by me under the guidance of **Dr. Gurunath C. Sankad**. I confirm that the content of this thesis has not been previously submitted to any other university or institution for the purpose of obtaining any degree.


DURGA PRIYADARSHINI GAMPALA

USN: 2BL19PMA03

Research Scholar

Date: 30/05/2024

Place: VIJAYAPUR

Dedicated to
My Parents
And
Family Members

ACKNOWLEDGEMENTS

I express my gratitude to the **Visvesvaraya Technological University (VTU), Belagavi**, and **Vachana Pitamaha Dr. P. G. Halakatti College of Engineering and Technology, Vijayapur**, specifically **the Department of Mathematics**, as well as my place of employment, the **Department of Freshmen and Engineering, Geethanjali College of Engineering and Technology, Hyderabad**, for providing me the privilege to pursue a Doctor of Philosophy degree and for providing support throughout my tenure at the institution.

I would like to extend my sincere appreciation and gratitude to **Dr. Gurunath C Sankad**, a highly esteemed teacher and research supervisor in the Department of Mathematics at BLDEA's CET Vijayapur. I am deeply thankful for his intellectual advice, insightful suggestions, scholarly guidance, invaluable discussions, consistent counsel, constant encouragement, meticulous attention, and continuous interest throughout the various stages of my work. Without his support, my progress would have been unattainable.

I would like to extend my profound gratitude to **Dr. Anand H Agadi**, department of Mathematics, Basaveshwar Engineering College (A), Bagalkote and **Dr. M. Y. Dhange**, Department of Mathematics at BLDEA's CET Vijayapur for their exceptional experience, invaluable counsel, and constant assistance that have played a pivotal role in shaping the course of this research endeavor. The valuable input and guidance provided by them have had a substantial impact on the overall quality of the work being performed.

In addition, I would like to offer my appreciation and heartfelt thanks to **Dr. S. C. Desai, Dr. A. B. Patil, Dr. Pratima Nagathan**, as well as **Mr. K. M. Chavan** and **Mr. Revu Metri**, for their helpful relationship and assistance during the duration of my studyeffort.

I would like to express my gratitude to **Dr. V.G. Sangam** for his invaluable assistance and motivation, as well as for facilitating the necessary resources during the duration of the study endeavor. I would like to express my gratitude to **Dr. Ramesh S. Malladi**, the Research and Development coordinator, as well as all the academic members and other staff members of the department.

I express a particular debt of gratitude to my parents **Sri. G. Sri Krishna Raja Rao and Smt. Manga Thayar** because they taught me the value of perseverance and hard work in the pursuit of goals. My husband, **Sri. V. Ramprasad**, who has always been an infinite source of love and support for me, is someone for whom it is difficult for me to find enough words to convey my gratitude. The love of our child, **Lekaa Sehari**, was one of the things that I missed the most while I was working on my Ph.D., and I cannot end this post without expressing my deepest gratitude to them. I express my gratitude to my beloved brother **Sri G. Kranthi Chaitanya** and my beloved Sister-in-law **Smt. Sravani** for their kind co-operation and everlasting encouragement during the course of my work.

I would also like to express my gratitude and sincere thanks to **Dr. G. Srinivas**, Professor, Geethanjali College of Engineering and Technology and **Dr. Umesh Bhujakkanavar**, Assistant Professor, Department of Humanities and Sciences, R.I.T. Sakharale for their kind support and valuable suggestions given to carry out my research work.

In conclusion, thank everyone who had a significant role in the development of this thesis into an accomplishment. I apologize for not being able to acknowledge each contributor individually.

Durga Priyadarsini Gampala

VIJAYAPUR, INDIA

2024

PREFACE

This research report presents the study of fluid through micro channels which often termed as “microfluidics” through the pulsating heat pipes (often termed as oscillating heat pipes) under various conditions and applications. The pulsating heat pipe is more frequent in many biological, medical and petrochemical industries. Fluid carrying pipes are not stationary in the above mentioned industries. The studies of such fluid flows are more complicated particularly in medical field. Most of these studies are frequent in non destructive methods. The present thesis is divided into **seven chapters**.

The first chapter deals with the overall introduction. The relevant literature survey is included here to demonstrate the motivation of selecting the problem.

In the **second chapter** we propose a Mechanically Pulsating Heat Exchanger (MPHE-MT) that uses microfluidic technology. Hence to accomplish this, walls are constructed inside the flow channel. Each vascular waveform includes its minimum, maximum, and median flow rate. Patients with cortical and lacunar stroke did not differ significantly on any measure of flow or pulsatility.

The **third chapter** describes a methodology of Heat Pipes with Pulsating Response Surfaces [HP-PRS] to find the effectiveness of heat exchangers. According to the results of the current heat exchangers, the PHP heat exchanger, when operated at evaporator temperature, is most effective and using water as the operating fluid.

In the **fourth chapter** we describe the temperature measurement. Microfluidics research has produced many temperature measurements. However, many of those lack short of expectations of performance and precision. In an effort to facilitate drug injection, a better method is created to account for and monitor the temperatures in microfluidics.

In the **fifth chapter**, for better separation and performance, we developed a novel PHP called Temperature Regulation in a Pulsating Heat Pipe Using Microfluidics [TRPHP-MF] that uses dividing barriers built into the channel itself. A change in the flow pattern of the liquid and vapor plugs may lead to enhanced thermal performance in the heat pipe. The heat transport model is validated by a comparison of theoretical and experimental results, which demonstrates its efficacy in enhancing separation while reducing energy use.

The **sixth chapter** introduces a novel approach, namely Deep Learning-Based Prediction and Enhancing Performance (DL-PEP), for improving the performance of PHPs. Initially, TiO₂ nanomaterials are introduced into the working fluid to augment its thermal conductivity. Subsequently, the PHP is infused with nanofluid, and a test rig is fabricated to assess its efficacy. The methodology entails altering the amount of heat input, gauging temperature profiles, and ascertaining the heat transfer properties. A model of an Artificial Neural Network (ANN) has been constructed to forecast the performance of PHP by utilizing empirical data. The findings indicate that incorporating TiO₂ nanoparticles leads to a notable enhancement in the thermal conductivity of the PHP. Furthermore, the constructed ANN model exhibits precise forecasts of heat transfer properties, accompanied by high correlation coefficients. The findings of this research offer significant perspectives on the possible utilization of nanofluids and deep learning-based forecasting to improve the performance of PHP, thereby facilitating effective and dependable heat dissipation in diverse thermal management systems.

The **seventh chapter** is spared for total summary of the entire research in the form of conclusions. The future scope of extension of this work and possible directions are mentioned in this chapter.

LIST OF FIGURES

Sl.No	Figure	Page
1	Figure 2.1.1 Flow in a stiff tube	18
2	Figure 2.2.1 Pulsating Heat Exchanger	20
3	Figure 2.2.2 Procedures for Handling Fluids at the Point-of-Care	21
4	Figure 2.3.1 Thermal Resistance	28
5	Figure 2.3.2 Flow Rate Analysis	28
6	Figure 2.3.3 Constant and Fluctuating Flow Methods	29
7	Figure 3.2.1 Domain of calculation models and grids in PHP	35
8	Figure 3.2.2 Chemical Process of a PHP	36
9	Figure 3.2.3 Visual representation of a PRS	37
10	Figure 3.2.4 Layout of the Current Experimental Setup	39
11	Figure 3.2.5 Comparison analysis of PHP geometrical parameters	40
12	Figure 3.3.1 Thermal Resistance	41
13	Figure 3.3.2 Filling Ratio	42
14	Figure 3.3.3. Efficiency Analysis	43

15	Figure 3.3.4. Temperature Profile	43
16	Figure 3.3.5 Surface Area Response Modeling	44
17	Figure. 4.2.1. The design and working process of the flowmeter	52
18	Figure. 4.2.2 The fabrication process of the flowmeter	55
19	Figure. 4.2.3 The setup connection for flowmeter-based temperature compensation and measurement	56
20	Figure 4.2.4 chips and design	57
21	Figure. 4.4.1 Glass surface temperature analysis	61
22	Figure. 4.4.2 Glass surface temperature analysis under the microfluidics condition	62
23	Figure.4.4.3. The increased fluorescence intensity analysis	63
24	Figure. 4.4.4 Heater resistance analysis of the proposed system	64
25	Figure. 4.4.5 Heater power analysis of the Mechanically Pulsating Heat Exchanger	65
26	Figure 5.1.1: Creating U-turns on a copper plate via a machine-engraved square channel of the PHP	68
27	Figure 5.1.2: Reduced pressure	69
28	Figure 5.2.1 PHP evaporator liquid film form	70
29	Figure 5.2.2 Correlating heat exchange between zones	72
30	Figure 5.2.3 Schematic Diagram	75
31	Figure 5.3.1 Accuracy Analysis	78
32	Figure 5.3.2 Thermal Insulation	78
33	Figure 5.3.3 Volume Flow rate	79
34	Figure 5.3.4 Performance Analysis	80
35	Figure 5.3.5 Efficiency Analysis	81
36	Figure 6.2.1 TEM image of TiO ₂ nanoparticles	85
37	Figure 6.3.1 Experimental setup for PHP	87
38	Figure 6.3.2 ANN architecture	91
39	Figure 6.4.1 Temperature distribution analysis of different time	92
40	Figure 6.4.2. Predicted thermal resistance analysis	93
41	Figure 6.4.3 Weights & bias analysis of the ANN system	94
42	Figure 6.4.4 Thermal resistance analysis vs. heat input analysis of different nanomaterials	95
43	Figure 6.4.5 Temperature analysis of PHP with different experimental time	96

LIST OF TABLES

Sl.No	Table	Page
1	Table 4.4.1 Flow rate analysis of the Mechanically Pulsating Heat Exchanger based flowmeter	65
2	Table 5.2.1 Comparison Analysis on Performance:	76
3	Table 5.3.1 Material Properties and Setup Dimensions	77

SYMBOLS

- u, v velocity components along x- and y-axes
- α is the volumetric expansion coefficient of the fluid
- β is the Casson fluid parameter
- f dimensionless stream function
- f' non dimensional velocity of the fluid
- ρ is the Casson fluid density
- λ is the slip parameter
- λ_1 is the temperature constant
- ρ_p is the density of nanoparticles
- ρ_m is the microorganism density
- γ is the average volume of microorganisms
- r heat capacity ratio of the fluid
- r_w shear stress
- r_{ij} stress tensor
- a_0 stretching rate
- B_0 Strength of magnetic field
- P_r Prandtl number
- T fluid temperature
- T_n ambient temperature
- T_w fluid temperature at the wall
- k_p Permeability constant.
- C Nanoparticle volume fraction
- C_n ambient nanoparticle volume fraction
- C_w concentration of nanoparticle at the wall
- N volume fraction of motile microorganisms
- N_w volume fraction of microorganisms at the wall
- Dn diffusivity of microorganisms

T_{∞} temperature at infinite distance from the wall
 C_{∞} concentration of nanofluid at infinite distance from the wall
 N_{∞} concentration of microbes at infinite distance from the wall
 k thermal conductivity
 Le traditional Lewis number
 Pe bioconvection Peclet number
 N_b Brownian motion parameter
 Nr is the buoyancy ratio parameter,
 Rb is the bioconvection Rayleigh number
 S mass flux parameter
 N_t thermophoresis parameter
 Sc Schmidt number
 σ bio-convection constant
 M modified magnetic parameter
 ν kinematic viscosity
 μ dynamic viscosity
 q is the Chandrashekhhar number
 q_r radiative heat flux
 T_r thermal radiation parameter
 ρ_{cp} density of nanoparticles
 ρ_{cf} density of the fluid
 l Characteristic length
 Le traditional Lewis number
 L_b Bioconvection Lewis number
 ρ_m microorganism density
 Tr radiation parameter
 D_B Brownian diffusion coefficient
 D_T thermophoresis diffusion coefficient
 Re_x Reynold's number
 R_b Bioconvection Rayleigh number

v_c suction or injection velocity

ψ stream function

η similarity variable

θ dimensionless temperature

ϕ rescaled nanoparticle volume fraction

χ dimensionless concentration of microorganisms

U_w stretching velocity

C_f skin friction coefficient

CONTENTS

Chapter No.	Title	Page No.
	Acknowledgements	i
	Preface	iii
	List of figures	iv
	List of tables	vi
	List of Symbols	viii
1	Introduction	1
	1.1 Objectives	1
	1.2 Motives	1
	1.3 Scope	2
	1.4 Literature Survey	2
2	Miniature channel with pulsating liquid dynamics	18
	2.1 Pulsating Liquid Dynamics	18
	2.2 Mechanically Pulsating Heat Exchanger employing Microfluidic Technologies [MPHE-MT]	19
	2.2.1 Pulsatile Flow	22
	2.2.2 Signal Generation with Pulses	24
	2.2.3 Constructing Droplets	26
	2.2.4 Improved Blending	27
	2.3 Results & Discussion	28
	2.3.1 Thermal Resistance Analysis	28
	2.3.2 Flow Rate Analysis	28
	2.3.3 Flow Scheme Analysis	29
	2.4 Conclusions	30
3	Dynamic heat pipe & heat exchanger performance	31
	3.1 An overview	31
	3.2 Heat Pipes with Pulsating Response Surfaces [HP-PRS]	34
	3.3 Results and Discussion	41
	3.3.1 Thermal Resistance	41
	3.3.2 Filling Ratio	42
	3.3.3 Efficiency Analysis	43
	3.3.4 Temperature Profile	43
	3.3.5 Surface Area Response Modelling	44
	3.4 Conclusion	45
4	Microfluidics temperature compensation and tracking for drug injection based on mechanically pulsating heat exchanger	47
	4.1 Background to the temperature measurement in microfluidics	47
	4.2 Proposed Microfluidics Temperature Compensation and Tracking Method	50
	4.2.1 Working principle and design	50
	4.2.2 Material selection	53
	4.2.3 Laser cutting	54
	4.2.4 Fabrication process	54
	4.2.5 Thermal flowmeter characterization setup	55

	4.2.6 Temperature calibration and solution delivery	58
	4.3 Numerical analyses	58
	4.3.1 Control Equation and Boundary Condition Settings	58
	4.3.2 Parameter settings in the simulation	60
	4.4 Result and discussion	61
	4.5 Conclusion	66
5	Microfluidic systems with a pulsating heat pipe	67
	5.1 Temperature Regulation in a Pulsating Heat Pipe Using Microfluidics [TRPHP-MF]	67
	5.2 PHP implementation of liquid film dynamics:	70
	5.3 Results & Discussion	76
	5.3.1 Accuracy Analysis	78
	5.3.2 Evaluation of Thermal Insulation	78
	5.3.3 Examination of Volume Flow rate	79
	5.3.4 Performance Analysis	80
	5.3.5 Efficiency Analysis	81
	5.4 Conclusion	81
6	Enhancing pulsating heat pipe performance using nanofluids and deep learning methods: an experimental analysis	83
	6.1 Proposed Deep Learning-Based Prediction and Enhancing Performance	85
	6.2 Material preparation	85
	6.2.1. Preparation and characterization of TiO ₂ nanomaterials	85
	6.2.2. PHP preparation	86
	6.3 Experimental setup	87
	6.3.1 Experimental procedure	88
	6.3.2 The building of the ANN model for prediction	90
	6.4 Experimental Analysis and Outcomes	92
	6.5 Conclusion and future scope	97
7	Conclusions and future scope	99
	7.1 Conclusions	99
	7.2 Future Scope	101
	References	102
	List of publications	119

INTRODUCTION

1.1 Objectives

The main aim of the research is to study the fluid flow through the micro channels due to its wide applications in various engineering and medical problems. The precise objectives are listed below:

1. To propose a Mechanically Pulsating Heat Exchanger (MPHE-MT) that uses microfluidic technology.
2. To describe a methodology of Heat Pipes with Pulsating Response Surfaces [HP-PRS] to find the effectiveness of heat exchangers.
3. To propose a better method to account for and monitor the temperatures in microfluidics.
4. To develop a novel PHP called Temperature Regulation in a Pulsating Heat Pipe using Microfluidics [TRPHP-MF] that uses dividing barriers built into the channel itself.
5. To improve the performance of PHP using Deep Learning-Based Prediction and Enhancing Performance (DL-PEP), TiO₂ nano-materials are introduced into the working fluid to augment its thermal conductivity.

1.2 Motives

Heat exchangers are important parts of many engineering and medical equipments. The pulsating heat pipe (PHP) in the study of microfluidics has wide applications. The pulsating heat pipe response study and the temperature measurements in PHPs play a vital role in the design of equipment. The nano fluid flow through the micro channels is the preferred mechanical system in most of the studies.

The mathematical model of such problems lands in to a typical governing equations and boundary conditions. It is observed from the literature that more cross sectional and theoretical studies are available but the study of the PHPs along the length has lot significance and end to end results are only useful in designing the equipment.

1.3 Scope

Heat exchangers depend on the materials and geometry. The experimental setup basically needs the Mathematical model and its solution. The study considered in this research work is the microfluidics through pulsating heat pipes. Which are most common in many heat exchangers.

This study proposes the better methods to for effective heat transfer and the better methods for the measurement of such temperature in the said systems. These are applied to the equipment and calibrated accordingly.

1.4 Literature Survey

Microfluidics' precision in manipulating liquids at the sub-millimeter scale has applications in many different fields, including materials engineering, Microphysics, in vitro research, pharmaceutical development, biotechnology quality assurance, and ecological assessment [52]. The new experiments demonstrate the importance of including pulsatile flow effects in models of liquid flow for smaller vessels [93]. Because of this further information, it is abundantly clear that a simplified fluid model cannot approximately describe the intricate flow of liquid in smaller ships [139]. At this point in the circulatory system, non-Newtonian and non-homogeneous liquid flow characteristics become most pronounced, highlighting the need for a suitable model in an accurate representation of liquid flow's physiological behavior [71].

Microfluidic systems are widely used in research institutions across sciences and engineering because of their capacity to mass produce and parallelize experimental setups [57]. One promising area of study for expanding microfluidic technology is the creation of open-source and inexpensive tools for manipulating fluids [14]. Point-of-care diagnostics in low-resource areas may benefit significantly from using open-source microfluidic devices [147]. Point-of-care diagnostics using microfluidics are on the rise, spurred by the need for individualized care based on each patient's unique symptoms and diagnoses [1]. Future point-of-care diagnostic tools could save money and be easier to use if they relied more on open-source software [100].

There are three fundamental parts to any microfluidic point-of-care diagnostic system: the microfluidic device, a system to read the assay output, and a system to regulate the flow of liquid reagents [92]. Microfluidic devices are typically

manufactured as single-use disposable cassettes from various inexpensive materials like polydimethylsiloxane (PDMS), glass, plastic, and paper [55]. Some essays are meant to be read by visual inspection, while others require using expensive computer systems, sensors, and microscopes to interpret the results. Accurate regulation of fluid flow is essential in most microfluidic systems [121]. Despite the existence of microfluidic systems that use sophisticated on-chip pipes for liquid handling, the widespread use of such devices in point-of-care diagnostics may be hindered by their high manufacturing cost, low flow rates, or both [3]. Off-chip pumps in microfluidic devices typically handle pressure and flow rate regulation. The microfluidics industry has seen the development of a wide variety of cutting-edge off-chip pumps, some of which are incredibly cheap and easy to use [99]. Repetitive compressions and contractions propagate along a deformable tube's wall, causing the pumping action known as peristaltic pumping. It is generally accepted that peristaltic pumping is a common mechanism for fluid transport in fluid dynamics [102].

Expanded research into peristaltic fluid pumping has been applied to various contexts. Simulations of the flow of fluids during peristalsis can be made with high accuracy using fluid dynamic principles; these forecasts have been utilized to design artificial peristaltic pumps [105]. Varying fluids (those with different viscosities and thermal properties, for example) are conveyed through a porous material. Researchers make the initial assumptions in the issue formulation, which are an extensive range and various Reynolds ratios [77]. Both the fluid flow formulae have been solved using the perturbation method. We have analyzed the pump's performance indicators, like pressure increase and frictional force [84].

Peristalsis is a widely observed process within living systems that help move most physiological fluids. This system allows for the gradual wavelike contraction and expansion of a distensible tube filled with fluid throughout its length. Capillary motility, urine in the ureter, and ovum transport in the fallopian lines are all examples of biological activities that rely on peristalsis. The concept of porosity is crucial to studying peristalsis in biological systems. For research into blood flow within obstructed vessels caused by clots and tumors, porosity profoundly affects fluid motion [98]. Constant attention has been paid to peristalsis in porous media studies. According to the findings of numerous studies, non-Newtonian fluid models provide a more accurate approximation of the behavior of biological fluids, thus inspiring further investigation in this area [24]. Models that deviate from Newton's laws of motion were studied here,

including the pair pressure fluid layer and the Jeffries fluid model. The results of these analyses show that the mean speed and flow rate in the pouring region are lower when the medium's permeability is higher. Heat transfer is another topic that has attracted much attention because of its relevance to various fields, including biology and industry [108].

Micro fabricated arrays of nozzles with diameters ranging from 10 to 100 μm were used in the first inkjet print heads to realize this potential, allowing for the rapid and precise delivery of ink droplets [18]. Because of their responsiveness, speed, and ease of automation, microfluidic inkjets have entirely changed the printing industry. Since the early 2000s, when micro-fabrication technologies became more readily available at reduced costs, the number of alternative applications for microfluidics has increased tremendously. Analytical solutions exist for laminar flows in circular and rectangular channels, while simulation software is necessary for highly accurate solutions to flows in more complex geometries. Investing in micro-fabrication allows for developing digital prototypes of microfluidic designs for testing and refinement [136].

Numerous authors [87, 29]) have investigated pulsating blood circulation in the arterial system. The existence of pulsatile flow throughout the microvasculature has been demonstrated beyond any reasonable doubt from the earliest studies by (Rappaport et al. [111] on pulmonary arterioles to the most recent measurements by (Gaehtgens [59] and (Intaglietta [62] in arteries and venules of catomentum and cat mesentery). These results suggest that simulations of blood flow in smaller veins need to account for pulsatile flow effects to be realistic. (Womersley [140] provided the upon of pulsatile flow predicated on a Newtonian fluid. It is evident that a fluid model simplistic that it ignores the intricacies of blood circulation in the vessels is not enough. Suppose a hemorheological model is to represent the physiological activity of blood accurately. In that case, it must consider the blood's non-Newtonian, non-homogeneous properties as it reaches this point in the circulatory system. The presence of wholly developed laminar flow at low flow rates is indicative of constant venous impedance (ratio of pressure loss to flow) (Misra et al. [96]). Researchers found that the stenosis's resistance was primarily determined by its lowest cross-section area instead of its duration (Chakravarty et al. [42]). Due to a specific stenotic region, the pressure drop can be predicted using analytical models. About 65% and 90% of the non-stenotic model's minimal area was used to produce the stenosis tube (Zohdi et al. [155]).

About one-third of all deaths can be attributed to this factor. Due to the increased resistance to blood flow caused by high-grade stenosis, the body must boost blood pressure to ensure adequate blood flow. High pressure and constricted blood arteries result in increased flow velocities, high shear stresses, and lower or even negative pressure at the stenosis's orifice, known as the throat. There have been a lot of studies on the fluid flows and stresses in a collapsing elastic tube, both experimental and numerical (Tang et al. [126]). Several investigations have found evidence of a connection between atherosclerosis and micro polar fluid flow.

In situations where the size of the red blood cell (RBC) is comparable to the diameter of the tube, the two different natures of fluid as a suspension become relevant. Some of the impacts seen in the lab and living subjects are listed below. (i) The Fahraeus-Lindquist effect, in which the apparent viscosity of a tube depends on its internal diameter; (ii) the Fahraeus effect, in which the hematocrit of a tube or vessel depends on its internal diameter; (iii) the existence of a cell-free or cell-depleted layer; (iv) the presence of a smooth velocity profile (v) The red blood cell and plasma phase separation effect occur at vessel forks. Several models to explain these effects have been devised (Pries et al. [131]). Verma and Srivastava (2013, p. 13) [35] employed a two-phase model to analyze the constant blood flow in a circular tube. In the central region, blood is thought to behave as a power law, while the cell-depleted layer is treated as a Newtonian fluid. The two-phase model proposed by Sharan and Popel [120] assumes that the plasma forms a thin layer at the vessel's periphery. At the same time, the erythrocytes are suspended in a denser core region. Moreover, (Santhosh Nallapu and G.Radhakrishnamacharya [11]) consider a two-fluid model of a couple-stress fluid flow through a porous (tiny holes that liquid can travel slowly) medium in a confined channel with slip (go quietly & quickly). As slip, hematocrit, and channel height increase, the couple-stress parameter drops, and thus does the effective viscosity. The flow is observed to have the abnormal Fahraeus-Lindqvist phenomenon.

Some researchers depict the blood flow in small tubes as two methods. Reference: (Maithilisharan and Popel [88]). Blood flow in narrow pipes has been studied extensively (Chein et al. [46]), and biophysical aspects of microvasculature blood flow have been examined (both in vivo and in vitro) by Pries et al. [109]. Nair et al. [97] employed a double and for the blood in simulating oxygen transport in arterioles, one of many models devised to interpret these effects. With the help of in vitro and in vivo data, it could empirically develop connections between the apparent comparative

viscosity and the average tube's hematocrit as parameterized combinations of pipe diameter and discharge hematocrit.

Triple connections for viscosities, tube hematocrit, and core hematocrit are often derived from the total mass and energy balance of the RBCs and fluid in a cylindrical tube in most mathematical representations of constant blood flow using a two-phase flow model. According to (Nallapu and Radhakrishnamacharya [118]), the human circulatory system comprises a network of blood vessels ranging in size from 20 to 500. Blood circulation in the tiny arterioles, capillaries, and venules is called microcirculation. Its primary roles include supplying cells with oxygen and nutrition, removing waste products like carbon dioxide and urea, and circulating chemicals and organisms that mediate the body's defensive and immune responses. Significantly, it aids in the recovery of damaged tissues. Microcirculation exhibits some peculiar phenomena, such as the Fahraeus-Lindqvist effect, the Fahraeus effect, and the presence of a cell-free or cell-depleted layer near the wall (Fahraeus and Lindqvist [56]). Here, (Nallapu and Radhakrishnamacharya [117]) investigate an and, in fact, the motion of a Jeffrey fluid through a porous medium in tubes of varying sizes while being subjected to a magnetic field. We suppose that a Newtonian (in terms of the rate of its contraction over time) fluid exists in the periphery, while a Jeffrey fluid makes up the central region. When discussing blood flow in small tubes, (Sharan and Popel [119]) have explored a two-phase model. Two-layer models for blood flow in narrow pipes with micro polar fluid at their center have been proposed (Chaturani and Upadhya [44], [43]). Analytical solution to the linear system equations of motion has been obtained and used by (Sankar and Lee [116]) to study the steady stream of Herschel-Bulkley liquid through catheterized arteries. For the cell-free layer, we derive formulas for the effective viscosity of the flow, the core hematocrit, and the mean hematocrit. We investigate the impact of essential factors on these flow variables.

After studying blood's mobility with Newtonian and numerous non-Newtonian models, researchers have concluded that the Herschel-Bulkley model provides the most accurate description. Herschel-Bulkley fluid flows steadily even when encountering multiple stenoses in an angled tube with a non-uniform cross-section, as reported by (Prasad and Radhakrishnamacharya [94]). To better understand blood flow in arteries that have been catheterized, then examined the Herschel-Bulkley model with two fluids. Herschel-Bulkley fluids in elastic tubes have been the subject of mathematical investigation (Vajravelu et al. [129]).

Flat plate pulsating heat pipes [F-PHP] are of unique focus due to the fact that differences from traditional tubular pipes cause them to exhibit different thermo-hydrodynamic behaviors; hence, Ayel, V. et al [31]. offered a summary of current experimental research on these topics. Because of the thermal spreading effect linked to the geometrical continuity of the plate and the capillary pumping that occurs in the corners of square or rectangular channels, the differences can be partially explained. It was further proven by comparison testing of channel shapes in FPPHPs that square channels evaporate faster than circular ones, which was supported by local studies of self-induced evaporation. Even more so than with tubular FPPHPs, the evaporator zone tends to dry out more frequently when tested horizontally. With this background in mind, we'll dive into a literature review of local hydrodynamic visualizations and physical analyses. This will help us make sense of the phenomenological aspects, which in turn will shed light on the following sections: thermal performances, potential improvement efforts, operating conditions, and the most important parameters (channel dimension, fluid/material, geometrical aspects and fluid/material type).

A group of researchers led by Yang, K. S [145]., created vertically-oriented pulsing heat pipe (VO-PHP) devices that facilitate the flow of heat between two parallel movable air streams. Both water and HFE-7000, in proportions of 35% or 50%, could be used to fill these heat exchangers. A 132 x 44 x 200 mm PHP system was considered, with evaporator temperatures ranging from 55 to 100 °C and airflow velocities from 0.5 to 2.0 m/s, in order to determine the heat exchangers' thermal resistance and efficiency. Based on the experiments, it seems that heat pipes filled with HFE-7000, regardless of the ratio, behave like a network of thermo siphons because the tube's disadvantageous inner diameter was present in every test. On the other hand, water-charged PHP has the potential to generate pulsating liquid and vapor slug movements at high enough evaporator temperatures, particularly at a 50% filling ratio. The thermal performance of the HFE-7000-charged PHP heat exchanger was less affected by the increase in evaporator temperature since the tube contained non-condensable gas. Water might be used as a working fluid in the PHP heat exchanger, as long as the evaporator temperature is greater than 70 C, according to an analysis of the efficiency of the present heat exchangers.

The work of Shang, F. et al [12]. was joined to develop the efficiency of heat transfer in a pulsing heat pipe (EHT-PHP) is heavily reliant on the heat input and the

inclination angle. This article investigates the heat transmission efficiency at several angles of incidence. At different inclination angles, the temperature distribution of the PHP is determined using thermocouples and infrared thermo graphic imaging equipment. When operating with the help of gravity, the results reveal that heat is dispersed symmetrically, and that the average minimum thermal resistance is 0.17 K/W at a 45° angle. Thermodynamic resistance rises to a maximum of 0.33 K/W when the working fluid cannot circulate due to gravity, resulting in a uniform distribution of temperature. At the same time, when operating in the gravity aid and suppression modes, the inclination angle just affects the temperature oscillation mode. The PHP's optimal mode of oscillation occurs at a 90-degree angle, where its heat resistance is 0.077 K/W.

The experiments described by Li et al [79]. were to examine the performance and thermal responsiveness of a PHP that used a Nano-suspension of graphene, water, and ethylene glycol. The heat pipe was tested extensively using a range of conditions, including varying filling ratios, condenser temperatures, and graphene Nano platelet concentrations (0.1 g/l to 2 g/l) in a water-ethylene glycol solution. The applied heat values ranged from 10 to 100 W. At different concentrations, the Nano-suspensions' thermal conductivity and viscosity were experimentally assessed. A model was developed by means of response surface methodology [RSM] to minimize the system's thermal resistance and optimize the heat pipe's thermal performance. The results demonstrated that both the concentration of graphene Nano platelets and the thermal resistance value is negatively affected by a heat load delivered to the evaporator.

At the moment, popular approaches include F-PHP, VO-PHP, EHT-PHP, 3D-CLPHP, and RSM. Nevertheless, some constraints need to be considered. This work presents a methodology for determining heat exchanger effectiveness using Heat Pipes with Pulsating Response Surfaces [HP-PRS]. One of the pieces of medical gear that clinics utilize the most frequently is an infusion pump. Mechanically Pulsating Heat Exchanger infuses medicinal liquids into a patient's circulation scheme in regulated amounts and at exactly predetermined rates, such as nutrition, medicines, and contrast agents [26]. Pump malfunctions can result in overdose, missing therapies, or disruption in therapy because of the nature of the fluids they are designed to deliver, particularly high-risk drugs. This has a substantial impact on the wellness and security of the sufferers. From 2005 to 2009, the U.S. Food and Drug Regulation recorded around 56,000 incidents of unfavourable infusion pump-related events, including several injuries and fatalities [5].The infusion pump's inefficiency when operated improperly is

the cause of one of its most well-known failures. While the infusing pump's clinical instructions call for correctness with a 5% maximum margin of error, current precision personalized medicine and treatment need tightly regulated medicines administered on schedule. Drug injections for new borns, babies, and young children, for instance, must be able to administer several doses of high quantities at slow fluid velocity [21]. Since supplying the low-volume liquid needs more accurate fluidic management than providing the huge volume, this medicinal requirement is a considerable issue in the smaller end (3.0 g/h). To maintain patient security, a flow-rate sensor that can calibrate the infusing pump within the low region is essential [104].

The Gravimetric Model (GM) is the foundation of the infusing pump's standardized calibrating process. The quantity of the injectable liquid is measured by the GM using a balance, and the mass increase multiplied by ignition timing is used to compute a traceable flow velocity (in the unit of g/h). To prevent any miscalibration caused by fluid drifting, vaporization, and bubbling, accurate GM needs precisely regulated equipment, such as draft screens, micro tubing, and dispensed syringes [53]. Due to these limitations, the GM is normally carried out in a carefully regulated laboratory setting and cannot be implemented in hospitals, homecare settings, outlying medical institutions, or while providing care while travelling. There is a high need for an alternative to the GM that is ideal for these infrequent, small-scale, and distance adjustments of the infusing pump. The development of downsized flowmeter platforms has proven to benefit from Microelectromechanical System (MEMS) technologies [35]. Optical, mechanical, and heating flowmeters are some of the MEMS measurements that have been studied thus far. The most popular of them are the heat flowmeters, which are made up of just a few components (such as metallic warmers and temperature monitoring) and are simpler and more sensitive than non-thermal flowmeters.

Direct connection and non-direct connection thermometer monitoring are the two primary approaches that have been documented for microfluidics temperature monitoring [9]. In general, the temperatures can be precisely measured, but contact assessment will change the natural temperatures of the intended micro fluids through external macro equipment [150]. Because there is no heat transfer when using non-contact measuring equipment, it is challenging to attain high precision by relying on variations in the targeted object's physical characteristics.

To apply indirect ways to flip the microfluidic temperatures, more and more microscopic heat exchange concepts have been discovered and examined in recent times. The impact of heat transmission from the pipe substance is not taken into account when, for instance, copper wire is wound across a microfluidic pipe to serve as a temperature shift resistor to detect microfluidic temperatures. Temperature-sensitive materials that turn green can be used to detect microfluidic thermal variations, but they typically work best at a single temperature and have a relatively limited range of uses. The use of liquid metals with low breaking temperatures as easy-to-handle compounds with excellent thermal conductance in microfluidic heat exchange has also received much study [64]. To obtain a ratio of thermal transmission, fluid metals can be utilized as heating conductive mediums to link the microscopic and the macroscopic worlds. The electromagnetic flow meter is made up of an electrically insulated fiber pipe. Electrodes positioned opposite the additional, magnetic coil installed on pipe to generate magnetic field, and further forth. The insulated pipe transports the liquid, the flow that has to be monitored. A temperature monitoring system maintains and controls the temperature of a certain environment. In recent years, temperature monitoring systems have become a vital component of healthcare, hospitals, clinics, the food industry, and other businesses. In a heat exchanger, conduction and convection operate in concert to transfer heat. Heat exchangers can feature four different flow configurations: cross flow, co-current or parallel flow, and hybrid flow. Regenerative and recuperative heat exchangers are neither of the primary kinds of heat exchangers.

The research offers a MEMS flow meter that combines a microfluidic channel with a small membrane and a heating element to provide a quick reaction time, a low level of ambiguity, and minimal power consumption using a Mechanically Pulsating Heat Exchanger. The efficiency of the gadget was assessed using GM as a benchmark [130]. The flowmeter's dimensions are 11.5 mm x 17.5 mm x 3 mm, making it suited for a variety of liquid-flow calibrating applications in the field. This study presents a unique indirect temperature measuring technique that integrates a fluid metallic sensor with a millimeter-scale platinum impedance commercial sensor to detect and track the temperatures of microfluidic chip channels. This approach is user-friendly, reproducible, and avoids direct contact between the detector and the microfluid. A measure to offset and compensate an unfavorable temperature affect is referred to as temperature compensation. A sensor's measured value should never again be impacted by a temperature change thanks to temperature compensation. The mechanical varieties of

water flow meters, which measure flow by turbine rotation with a propeller, shunt, or paddle wheel design, are the most popular and cost-effective kind of water flow meter. Glass-based microfluidic devices have emerged as a game-changer in the field of microfluidics because of its many advantages over silicon, MFTCTM, and paper in terms of photonics, electronics, and thermo-chemistry.

Research into innovative technologies that can disperse more power in less space while yet meeting high reliability criteria is being driven by the ongoing need for innovative heat transfer techniques enable miniaturization and power density in electronics [128]. The Pulsating Heat Pipe (PHP) is a relatively recent addition to the heat pipe family; the original patent was submitted around 30 years ago [54]. For future ground and space applications, PHPs may constitute an alternative to cooling systems due to their ease of construction, capacity to dissipate heat even in microgravity, and compact size [22]. There has been growing interest in droplet microfluidics among researchers and industry professionals over the past two decades, and this has resulted in the publication of a number of publications detailing both theoretical developments and practical applications [91]. Some businesses, like Dolomite Bio, have even caught up to the created advancements [65]. Due to the carrier fluid's ability to isolate droplets from each other and the channel walls, droplets can be employed as micro reactors for chemical or biological synthesis, as well as enclosed cargo platforms for cells, particles, or biomolecules (DNA, proteins) [81].

Miniaturization of electronic components during the past few years has resulted in increased heat flux generation [27]. This element, along with strict criteria for aeronautics, transportation, and energy applications, has resulted in difficult problems in thermal management [61]. One of the most exciting developments in cooling technology, for electronic devices, the pulsing heat pipe is an extremely effective passive heat transfer mechanism (PHP) [60]. PHPs are two-phase passive devices driven by temperature changes, and they function by utilizing the capillary forces and liquid motion brought about by a phase shift [73]. As power density in high-performance electronic devices and small-size portable devices grows, thermal properties have become a barrier to further reduction of rising circuit boards, creating an urgent demand for thermal management [67]. A heat pipe uses the vapor-liquid phase shift inside the pipe to passively and efficiently transmit heat from the heated end to the cool end [153].

The reduction of mass is one of the current technological design difficulties of many products [82]. In order to lessen their impact on the environment, this is necessary [36]. Due to the weight savings afforded by synthetic materials, they are increasingly being used in place of metals [58]. Nevertheless, these materials are poor heat conductors, necessitating novel thermal management systems for cooling electronic components [74]. Conditions such as temperature fluxes of several hundreds of W/cm², long-term dependability, and very cheap prices for commercial market items are all issues with traditional cooling systems that have arisen as a result of device miniaturization [146]. Because of this, we urgently need cutting-edge new methods of cooling. Heat pipes, specialized devices designed to transport surplus heat to a cooler location, are gaining in popularity [151]. As the fluid velocity along the plug axis must be counter clockwise to ensure liquid mass conservation, this results in the formation of rolls within the plug [123]. Microfluidic systems and pulsing heat pipes are two applications of these techniques. Explore fluid dynamics as well, explaining the differences between laminar and turbulent flows and how Reynolds and Capillary numbers play a role. Highlight the significance of phase change phenomena, especially evaporation and condensation, to heat transmission in closed systems. There should be definitions of terms as they are introduced, visual aids for complicated ideas, and comparisons to established standards in the presentation. It is important to highlight the lack of explicit material qualities, experimental dimensions, and a technique when discussing the presentation's flaws. The scientific credibility and readability of the article will be improved by revitalizing these elements. The designers are forced to use synthetic materials that are lighter than metals but poor heat conductors, necessitating novel approaches to cooling the electronics inside [70]. When compared to other heat pipe designs, PHPs have superior efficiency because of this occurrence [107]. The expanding vapor then travels to the condenser where it condenses. Transfer of heat occurs because latent heat is absorbed in the evaporator and released in the condenser [47]. The heat pipes work very well because of the high latent heat. Many varieties of heat pipes exist. The geometry and the means by which liquid is moved from condenser to evaporator set them apart [80]. Due to miniaturization and increased heat production, this research tackles a pressing issue in modern microelectronics: maintaining an acceptable operating temperature. The importance lies in the requirement for effective heat transmission, which has led to research into the Pulsating Heat Pipe (PHP) as a passive, high-efficiency heat transfer solution. This study looks into PHPs, which can improve heat management over active technologies thanks to their fluid and vapor

phases contained within a closed capillary channel. Specifically, the researchers use a new PHP configuration called "Temperature Regulation in a Pulsating Heat Pipe Using Microfluidics [TRPHP-MF]" to improve separation and efficiency by inserting partitioning barriers within the channel. The research validates the heat transport model using simulations and real-world data. The results demonstrate that TRPHP-MF's thermal performance is enhanced due to the flow pattern modification generated by droplet production within the heat pipe. The work highlights the necessity for thorough understanding driven by physics-based inquiry, and it highlights the constraints of relying on empirical correlations in non-stationary systems like PHPs.

By suggesting a concrete method for incorporating microfluidics into PHPs, this research goes beyond past efforts in the literature. While previous works have investigated PHPs' passive heat transmission capabilities, the current work goes farther by presenting a realistic design adjustment utilizing separating barriers. In addition to making a substantial contribution to the field of passive heat transfer solutions, this discovery has the potential to enhance heat transmission in microfluidic systems. The results of the study highlight the need for additional thorough investigation to fully realize the promise of PHP-based thermal control solutions.

Droplet generation is typically the first and most crucial stage, with results that are steady and predictable [95]. Methods like biochemical testing, click chemical and the DNA polymerase chain reaction are just a few examples of the many applications that necessitate a tightly regulated droplet formation process for reliable outcomes [133].

Mangini, D et al. [90] developed a Single Loop Pulsating Heat Pipe (SLPHP). It's been tested in both hyper and micro gravity and has a 2 mm internal diameter. Two sapphires tubes join the hot and cold sections of the system, allowing for simultaneous increased imaging of fluid flow with a large camera and direct to fluid IR analysis with a Medium-Wave Infrared Camera (MWIR). By strategically placing three separate heaters at the evaporator, power may be distributed in a number of ways, and various flow motions can be encouraged by tailoring the heaters' temperatures and placement. Moreover, two very accurate pressure transducers monitor the pressure difference between the condenser and the evaporator.

Cui, W et al. [51] proposed a novel approach to droplet formation in microfluidic systems (DF-MF) with integrated microwave heating. Microwave heating causes an

Inertial pressure at the contact Laplace, allowing droplet production on demand. Scientists have shown that the power of the microwave stimulation and the length between the contact and the junction play a role in droplet formation. Applications needing dynamic tuning of material properties in droplets can benefit greatly from the method's incorporation with microwave detection, which can be used as feedback to govern the supply flow of materials, despite the method's limitations in creating droplets at a high rate.

Ayel, V et al. [31] elaborated and provides a summary as a result of their structural variations from standard tubular pipes, flat plate pulsating heat pipes exhibit a wide range of thermo-hydrodynamic phenomena, which have recently been the subject of experimental research. Most of the distinctions may be traced back to whether the channels are rectangular or square in shape, which affects capillaries squeezing at the channel's corners, and the thermoelectric expanding impact linked with the plate's geometrical continuity. In illumination of these concerns, a review of literature of local hydrostatic visual representations and physiological evaluations is introduced in to fully comprehend the experiential facets, which will aid in the assessment of the subsequent subsections on: the most key variables (connection space, liquid, simple geometric aspects, processing parameters); thermoelectric showings and tries at major improvements; and, eventually, the promising therapeutic fields of appl.

Chen, X et al. [2] incorporated flat-plate oscillating heat pipe (FP-OHP) which is employed electronic equipment cooling when subjected to uneven heat production from a number of sources, using a plan that has Under different inclinations, thermal loads, and levels of heating inhomogeneity, a "center-multiple-heat-source nonuniform heating and two-end air cooling system is created. The thermal performance disparities among two mirror-symmetric regions of the flat-plate OHP are analyzed with the use of different flow drawings and thermal version. The results show that nonuniform heating, in contrast to uniform heating, yields higher thermos hydrodynamic performance at low heat loads with quasi-steady "stop-oscillation" fluid motion in the OHP, lower performance at high heat loads when continuous fluid flow can be maintained in the flat-plate OHP. Nikolayev, V. S et al. [99] exhibited discuss the evolution of theoretical PHP (T-PHP) research and its implications for the future. At first, we examine the physical events occurring at the scale of a single bubble or liquid plug. To begin to understand PHP and validate models, it is described here how the simplest, single-branch PHP can be modelled. Next, how the generation and disappearance of bubbles, as well as the

evaporation of plugs, can be modelled. Finally, the differences and similarities between the regarding the existing modelling as well as simulation methodologies for the multi-turn PHP are discussed.

For the purpose of selecting the best polymeric materials for creating flexible pulsing heat pipes, the multi-criteria decision-making (MCDM) model developed by M. Ordu et al is presented. Since there are so many different competing materials on the market today, each with its own unique set of qualities, applications, benefits, and downsides, making a decision on which polymeric material to employ requires weighing a number of factors. Findings from this research lend credence to prioritizing material choices with MCDM methods in order to improve the selection process. Both business executives and researchers in the academic world who are responsible for choosing polymeric materials would benefit immensely from this study.

According to the review of relevant works, microfluidics-related studies have included temperature measurements. However, they fall short in terms of precision and efficiency at higher levels. Therefore, a more effective system is developed to account for and measure temperatures in microfluidics to facilitate drug injection.

The present literature review on PHP analysis offers a thorough and inclusive examination of the extant scholarship and understanding in the domain, encompassing the fundamental tenets, operational mechanisms, and progressions in PHP technology. The text functions as an essential basis for the intended investigation, setting the stage and pinpointing areas of deficiency that the present inquiry endeavors to rectify.

Xu et al. present a comprehensive overview of PHP, focusing on selecting working fluids, operational mechanisms, and practical applications [144]. The study emphasizes the importance of careful fluid selection and design considerations. The results delineate the functional attributes of various working fluids and their influence on the performance of PHP, thereby facilitating the enhancement of PHP configuration to achieve proficient heat transfer. Li et al. analyzed operations and evaluated the performance of a pulsating heat pipe in the context of low-temperature heat recovery [78]. The proposed method involves analyzing PHP's response characteristics and heat transfer performance. This analysis aims to better understand the operational behavior of PHPs in varying conditions and their potential for use in heat recovery applications.

The study conducted by Zhang et al. pertains to an experimental investigation of a pulsating heat pipe utilizing a silica nanofluid [149]. The research focuses on the visualization of flow and heat transfer. The results offer significant insights into the augmentation of heat transfer efficiency by applying nanofluids, which enhance thermal conductivity and flow properties. In their study, Kim et al. conducted an empirical examination of the selection of working fluid in a micro-pulsating heat pipe, scrutinizing the impact of different fluids on the efficacy of heat transfer [69]. This study conducts a comparative analysis of various working fluids and their corresponding effects on thermal resistance. The objective is to facilitate the identification of appropriate working fluids that can enhance the operational efficiency of a PHP.

The experimental investigations on the heat transfer mechanisms of a pulsating heat pipe were conducted by Jo et al. [6]. This research offers valuable insights into the primary modes of heat transfer in PHP: evaporation, condensation, and capillary action. These findings enhance our comprehension of the fundamental heat transfer mechanisms that govern PHPs. The study by Xu et al. pertains to an experimental investigation of the heat transfer performance of PHP utilizing hybrid working fluids [143]. The method under consideration investigates the utilization of amalgamated working fluids for augmenting heat transfer. The results indicate a superior thermal performance compared to working fluids with a single component.

Khalilmoghadam et al. introduce a new energy storage mechanism that utilizes phase change material and PHP to recover latent heat in solar stills [68]. This study examines the utilization of Phase Change Materials (PCMs) for efficient energy storage and latent heat recovery to enhance solar energy utilization. Specifically, the study focuses on applying PCMs known as paraffin wax for this purpose. The study by Kang et al. is a numerical investigation of a newly developed single-loop pulsating heat pipe that incorporates separating walls within the flow channel [66]. The proposed design incorporates partition walls to augment heat transfer efficiency. The outcomes indicate enhanced heat transfer properties and decreased temperature differentials. The thermal behavior of a micro pulsating heat pipe is characterized by Iwata et al. through local heat transfer investigations [63]. This research offers valuable perspectives on the heat transfer mechanisms and thermal efficiency of micro PHP, which can facilitate the enhancement and comprehension of their functionality in microscale contexts.

The study by Ayel et al. examines the thermal performances of a flat-plate pulsating heat pipe under varying working fluids, such as water, aqueous mixtures, and surfactants [30]. The results underscore the impact of the composition of the working fluid on the heat transfer properties, providing insights into the most advantageous choice of working fluids to enhance the performance of the pulsating heat pipe. The literature review offers significant perspectives on diverse facets of PHP, encompassing working fluids, design factors, heat transfer mechanisms, and practical implementations. The survey underscores the necessity for a sophisticated approach, such as prediction based on deep learning, to precisely gauge the performance of PHP and improve its overall effectiveness. This approach can help bridge the gap between experimental analysis and optimization, leading to optimal thermal management solutions.

MINIATURE CHANNEL WITH PULSATING LIQUID DYNAMICS

2.1 Pulsating Liquid Dynamics:

This past decade has seen the development of several inertial microfluidic strategies that aim to take advantage of inertial effects in fluid combining and particle transport by increasing flow velocities to $Re > 100$. One other method for guaranteeing adequate reactant blending until the next microfluidic operation is to lengthen the channel. There is a trade-off in energy efficiency between extending the track and increasing the flow rate for incompressible flow in microchannel with a constant cross-section.

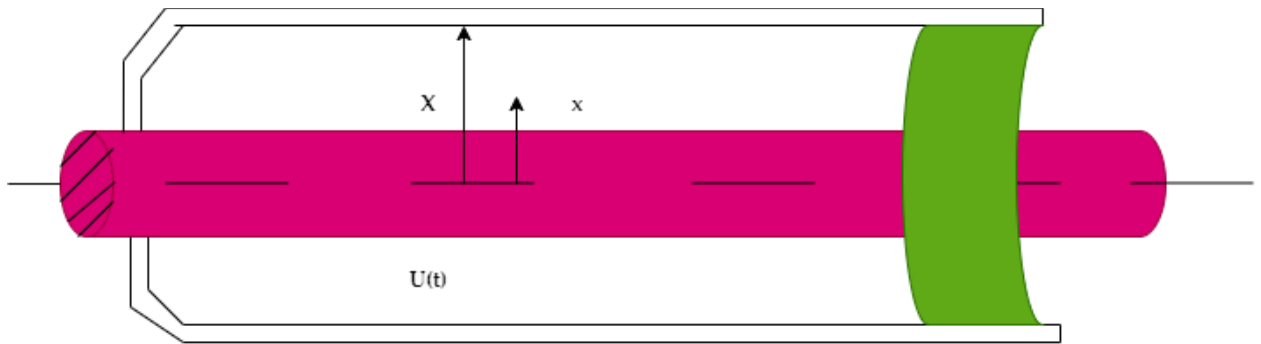


Figure 2.1.1 Flow in a stiff tube

The following discussion examines the effects of a periodic pressure gradient on the motion of a liquid inside a closed conduit of suitable length. We assume that the pressure gradient is time-dependent, with no contribution from the onset, termination, or presence of particular walls. When it comes to fluid dynamics, the streamlined momentum equation is

$$\sqrt{\phi} = \sqrt{\partial + \alpha^{1/2}} \left(\sqrt{\frac{dy}{dx}} \right) \quad \text{if } \phi \geq \phi_y \quad (2.1.1)$$

The yield stress and shear-dependent viscosity of fluid whose structural connections in time-varying shear are given by the above equation (2.1.1).

$$\frac{dy}{dx} = 0 \text{ if } \phi \leq \phi_y \quad (2.1.2)$$

However, the Newtonian features of the cell-free wall layer that functions as a lubricant can often outweigh the effect of the cell-rich, non-Newtonian centre on the overall flow characteristics.

The pressure gradient is thought to be time-dependent, with no entrance, end, or special wall effects. When it comes to fluid dynamics, the streamlined momentum equation (Navier-Stokes Equation) is

$$\rho * \frac{du}{dx} = - \frac{dP}{dx}(t) + \frac{1}{r} \frac{d}{dx} (r\phi) \quad (2.1.3)$$

These terms represent the equilibrium between the forces of inertia, pressure, and shear. The above equation can define the equations that need to be solved, and it is vital to note that the system contains nonlinear interactions (2.1.3). In addition, the starting point of the plug flow region is identified by the solution. The problem's opacity makes it difficult to approach it straight forwardly.

2.2 Mechanically Pulsating Heat Exchanger employing Microfluidic Technologies [MPHE-MT]:

Our analysis is carried out by first converting the motion equations to a non-dimensional form and then doing a fundamental perturbation analysis on the distinctive semi-fundamental flow. New to this work is a method for pinpointing the yield plane when initial inertial effects become significant.

$$\rho * \frac{du}{dx} = \frac{dP}{dx}(t) + \frac{1}{r} \frac{d}{dx} (r\phi) \quad (2.2.1)$$

where ϕ is the shear stress ϕ_{ry} , as new non-dimensional variables, we introduce quantities written in the dimensional form.

$$\begin{aligned} \phi^1 &= \frac{PR}{2} \phi, \\ r^1 &= Rr \\ u^{-1} &= \frac{P_0 R^2}{2\delta} \partial \\ t^{-1} &= \frac{t}{\delta} \end{aligned} \quad (2.2.2)$$

where P_0 is the magnitude in absolute terms of a standard pressure gradient

R is the radius of the tube

∂ be the viscosity signature at high shear rates.

The formula for the pressure difference is

$$-\frac{dP}{dx} = -P_0 P(t), \quad P_0 = \left| \frac{dP}{dx} \right|_{\text{typ}} \quad (2.2.3)$$

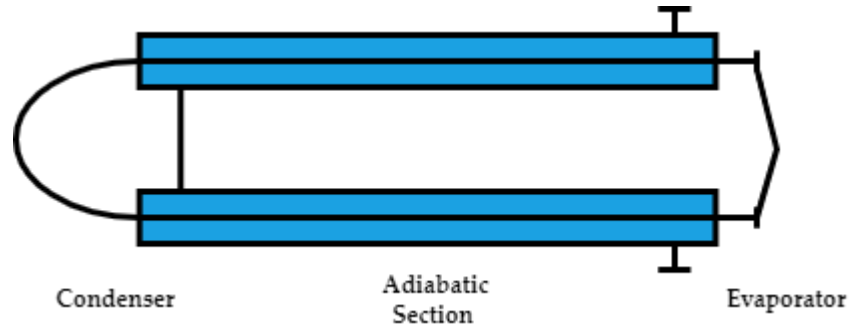


Figure 2.2.1 Pulsating Heat Exchanger

The above figure 2.2.2 shows the pulsating heat exchanger. The 2D single loop pulsating heat pipe was chosen to analyse the effect of the thin separating wall in the heat pipe channel. All of the conventional and innovative PHPs were 100 mm in length. PHP had a total channel width of 2 mm, with 15 mm between its two major, straight branches. In addition, the evaporation, isothermal, and condenser sections are 50 mm, 55 mm, and 45 mm in length. The novel PHPs have a dividing wall of copper 0.3 mm thick. Specifically, the distances between the split system's inner side and the fluid flow's inner side were 1.1 mm, 1.56 mm, and 2.46 mm when the separating wall was placed on the inner, middle, and outer sides of the flow channel, respectively. The heat pipe channel's inner side was separated from the remainder of the pipe by walls at the quarter, half, and three-quarter marks of the main channel's cross-section.

As a function of atmospheric pressure, the saturated heat for water vaporization and condensation is given by

$$\text{Sat. Temp} = C * \ln \left(\frac{\text{Pressure}}{\text{Const}} \right) + C \quad (2.2.4)$$

The above equation shows the saturated temperature where C the constant value at a given set is, and pressure and const are considered.

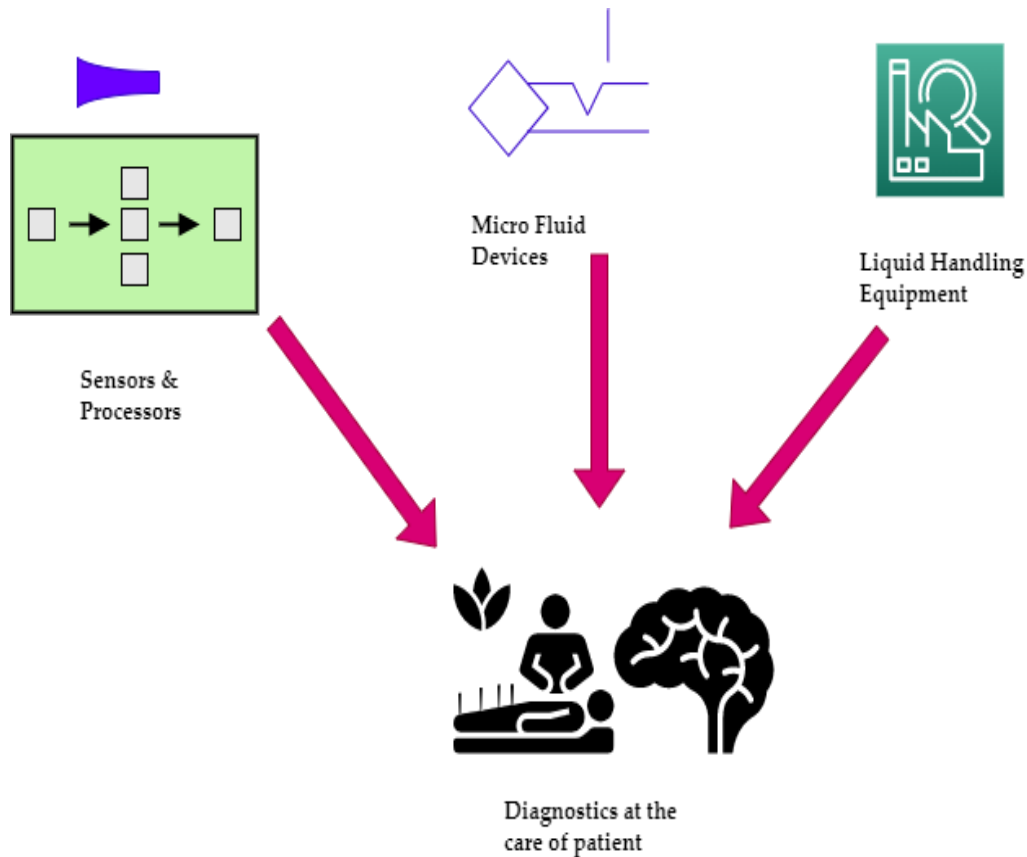


Figure 2.2.2 Procedures for Handling Fluids at the Point-of-Care

Off-chip pumps in microfluidic devices typically handle tension and flow rate regulation. There are a wide variety of off-chip pumps for microfluidics, ranging from inexpensive syringes to programmable piezoelectric pumps to simple; ultra-low-cost reinforced latex balloons exaggerated to include a steady pressure source. Pumps of various kinds are used in laboratory microfluidics, with syringe pumps being ubiquitous. With feedback control, syringe pipes can be programmed to maintain a constant flow rate or pressure. However, there are some situations where syringe pumps just don't cut it. Unfortunately, syringe pumps can only dispense liquids up to the volume of the syringe, and they can't be used to power recirculating flow in a closed system. Not only are high-quality syringe pumps like those made by Harvard Apparatus typically used in research labs, yet their price makes them unfeasible to implement in low-resource clinical settings. Peristaltic pumps are alternatives to syringe pumps, which are best suited for some applications. A liquid is pumped by cyclically compressing a tube against a rigid accommodation in these devices. Here, we give the blueprints for a microliter-range liquid-handling peristaltic pump that is inexpensive, open-source, and three-dimensional in design—perfect for diagnostic microfluidic devices.

2.2.1 Pulsatile Flow:

Microfluidic devices have advanced significantly over the past decade, allowing for faster cell sorting, more sensitive analyte detection, precise micro-pumping, and the purification of bio samples in less time. However, the conductivity value of the reagents restricts the mixing velocity in low Reynolds number (Re) flows. It can mix lengths over a thousand times the channel's width for rectangle micro channel. While laminar flows in simple geometries such as circles and rectangles have analytic solutions, more complex geometries require using simulation tools to arrive at reliable results. Because of this, digital models can prototype and refine the microfluidic design before any micro fabrication is undertaken. While this ease of setup is welcome, laminar transport presents several difficulties, including those associated with reagent mixing.

Increasing the short-channel effects is another approach for ensuring sufficient reagent blending before the following microfluidic procedure. For incompressible fluids flowing through micro channel of constant cross-section, the needed differential pressure is proportional to both the channel length and the flow velocity; thus, expanding either strategy (channel length or flow velocity) incurs a high energy cost. Because of the high pressures, rigid fabrication materials like glass and silicon are often required. It presents a severe challenge to moment-in-time or business products due to the high manufacturing cost and the lack of readily available external high-pressure sources. Using fluid oscillations as an alternative to constant, unidirectional flow is another possibility.

In pulsating flows, the properties of the flow can be broken down into a time-averaged value and an oscillatory value. Oscillatory flows are a particular case of pulsatile flows that are made solely of oscillations and not any time-averaged components. As mentioned before, the viscosity nature of these low- Re flows can be used to one's advantage in the blending problem described. An alternative to stretching the channel's physical dimensions is to use an oscillating velocity to alternate the flow's direction at regular intervals, resulting in a longer "pipe" without needing a boost in pressure. The examples of pulsatile flow in microfluidics presented in recent literature are typically much more complicated than this improvement in effective duration. Pulsatile flows' time-varying pressure, velocity, shear stress, and other flow characteristics have been exploited for improved separation and mixing, automating

processes effectively on-chip, preventing clogs, and pinching off droplets are all examples.

There is significant biological relevance to pulsatile flows, and they add complexity for improved microfluidic functions. Almost every multicellular organism uses a beating heart to power fluid transport, whether the system is open or closed. Many models of cardiovascular flows include chambers or channels and incorporate pulsating flow. Many organisms, including jellyfish, sponges, and fungi, that lack a heart or complicated circulatory system rely instead upon and flow of the water around them to transport nutrients and waste. Many cells depend heavily on the pulsating environment for their survival, migration, and development.

Most microfluidic systems have used steady flows inside immobile or malleable apparatuses. Recent research has concentrated on how to take advantage of pulsatile flows to make possible new functionalities. The wax and wane of a pulsing flow are associated with a unique temporal scale, in contrast to the invariant time nature of a steady flow. A common source of motivation for such systems is a harmonically oscillating field from the outside.

Micro channel flow driven by a pulsatile differential pressure can be expressed mathematically as ppd.

$$\Delta ppd = \Delta ppd_0 + \partial * ppd - e^{i\phi t} \quad (2.2.5)$$

where Δppd_0 is the time-weighted pressure, ∂ represents the fluctuating pressure's amplitude, ϕ is the rate of repetition, and t is the time. This expression can be used to define several distinct flow fields. Time variance disappears, and classical steady flow is established when the oscillation amplitude is zero ($p = 0$). There are two categories of harmonic flow; when $p > 0$, the flow is said to be pulsating. A mean advection of flowing fluid is superimposed with an oscillatory motion having an amplitude of p and a frequency of $f = \phi / (2\pi)$.

When $p = 0$, fluid particles do not undergo net fluid motion over time and instead oscillate about a fixed point, a situation known as oscillatory flow. It is essential to consider system characteristics when describing the impact of flow oscillations on different microfluidic chip designs. In a flow, the Reynolds number quantifies how much more dominant inertial forces are compared to viscous forces (Re). Since viscous effects are typically more prominent in microfluidic devices, laminar flows generally are

observed. However, the temporal properties of groups on the surface and oscillatory flows are not currently accounted for in Re due to a lack of appropriate parameters. Even at low Re , the pulsating nature of the system can cause the fluid flow to encounter viscous resistance and inertia. The situation here is distinct from the constant stream in micro channels, where only the viscous resistance plays a role. Thus, it is necessary to introduce a new dimensionless parameter. Womersley's number (Wom) compares the momentary inertial effects to the viscous forces.

$$Wom = \sqrt{\phi * V + LS} * V \quad (2.2.6)$$

Here V and LS denote the velocity and length scale characteristics, respectively. With $Wom < 1$, the flow is dominated by viscous effects, and the oscillation frequency is low enough that a steady velocity profile can develop throughout each cycle. At sufficiently high oscillation frequencies, such that at low velocities ($wom > 1$), the mean flow profile is drastically altered by the oscillatory inertial force. As the pressure gradient changes direction, a corresponding phase difference in the fluid flow happens in this regime.

It is possible to perform analytical settlement of a single stream in the laminar regime, which has been considered for describing physiological flows, among other applications. However, this review will mainly exclude the influence of flexible fluidic streams on pulsatile flows. It is still an active research area because of the system-specific nature of the effects of compliance and harmonic currents.

2.2.2 Signal Generation with Pulses:

Oscillatory signals both generated internally and externally can propel pulsatile or oscillatory flow in micro channels. The simplest is to use an external input, such as digitally regulated pressure controllers or peristaltic pumps. Oscillatory pressure signals can be superimposed on a constant flow through specialized pneumatic conduits to create complex pulsatile flows. While external sources have the advantage of simplicity and durability, they are not practical for use in point-of-care or field settings because they require more space and energy. Another restriction is that they can't handle signal frequencies higher than about a few Hz. Consequently, a wide variety of on-chip methods have been investigated.

On-chip mechanical oscillatory signal generation is still in its infancy. Hence to create pulsating flows with constant flow inputs, asymmetric elastomeric components

have been incorporated into microfluidic channels. This method, similar to an electronic switching circuit, has a frequency that has been demonstrated to be no higher than 1 Hz and requires a well-designed device to produce the desired signal. It has been shown that oscillator fluid circuits can achieve flow rates of up to 0.5 m/s at frequencies of up to 10 Hz when operating at a constant water head pressure. Oscillators like these are one-of-a-kind because they can produce variable flow rates from an endless pressure supply. Despite the prevalence of incompressible flows in microfluidic applications, it has been shown that silicon microfluidic oscillators can operate at frequencies close to 1 kHz.

An oscillating electrical signal is typically used to create pulsing flows on a chip. Thermal bubble micro-pumping, which has its roots in inkjet printing, entails using an integrated micro heater to propel the growth of a stationary bubble. It has been used to enforce a frequency-dependent oscillatory flow and can be accomplished with a unit of energy or thermal management to control bubble growth. Fluid motion can be induced over a broad frequency range using piezoelectric diaphragms. Electrodynamic phenomena can drive pulsatile flows. Electro wetting involves applying a voltage to control the surface energy of a fluid's interaction with a dielectric-coated electrode. Since capillary flows can be caused by surface tension alone, this is ideal for microfluidic applications. Electro wetting systems are easy to make because they only need a single layer of patterning on the electrode for the bare minimum of functionality. It is possible to control fluid motion over the patterned working electrode at kilohertz actuation frequencies, which makes electro wetting and droplet-based techniques a powerful combination for improving micro scale mixing. The electro kinetic phenomenon of electro osmosis uses an electric field to propel a fluid's bulk flow through a network of tiny channels, such as a capillary. Like electro wetting methods, electro osmotic flow (EOF) can be easily implemented across the board. It is sensitive to electrochemical properties and Joule heating, which can restrict the types of samples used. Recent years have seen a proliferation of theoretical studies on oscillatory EOF, which is still in its infancy. Low cost, small footprint, and straightforward implementation are just some of the benefits of this device, and it has already been shown to be effective in generating oscillatory flow rates in microfluidic systems. This overview demonstrates the extensive toolkit available for generating oscillatory signals, which includes active, passive, outer, and on-chip approaches. Microfluidic systems operating over a broad flow range or processing samples with varying steam, high voltage, and viscous properties benefit greatly from this diversity.

Because of this variety, however, it is challenging to generalize the effects of pulsing flows in many different settings. Many of the methods above focus on the frequency of oscillations, yet only a few highlight the importance of flow rate or oscillatory amplitude. For critical comparisons of methodologies and pulsatile studies to be standardized across fields, a more precise description of pulsatile parameters will be required.

2.2.3 Constructing Droplets:

The generation and manipulation of droplets is a classic application of microfluidic technologies. It has expanded to new fields such as single-cell analysis, high-throughput biochemical screening, and material synthesis. The benefits of droplet-based systems include efficient use of reagents, the ability to produce droplets in abundance, a large surface area to volume ratio for quick responses, and the ability to control individual droplets' size independently. While most uses necessitate droplets of consistent size, there are a few that call for carefully orchestrated sequences of droplets of varying volumes. Droplet coalescence must be managed if micro droplets encapsulate minute reaction volumes. Precise regulation of droplet formation, growth, and motion is necessary. In the first generation of systems, droplets were generated passively by maintaining a constant flow rate or pressure across a microfluidic junction between two fluid phases. Syringe pumps or pressure regulators power the flow, and some of the system's energy is transferred to the destabilizing effect of the liquid-liquid interface, which can lead to the formation of droplets or grooves in the jet. Droplet formation can be triggered using passive methods if Rayleigh-Plateau instabilities are allowed to grow independently. While pressure and flow rate are the only variables that actively affect droplet breakdown, the shape of the connection can be passively altered to encourage or discourage it. Because electric fields can act as particle breakdown in dielectric jets, this method calls for electrically conductive working fluids.

As a result, passive methods are restricted in terms of droplet size, frequency of generation, and suitable fluid. In its place, active techniques have emerged to reduce the lag time between system input and output, which is essential for stable droplet production without compromising the range of possible droplet sizes or production rates. Many methods for creating active droplets rely on pulsatile flow. Additionally, the pulsatile condition allows for more command over droplet formation by eliminating its reliance on the expansion of the Rayleigh-Plateau instability. When it's necessary to

generate droplets with a very low interfacial tension, external forcing of the droplet formation can be very helpful. Finally, it's important to remember that pulsating flow conditions aren't always optimal for creating droplets. Systems with low interfacial tension, where the normal uncertainty expansion is slow or non-existent, benefit from periodic perturbations to trigger instabilities. Droplet formation may be non-uniform in systems with high interfacial tension due to the interaction of pulsatile pressuring and natural instability growth.

2.2.4 Improved Blending:

Mixing plays a critical role in many applications of functional microfluidics, including material synthesis and bioassays. Traditional microfluidic devices typically function in a low-Re domain characterized by laminar airflow profiles where diffusion limits mixing. Since the interfacial area between the fluids increases, the mixing process is accelerated when complex geometries are present in steady flow regimes. The term "chaotic mixing" describes this procedure. Hydrodynamic focusing and geometric elements like herringbone and serpentine channels are used to fold segregated liquids and increase mixing times repeatedly. Additionally, mixing times can be drastically improved with the help of pulsatile strategies, primarily when used in conjunction with other improvements.

The simplest method for pulsating mixing involves incorporating an oscillatory component into an otherwise stable mixing interface. A peristaltic pump was used to provide the mean flow, and a pinch valve was placed on each arm of a y-connection to create strong pulsations. Pulsatile flows have significantly improved one of the essential microfluidic operations, mixing. Reversing the flow direction, using high-frequency fluid oscillations to generate chaotically mixed, and internal circulatory using droplet techniques are all examples of pulsatile strategies that can significantly improve mixing times compared to their steady-flow counterparts.

2.3 Results & Discussion:

2.3.1 Thermal Resistance Analysis:

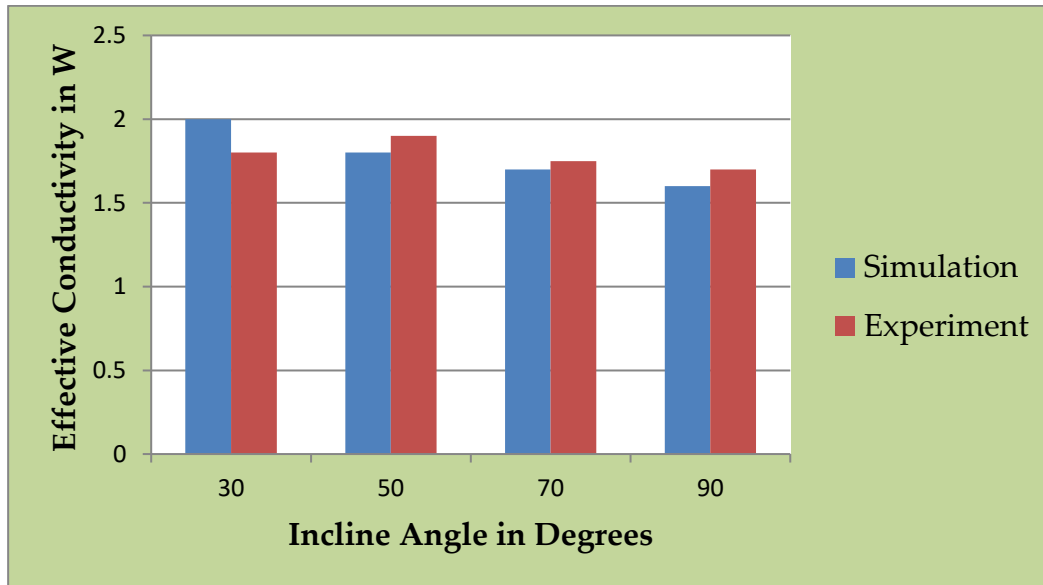


Figure 2.3.1 Thermal Resistance

Figure 2.3.1 depicts the test procedure for the thermal resistance analysis ratio. The inclination angle variation (X-axis) is compared to the conductivity (Y-axis) to understand the two better. The comparison between both is predicted and shown above.

2.3.2 Flow Rate Analysis:

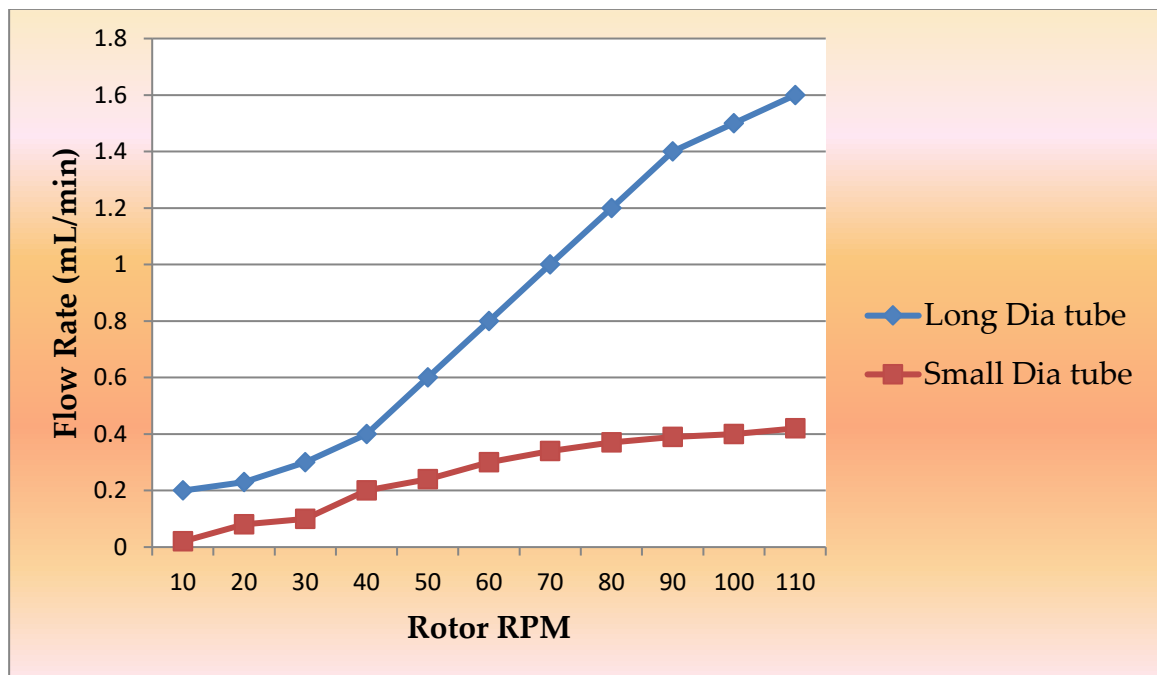


Figure 2.3.2 Flow Rate Analysis

Figure 2.3.2 depicts the results of a test of a ratio for analyzing flow rates. By contrasting the rotor RPM (X-axis) with the flow rate (Y-axis), we can learn more about both variables. They are compared as expected and demonstrated above.

2.3.3 Flow Scheme Analysis:

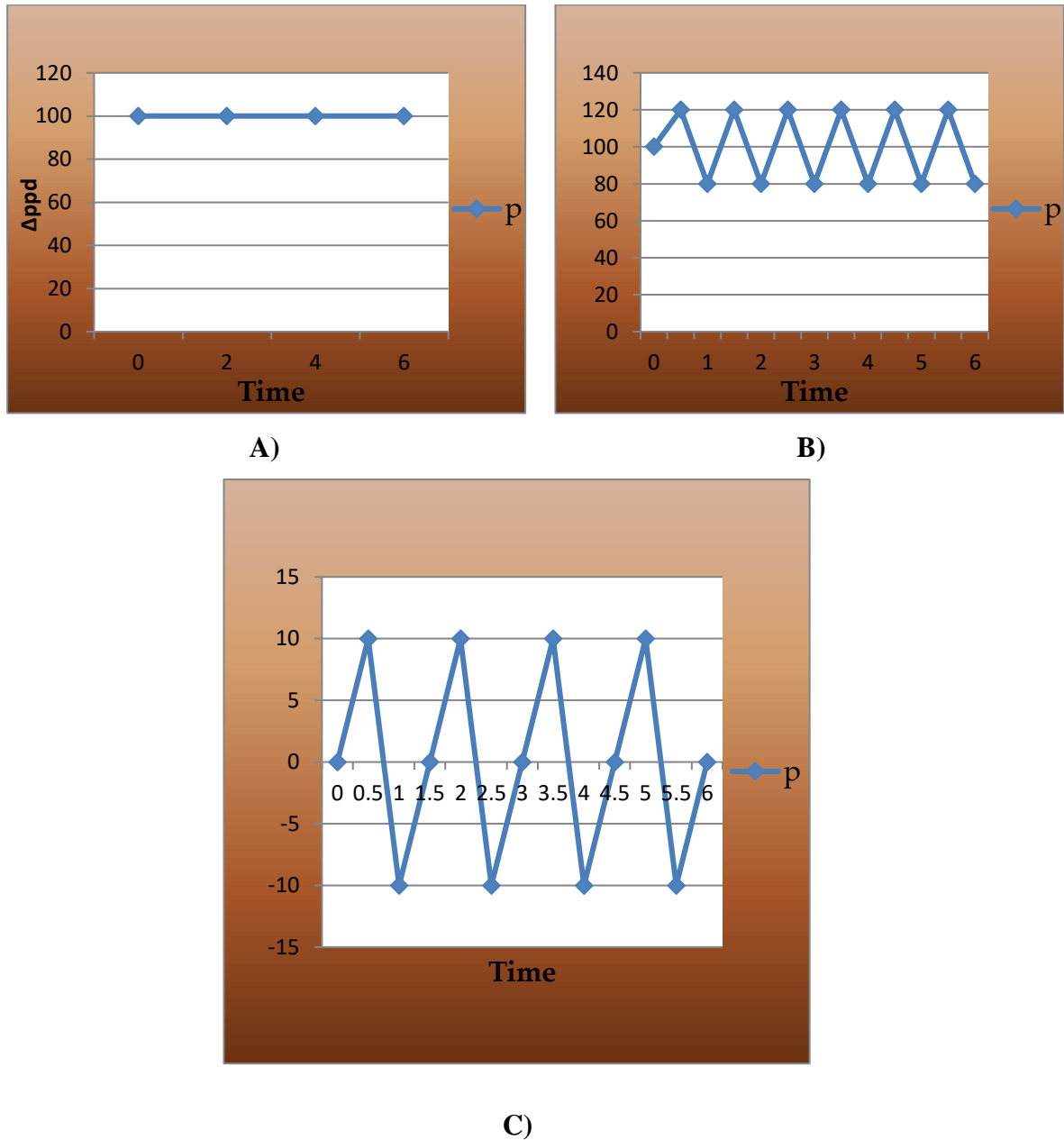


Figure 2.3.3 Constant and Fluctuating Flow Methods

The above figure 2.3.3 shows many flow fields are definable. When the oscillation amplitude is zero ($ppd = 0$), temporal variance vanishes, and classical steady flow is restored (Figure 6A). When two different kinds of harmonic flow can be defined for $p \neq 0$. When $ppd \neq 0$ is less than zero, as depicted in Figure 6B, the flow is characterized as pulsating. A mean increase in the flow of fluid particles is superimposed here with a

cyclical amplitude of p and angular frequency of $f = \partial / (2)$. In the scenario where $ppd_0 = 0$, particles in the fluid do not undergo net convection over time; instead oscillate around a fixed position, a phenomenon known as oscillatory flow. Consideration has been given to using a rigid microfluidic device to perform analytical precision of a single stream in the laminar domain for use in describing flows of a physiological nature.

The cardiovascular system is not the only organ where pulsating flows occur in the body. Blinking produces an oscillating flow of tears over the eyes. Redistributing tears helps keep the cornea moist, and blinking helps remove foreign bodies from the eye.

2.4 Conclusions:

Over the past two decades, microfluidic devices have seen increased usage due to the many benefits brought about by miniaturization. Because of their compact size and wide range of features, they are ideal for on-the-go use with a minimum learning curve. Due to their small size (on the order of millimetres), low-Re flows are frequently the consequence. These flows can begin and end abruptly and reliably. Features on a micrometre scale allow for the exact manipulation of particles as RBC, tumours, germs, viruses, and micro- and nano-particles all fall into this category. Oscillatory or pulsatile flows have the potential to address multiple issues with microfluidic devices. Numerous reports have surfaced showing that oscillatory improvements may be made to mixing, the formation of droplets with particle manipulation, low interfacial tension, and the prevention of clogs. This chapter aims to optimize axial velocity and temperature perturbation systems for typical values of variable liquid properties. Closed-form concentration solutions can be obtained by solving for the temperature perturbation. The present study is one of the first to shed light on how non-Newtonian fluids' heat and mass transfer characteristics are affected by external magnetic fields and variations in liquid properties. A stepper motor drives the pump's mechanical system, separated from the electrical system by a power supply and a microprocessor. In this work, we propose a Mechanically Pulsating Heat Exchanger (MPHE-MT) that uses microfluidic technology. Hence to accomplish this, walls are constructed inside the flow channel. Each vascular waveform includes its minimum, maximum, and median flow rate. Patients with cortical and lacunar stroke did not differ significantly on any measure of flow or pulsatility.

DYNAMIC HEAT PIPE & HEAT EXCHANGER PERFORMANCE

3.1 An overview:

The majority of industrial goods, machinery, processes, and combustion by products are responsible for producing low temperature waste heat [32]. So, heat exchangers, not thermoelectric devices, would be crucial for low-temperature waste heat recovery [7]. In the industrial sector, any operation that produces heat will inevitably result in waste heat. Waste heat is typically categorized according to its temperature, which can be low (<120 °C), medium (120~650 °C), or high (>650 °C) [4]. Since thermal pollution and energy loss result from waste heat dissipation, waste heat recovery is crucial for improving energy efficiency and reducing thermal pollution [25]. Commonly abbreviated as "HPs," these tiny but mighty devices can transfer massive amounts of heat from a hot source to a cold one across a relatively small and relatively energy-free area [13]. Because of their adaptability, they find use in many different contexts, such as solar thermal receivers and systems, cooling microelectronics, and other high-temperature applications [16]. A heat pipe typically consists of an evaporator, which takes in heat, an adiabatic portion, which transports heat without losing any heat to the environment, and a condenser, which either lets some of the absorbed heat escape or releases it all to the cold environment [8].

Due to the growing need in the aviation and information technology industries, space-saving heat transfer equipment is in great demand. The technology behind tiny heat pipes has advanced through multiple phases in the past few years [83]. A pulsing heat pipe serves as the cooling device. A system's thermal performance is largely dependent on the heat transfer fluid used by the HPs. This fluid allows a working fluid that is liquid-phase to absorb heat that is received in the evaporator [37]. The removal of the working fluid can be achieved through phase changes such as evaporation or nucleate boiling, which are dependent on the heat flux that is applied. The recent trend towards miniaturization of electronic components has led to a dramatic rise in heat flow [124]. Challenges in thermal management have been exacerbated by this component, which has to meet stringent requirements for use in aircraft, transportation, and energy applications, including compactness, light weight, and minimal power usage [15]. When it comes to passive heat transfer systems, pulsating heat pipes are among the most

promising options for cooling electronic equipment. Two-phase passive devices that are heated can be powered by PHPs through the application of capillary forces and liquid motion caused by phase changes. They resemble a capillary or tube that has been twisted in a web of connections [17].

Partially filling the tube with a working fluid in a liquid/vapor saturation state causes the fluid to be distributed as vapor plugs and liquid slugs due to surface tension effects [39]. A number of complex two-phase flows, such as bubbly, slug/plug, and annular flows, are produced in reaction to heat sources; these in turn affect the total heat flux that the PHP transports from the heated to the cooled zones [33]. Since the protocol's start, extensive research on PHP's inner workings and thermal transmission properties has been conducted. Complexity abounds throughout the PHP code. Rapid volume expansion, accompanied by the formation of bubbles, occurs as the working fluid is heated in the evaporator [76]. A dramatic reduction in volume occurs in the condenser. Because of the internal phase shift, the operating fluid can be continuously pumped to the spot between the evaporator and the condenser. The fluid achieves directional circulation flow after condensation by returning to the evaporator section [34].

The main parameters that impact the operation, as per the specifics of the PHP operating mechanism, are the pipe's shape, the inclination angle, the working fluid, the heating medium, and the structure of the unit [114]. Research has mainly focused on three areas: structure, working fluid, and liquid filling ratio. In terms of advantages, PHP stands out due to its easy organization and straightforward architecture [110]. Finding that PHP is more suitable for usage in electronic and military applications, the researchers adjusted the settings. One of the most effective cooling systems, boiling heat transfer, has found widespread use in electronics, mobile devices, and other high-performance engineering applications [125]. To dissipate a large amount of heat with a relatively little temperature change, boiling heat transfer makes use of the working fluid's latent heat of vaporization. Pool boiling HTC is also at least five times more than single-phase natural convection [48].

The effect of surface characteristics on nucleate boiling heat transmission is becoming an increasingly important area of study. Wettability as well as microstructure/roughness is critical parameters in boiling heat transfer. In several cases, the critical heat flux (CHF) for boiling heat transfer was higher on hydrophilic surfaces than on their

untreated equivalents [132]. At the same time, a pipe with a variable diameter outperforms a pipe with a fixed diameter in terms of heat transmission in the same channel. It has been shown that using Nano-fluid as the operating fluid makes the PHP easier to start and improves its heat transfer capabilities [134]. The filling ratio is another important factor that affects the efficiency of heat transfer. With a low liquid-to-gas ratio, the PHP is easier to work with initially, but it dries faster. When the ratio of fluids to fill is optimal, the PHP is difficult to start but not to dry [134].

The significant contributions to this paper are as follows:

- In this paper we present a methodology for determining heat exchanger effectiveness using Heat Pipes with Pulsating Response Surfaces [HP-PRS]
- Water is the PHP's most effective working fluid heat exchanger when worked at evaporator temperature. The suggested approach aimed to minimize system thermal resistance and maximize the heat pipe's thermal performance.
- The findings the thermal resistance value drops with increasing graphene Nano platelet concentration and evaporator heat load.

Presented here are the findings from experiments conducted on pulsing heat pipes with flat plates: First, we have an overview of pulsating heat pipes; second, we cover the relevant background research; third, we go into detail about the Heat Pipes with Pulsating Response Surfaces [HP-PRS] fourth, we discuss and analyses the experimental results; and finally, we arrive at a conclusion.

The present work quantitatively investigates a three-dimensional closed-loop pulsing heat pipe (3D-CLPHP) that was introduced by Wang, J et al. [135], charged with deionized water and featuring varying degrees of wettability. We derive the CLPHP thermal performance and bubble dynamics for a range of input heat loads. The results show that surface wettability and input heat load both have an impact on CLPHP performance. When applying less input heat, hydrophobic CLPHP (including super hydrophobic surfaces) show less thermal resistance than hydrophilic CLPHP. Meanwhile, CLPHP with a hydrophilic surface can start up faster and show better thermal performance even when exposed to a higher input heat load. The thermal resistance of CLPHP with a super hydrophilic surface is 10.8% lower than that of CLPHP with a hydrophobic surface when tested with a 20 W input heat load, specifically. Also, CLPHP that is hydrophobic on one surface and hydrophilic on the other exhibits flow reversal, but always keeps consistent directional circulation. Various

forms of capillary resistance are caused by dynamic contact angle hysteresis, which is the difference between the two angles. Hydrophilic CLPHP surfaces further enhance the dry-out input heat load through the liquid film effect and decreased flow resistance.

3.2 Heat Pipes with Pulsating Response Surfaces [HP-PRS]:

One efficient way to move a lot of heat from a hot source to a cold one is through a heat pipe, which is a small yet very effective device that typically doesn't need any outside energy to operate. Therefore, they have a wide range of potential applications including cooling microelectronics and high-temperature applications like solar thermal receivers and systems. The three primary components of a heat pipe are the evaporator, which absorbs heat, the adiabatic section, which transfers heat to the environment without loss, and the condenser, which returns all of the absorbed heat to the cold environment. A working fluid in the liquid phase absorbs heat received in the evaporator; this is achieved mostly through the fluid used for transferring heat within the HPs it is an essential part of the system's thermal performance. Two processes controlled by the applied heat flux—evaporation and nucleate boiling—are employed to extract the working fluid.

In this paper, we will examine a subset of PHP called Heat Pipes— Pulsating Response Surfaces [HP-PRS]. This type of PHP is characterized by a flat plate with a single, typically square or rectangular, channel that runs serpentine between multiple hot and cold sources. The channel can be engraved, machined, or obtained through additive or fetching manufacturing. A smooth-surfaced plate cover is utilized to seal the channel. Conversely, due to their exceptional thermal interactions, flat heat sources are perfect for heat transmission. The design is far more involved and can necessitate intricate or costly production procedures on occasion, in comparison to a tubular PHP. Nevertheless, it may be easily reduced in size, which opens up a world of possibilities for micro-electronic cooling applications.

A lot of research has gone into PHPs since 2000 so that we can replicate their pulsating, self-exciting working fluid movement. The purpose of these researches has been to identify the variables that affect PHP thermal performance and the smooth launch of this movement. To further our understanding of this thermal performance, we have also performed experimental testing using transparent PHPs, which let us to see the fluid movement.

$$HT = \phi_{cd} + \phi_{ad} + \phi_{ev} \quad (3.2.1)$$

Equation (3.2.1) denotes the heat transfer content which is the sum of 3 components of tube which are ϕ_{cd} be the condensing part, ϕ_{ad} be the adiabatic section and ϕ_{ev} be the evaporation part.

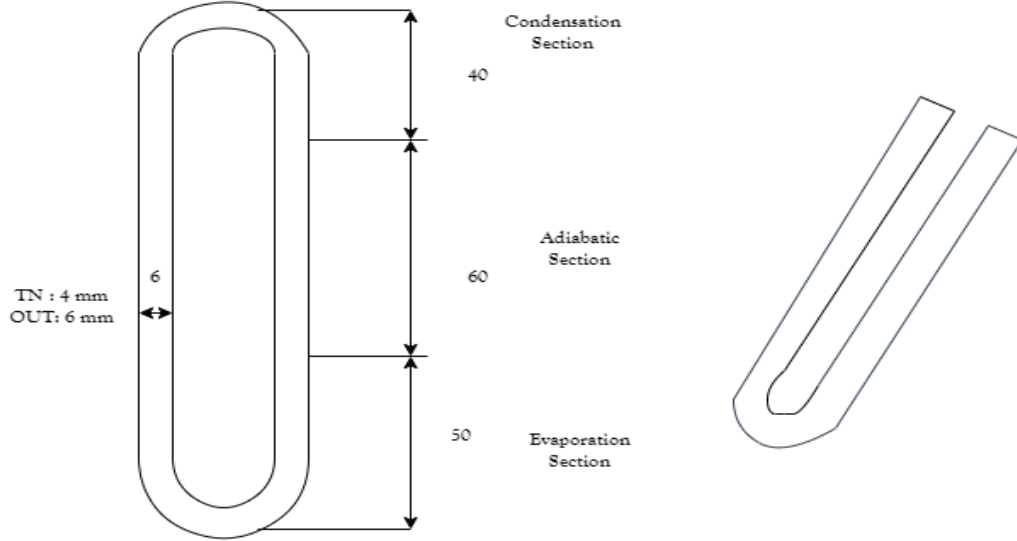


Figure 3.2.1 Domain of calculation models and grids in PHP

Figure 3.2.1 shows the establishment of a three-dimensional PHP having a 4 mm internal diameter of 6 mm, and a total width of 32 mm. The current numerical simulation relies on this accurate data acquisition. Meanwhile, the physical model utilized in this work is vertically arranged. Extraction (50 mm), absorption (60 mm), and condensation (40 mm) sections are measured at different lengths. The PHP is made of quartz glass and operates on deionized water. Quartz glass has a relatively low thermal conductivity, but it nonetheless manages to transfer a significant amount of heat through its wall. When heat is transported in a radial direction, the wall, liquid film, and liquid plug of the PHP all work together like a series circuit. A liquid layer that was far thinner than the wall was found. So, the wall and the liquid sheet work together to establish the radial heat conductivity. In this numerical simulation, the whole PHP environment is the computational domain. This method is used to generate hexagonal structured grids. Also, the grids near the PHP wall are locally densified to account for the wall's impact on heat transmission and working fluid flow.

$$\frac{dh(t)}{dt} + \partial(t) + HT = TR \quad (3.2.2)$$

Equation (3.2.2) represents the TR which is thermal resistance of the PHP tube taken for consideration whereas $\frac{dh(t)}{dt}$ be the pace at which change of heat factor regarding t to time. $\partial(t)$ Be the heat constant.

Substituting equation (3.2.1) in (3.2.2) gives equation (3.2.3) which is given by

$$\frac{dh(t)}{dt} + \partial(t) + \phi_{cd} + \phi_{ad} + \phi_{ev} = TR \quad (3.2.3)$$

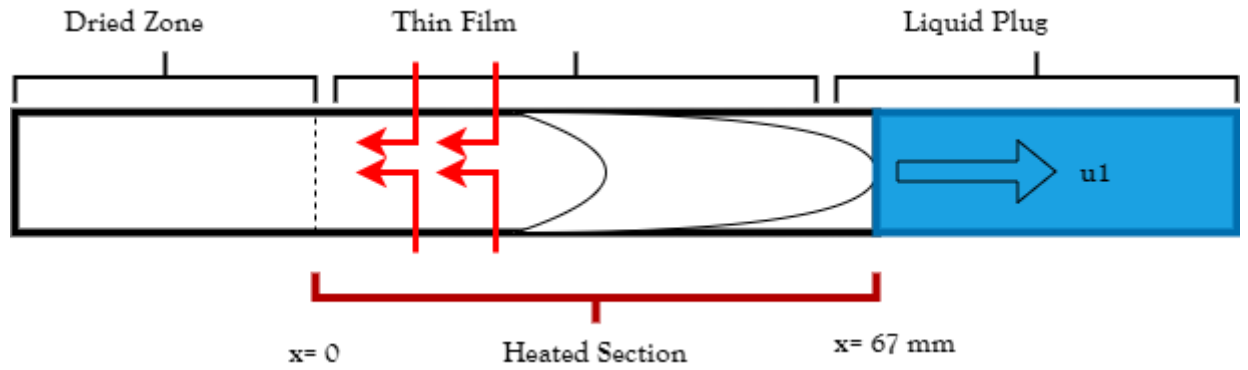


Figure 3.2.2 Chemical Process of a PHP

The process is carried out by monitoring the temperature of a thin liquid coating as it evaporates in a 2 mm capillary copper tube as illustrated in figure 3.2.2. This shows the chemical process happening in PHP when it's heated. Dried zone, Thin film, Liquid plug are notified as per the figure. Within a capillary tube heated by the Joule effect and coated with black paint, there was a flow of semi-infinite liquid slugs (with retreating menisci as their termini, a thin film as their deposit, and, theoretically, a vapor phase at saturation state). The tube's wall thickness was 0.2 mm. Using infrared thermography, we were able to determine the temperature field at the tube's top line and identify the four distinct locations of heat transfer during the initial heating phase, when the liquid slug passes through the heated region.

$$LP_u - LP_n = D_z - D_n + T_f + T_n \quad (3.2.4)$$

Equation (3.2.4) specifies the chemical process of PHP whereas D_z be the dried zone, D_n for n number of tubes, T_f be the thin film, T_n be the total film content, LP_u be the liquid plug for u_1 case and LP_n be the total number of plugs.

$$HS = \frac{LP_u - LP_n}{D_z - D_n + T_f + T_n} + x \quad (3.2.5)$$

The above equation (3.2.5) shows the heated section in PHP tube which is the ratio of liquid plug and dried zone and thin film where x takes the value between 0 and 67 mm.

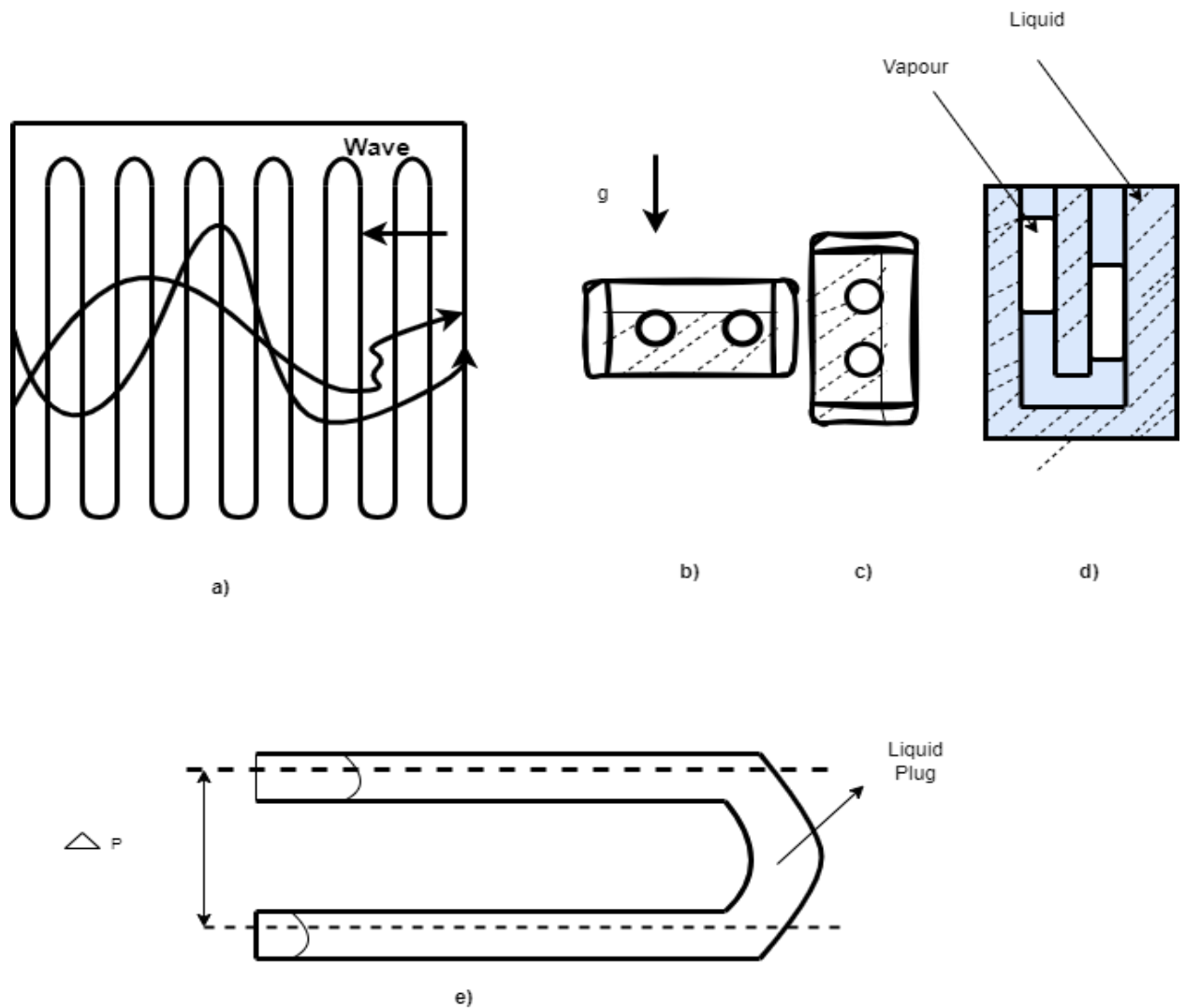


Figure 3.2.3 Visual representation of a PRS

At each flow channel, the endpoints of lengthy liquid slugs are connected by a fast waveform, as shown in Figure 3.2.3 a. One scenario involves right-handed wave generation, left-handed wave growth, and right-handed wave damping and disappearance until the following cycle. Variation in oscillation frequency is caused by heat conduction as well as thermal energy storage in solid walls. Their big channel PRS was tested in microgravity during a parabolic flight campaign. They saw oscillations of fluid flow with very high amplitudes, alternating between stopover periods and waveforms, and eventually the menisci ruptured. The flow pattern changes to slug flow when gravity is absent, even in channels of vast dimensions, because weak capillary

forces are sufficient to keep fluid slugs ensnared between vapour bubbles. On the other hand, when the hydraulic diameter is big, the capillary and friction forces are low, causing the liquid slugs to travel impulsively, the menisci to break, and the flow pattern to become more chaotic. Isolated liquid plugs may readily move, even in the presence of minor pressure changes, improving heat transfer during working periods, while the fluid tends to dry out in the evaporator under these conditions.

Figure 3.2.3 b), c) and d) shows that horizontal, edge and vertical sides respectively. Figure 3.2.3 e) shows the decrease in gravitational pressure due to a single edge bend. Since there is a disparity in height at each U-turn, there is a particularly high gravity pressure head at the last surrounding bend, which causes the liquid slugs to be pressure imbalanced. This causes all of the slugs to oscillate continuously over long periods of time, even with the lowest heat powers applied, and there is no dry-out at the evaporator. In the evaporator zone, the liquid slugs move from the top to the bottom in a waveform, as shown in the figure. The velocities and amplitudes of these oscillations grow when the heat input is increased.

$$Amp = \sqrt{\frac{H}{2} + V * p^e * HI} \quad (3.2.6)$$

The above equation (3.2.6) shows the amplitude of the oscillations where Amp be the amplitude of the oscillating wave, H be the horizontal side, V be the vertical side of the tube and p^e be the probability density for edge and HI be the heat input.

$$Vel = \sqrt{LP} * HI + \theta \quad (3.2.7)$$

The above equation (3.2.7) represents the Vel which is the velocity of the oscillating wave may be sin or cos. θ be the angle of deviation of the corresponding oscillating wave and LP be the liquid plug.

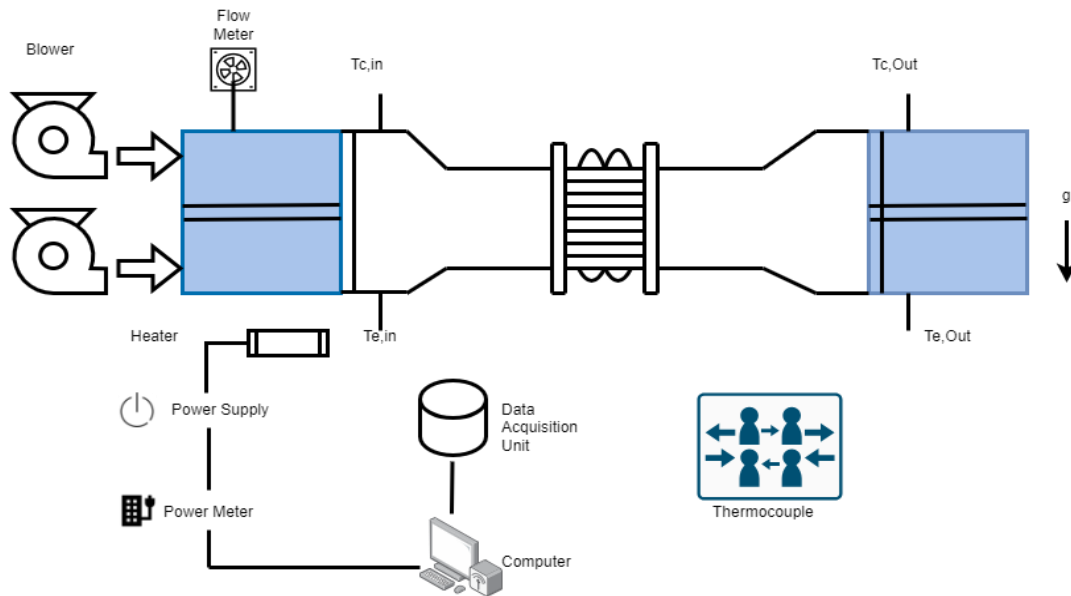


Figure 3.2.4 Layout of the Current Experimental Setup

Figure 3.2.4 shows the setup of the current experimental setup, which consists of a PHP heat exchanger, devices for monitoring temperature, and systems for supplying air and a data acquisition system. This setup was set up in a room where the air temperature can be consistently maintained at 30 °C and the relative humidity at 70%. The air supply system made use of two inverter centrifugal blowers to ensure that the two air streams were directed to flow in parallel through their respective ducts. The air temperature at the duct's inlet was controlled by a heater that was placed behind the inlet; a power meter measured the heater's output. At the intake and exit of both air ducts, T-type thermocouples were set up to measure the air streams' temperatures with a resolution of 0.1 °C. to measure the air temperature at both the intake and outlet cross sections of the air ducts, figure 4 shows the positioning of the T-type thermocouples. Furthermore, the airflow rate in the cold the air duct was recorded by means of a vortex flow meter with a volumetric flow rate accuracy of 1.5% (ranging from 8 to 300 m³/h), while the airflow rate in the a conduit for heated air was measured by a flow rate accuracy of 3% (ranging from 0.8 to 229 m³/h). When we have the inlet's volumetric flow rate, we can divide it by the air density and the inlet's cross-section area to get an approximation of the air flow velocity. Before further processing, all observed signals were transferred and recorded by a personal computer through a data capture unit.

$$T_{out}(c) = T_{in}(c) + T_{in}(e) + BL + FM \quad (3.2.8)$$

Equation (3.2.8) represents the $T_{out}(c)$ which is the temperature of the condenser at output side whereas $T_{in}(c)$ be the temperature of the condenser at input side, $T_{in}(e)$ be

the temperature of the evaporator at input side, BL is the blower value and FM be the flow meter reading.

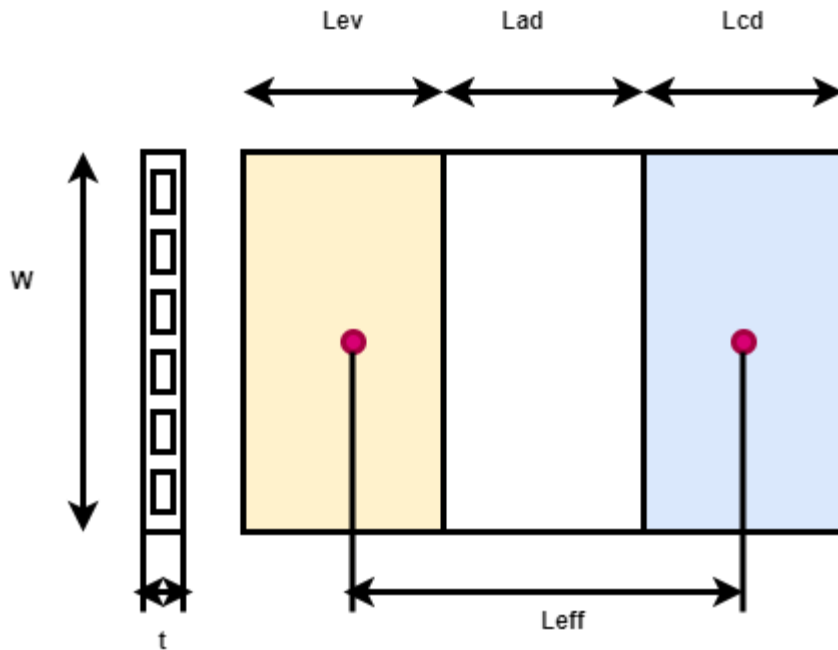


Figure 3.2.5 Comparison analysis of PHP geometrical parameters

Notably, there are one-of-a-kind publications that offer comprehensive details regarding the mathematical components depicted in figure 3.2.5. These components relate to the variables used in the experiment, such as the evaporator and condenser temperatures, effective thermal conductivity, and heat input or power. In the first instance, we solely looked at 1-layer channels PHPs, where the condenser and evaporator zones were located at the sides of the device. With respect to the efficient heat transit.

$$L_{eff}(h) = (L_{ev} + L_{ad} + L_{cd}) * wt \quad (3.2.9)$$

The term L_{eff} refers to the device's effective length. L_{ev} represents the evaporation, L_{cd} represents the condensation, L_{ad} represents the adiabatic section at width w and time t .

The flow meter that measures the efficiency of heat exchangers by compensating for and measuring the temperature of heat pipes with pulsating response surfaces (HP-PRS) is described throughout this portion, along with its design and operating structure. Using the mathematical model, we were able to achieve more efficient and less thermally resistant outcomes.

3.3 Results and Discussion:

Various operational characteristics are covered here, among various items, are the impact of thermal resistance, temperature profile, responsiveness, and filling ratio on the PHP's performance in efficiency.

3.3.1 Thermal Resistance:

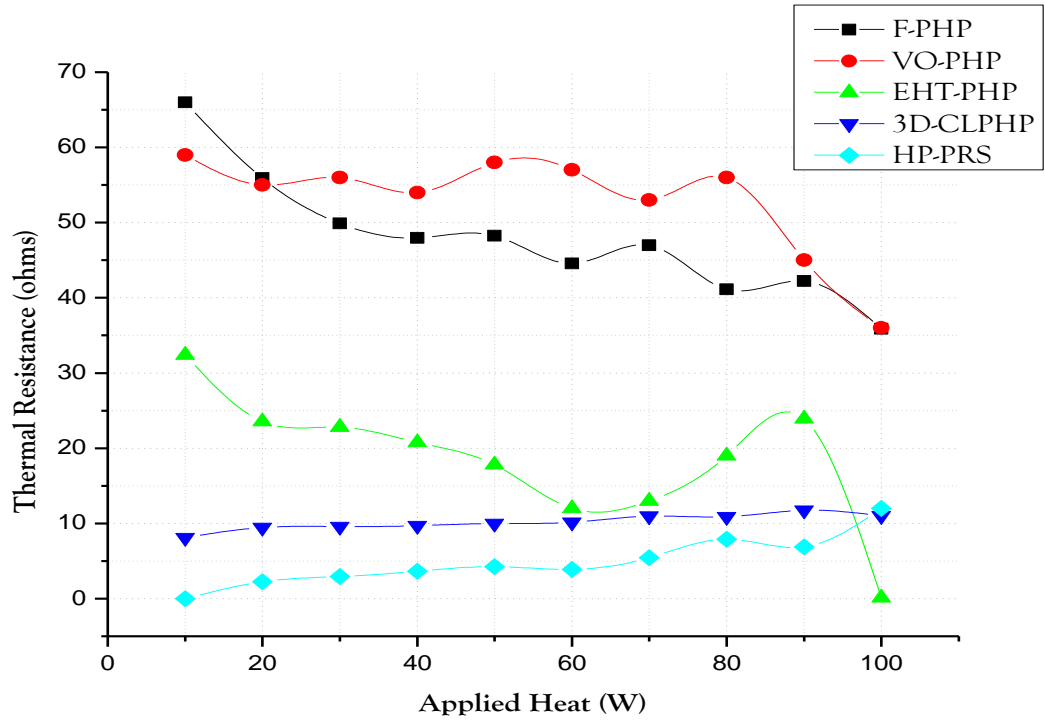


Figure 3.3.1 Thermal Resistance

When heat is delivered from the hot source (Ni-Cr wire) to the evaporator, figure 3.3.1 shows how the measured thermal resistance (THR) of the PHP varies. The THR value drops nonlinearly as the applied heat rises, as is clearly seen. With sufficiently high applied heat, the PHP's THR exhibits an asymptotic trend that, interestingly, reaches a zone with constant value. This finding is in line with previous research on Nano suspension, which found that raising the concentration of further decreased the system's THR value. Results showed that when PHP is run at maximum applied heat and high concentration, the THR value drops to its lowest.

3.3.2 Filling Ratio:

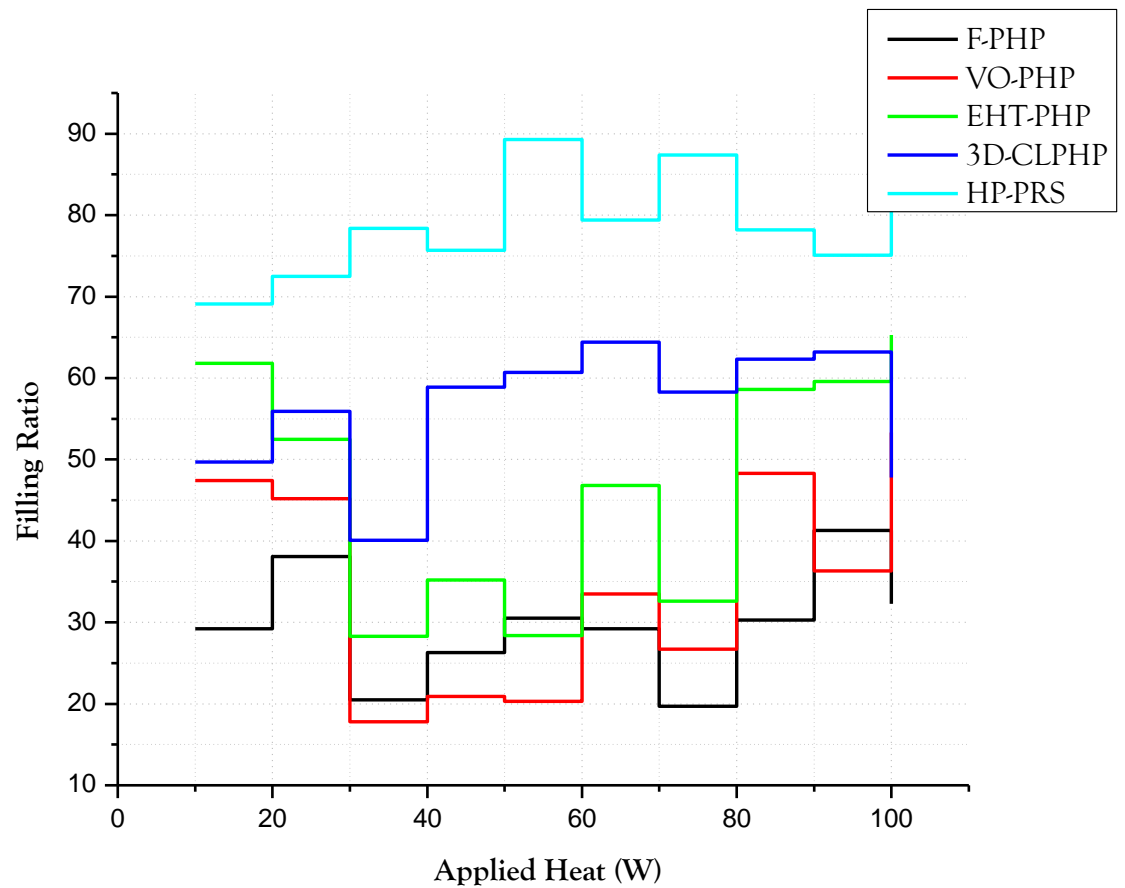


Figure 3.3.2 Filling Ratio

Figure 3.3.2 shows the filling ratio for the application of tube at different heats. Despite numerous experimental investigations into the impact of filling ratio, conclusive findings have proven elusive due to the fact that ideal filling ratios are very conditional on operational factors such as orientation (horizontal or vertical inclinations), working fluid type, distance between evaporator and condenser, lengths of both, etc. A change to semi-annular flow, characterized by liquid slugs in the channels, occurs as FR increases. FR outperforms 60% in terms of thermal performance.

3.3.3 Efficiency Analysis:

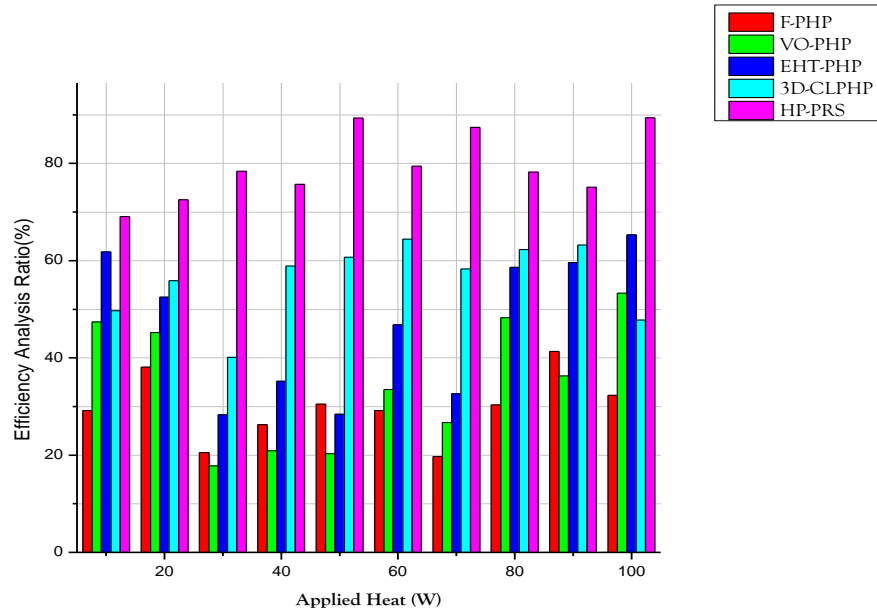


Figure 3.3.3. Efficiency Analysis

The above figure 3.3.3 shows the efficiency analysis where the graph is plotted against efficiency and applied heat (w). In this analysis efficiency is greatly achieved as HP-PRS stands high in ratio compared to the existing models such as F-PHP, VO-PHP, EHT-PHP, and 3D-CLPHP.

3.3.4 Temperature Profile:

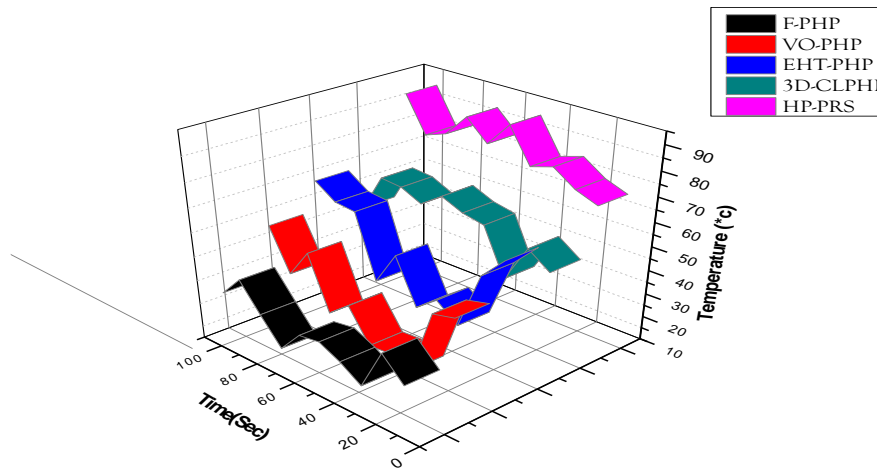


Figure 3.3.4. Temperature Profile

The experimental setup includes a PHP, data gathering hardware, and a heating system. A power meter, an ammeter, and transformers make up the heating system. Through the process of natural convection, the condenser part dissipates heat into the surrounding air. By utilizing K-type thermocouples, the variation in evaporator temperature was quantified. Infrared thermal imaging equipment records the heat flux distribution of the PHP. The PHP is built from ribbed-plate copper U-tubes. The working fluid's thermos physical characteristics in a copper pipe are temperature dependent. The working fluid's physical and thermal characteristics determine the PHP's critical diameter. When deionized water is poured into the copper pipe, the temperature of the evaporator and condenser are balanced. A direct representation of the PHP's operation may be seen in the temperature fluctuation of the evaporator and condenser sections on the same pipe. The three distinct steps involved in executing an operation on PHP are illustrated by figure 3.3.4, which indicates the current temperature of the process. When the first temperature oscillations are over and the temperature differential between the PHP's evaporation and condenser sections abruptly spikes, the system enters a quasi-steady oscillation phase. As the name implies, steady-state functioning is defined by stable oscillation, little temperature differential, and high oscillation frequency.

3.3.5 Surface Area Response Modelling:

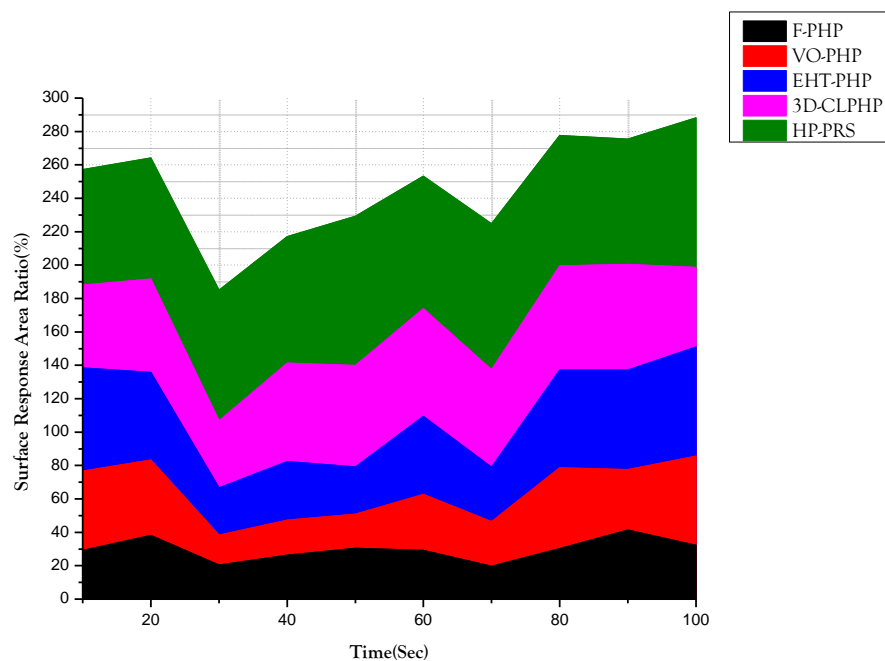


Figure 3.3.5 Surface Area Response Modelling

The optimization and minimization of the PHP's THR are very conditional on the operating conditions and concentration profile, as shown in the previous sections. As a result, optimizing PHP's operation through a battery of trials was a costly and laborious process. Therefore, a response surface technique model was developed to ascertain the impact of operating conditions on PHP's thermal performance. Reducing the time and money spent on experiments is one of the main goals of an RSM model. The current study includes the development and introduction of input parameters at three levels: low, center, and high bounds.

Graphene oxide and other Nano-suspensions are quite costly, and preparing them takes a lot of time and involves stability tests and characterizations. Therefore, equations derived from costly experiments are one-of-a-kind and useful for developing preliminary models in the absence of such trials. The experiments presented here are supported by the suggested model developed here.

3.4 Conclusion:

The present research utilized a battery of tests to assess the reaction and functionality of a PHP system that utilized graphene Nano platelets under diverse operational circumstances, such as varying applied heat values, concentrations of GNPs, ratios of filling and temperatures of the condenser. According to the findings, the filling ratio had no effect on PHP speed. But when the condenser temperature and this parameter were both optimized, the PRS model showed that they work together to decrease the THR value. Both the concentration and the amount of heat supplied were critical operational parameters that determined the PHP's efficacy. While increasing the concentration of graphene Nano platelets did not improve the thermal performance of the PHP, adding more heat to the evaporator had a multiplicative effect. The pipes are not at a right angle, the heat is evenly distributed, the oscillation mode is marked by abrupt changes, and the PHP shows very little resistance to heat. Further, the shape of the heat distribution is unaffected by the inclination angle during gravity-assisted circulation of the working fluid, but the way in which temperatures oscillate is. When subjected to gravity-inhibited circulation at angles larger than 90 degrees, a single tube exhibits small-amplitude oscillations and a homogenous temperature distribution. By filling them with water, we assessed the heat exchangers' performance. Here, we introduce HP-PRS, a method for calculating heat exchanger efficiency by means of heat pipes equipped with pulsing response surfaces. The outcome is a strong thermal

resistance for this mode. A symmetrical distribution of heat exists even when the angle is one degree. But it seems like the way things are done doesn't change too often. At this very moment, the PHP has the lowest heat transmission resistance. We can find out how different materials with different wettability behave thermally by doing numerical simulations. When surfaces are wet or dry, the advancing and retreating angles change, which in turn affects the capillary resistance. Since the resistance increases as the number of liquid plugs increases, more hydrophobic plugs, as opposed to more hydrophilic ones, will result in a higher capillary resistance.

MICROFLUIDICS TEMPERATURE COMPENSATION AND TRACKING FOR DRUG INJECTION BASED ON MECHANICALLY PULSATING HEAT EXCHANGER

The remainder of the research is organised in the following manner. Section 4.1 indicates the background to the temperature measurement in microfluidics. The proposed Microfluidics Temperature Compensation and Tracking Method (MFTCTM) is designed and analysed in section 4.2. Section 4.3 illustrates the simulation analysis and the findings of the study. The conclusion and the findings of the research are shown in section 4.4.

4.1 Background to the temperature measurement in microfluidics

Including sample collection, processing, and storing, sample processing, signal conversion and enhancement, mechanical sensing, and power providing, well-designed microfluidic systems may achieve great multiple functionalities in wearable technology. Furthermore, wearable microfluidic gadgets have shown potential uses in clinical evaluation, monitoring of wellness, and communication between intelligent gadgets and people. This study primarily concentrates on the general functionalities and architectures of multipurpose wearable technology based on microfluidic gadgets, as well as their specific implementations in physiological signal surveillance, clinical diagnostics and treatments, and healthcare [45].

The research created a microfluidic device with high-precision platinum (Pt) thermo-sensor integrated that can cultivate cells and track the temperatures of the cells in real-time [151]. A fixed temperature system with 0.015 °C of reliability was used during the detection process. The Pt thermo-temperature sensor's coefficients of impedance were 2090 ppm/°C, giving it a temperature precision of less than 0.008 °C. As a result, the thermo gravimetric microchip combined with tissue culture may be a non-disposable and label-free instrument for tracking cellular temperatures used in the research of physiology and disease.

To examine algal development under various culture settings, the research offers gradient-based microfluidic devices [115]. Using the gadget it gives the chance to create droplets with various medium nutrient availability in 200 seconds, saving the time and reagent from having to prepare these solutions the traditional way. The system is

regarded as the third attempt to use a gradient chip in the field of algae biotechnology. It is exceptional, easy to use, and produces very competent outcomes.

The research created a portable microfluidic device that combines Repressor Polymerase Multiplication (RPM) with a person's body heat for an easy and quick multiplication of HIV-1 DNA [72]. In the ambient setting, the normal body temperatures at the wrist ranged between 33 and 34 °C, which is suitable for RPM responses. This device consistently identified HIV-1 DNA in the range of 102 to 105 copies/mL with a log predictability of 0.98 in 24 minutes using a cellphone-based fluorescent detection approach. These findings show that in terms of speed, mobility, and electricity autonomy, this wearing Point-Of-Care (POC) nucleic acid monitoring approach outperforms conventional PCR and alternative isothermal polymerase chain reaction PCR techniques.

This study discusses a variety of microfluidic techniques, including culturing and tracking adhering and non-adherent cells, as well as several microfluidic device characteristics [49]. The paper compares the systems that are now accessible with high throughput research, automation capabilities, interface to devices, and connectivity. Factors, such as the operating adaptability of the gadgets, are assessed in terms of their diagnostic effectiveness. Advanced microfluidics' ability to perform multiple functions has led to the discovery that a significant amount of scientific results can be obtained from a single system, enabling complex innovative power and effective data correlation—both of which are crucial when considering biomedical research.

For temperature control in microfluidic devices, the research provides a modular, adaptable, and self-sufficient convection heat transfer [153]. The heat transfer is made of polymeric tubes that are totally immersed in elastomer blocks and wound around with a polymer pole to be installed into the microfluidic chip with ease. It works with a variety of microfluidic substrates and geometries. To move the heat-carrying fluid through heat transfer at the necessary fluid velocity and heat, miniature, battery-powered vibrating pumps are used.

The research describes a sensor device to track the oxygen intake by mammalian cells as a direct signal for metabolism while taking the needs for utilization in Bio labs into account [38]. This entails accurate oxygen sensing, a compact configuration devoid of complex external apparatus, the use of appropriate components, and the capacity to achieve a high level of connectivity and robotics. A system that comprises heaters, a

temperature probe, external optical reading, a hydrodynamic chip with an embedded oxygen-sensitive phosphors layer, 3D-printed supports, and an enclosure satisfies these criteria.

To achieve accurate and quick temperature management in the region between 2°C and 37 °C, a combined microfluidic gadget with active components for cooling and warming was designed [106]. The system, which was made up of a desiccator, a micro heater, and a temperature probe, managed to change the local heat on the chip actively through responses. The linked modelling of heat transmission, flow properties, and Heat conduction involved multiphysics simulations. The design parameters for achieving precise and rapid control of on-chip local thermal control were confirmed by the simulation and modelling methods.

The production of materials with nano- or micro scale dimensions has been a research priority for many years, and the development of microfluidic techniques offers alternate methods for doing so [85]. The latest events in the manufacture of nanoormicrosized nanoparticles with specified characteristics employing various Microfluidics (MDs), including continuously laminar flow, segmented stream, droplet-based, and other non-chip centred micro reactors, are discussed, along with their biological implications.

Quick halide transfer of inorganic polycrystalline nanocrystals is described in a simple room-temperature method [19]. Using a flexible microfluidic technology called the Quantum Dot Exchanger, the research isolates reaction percentage from precursor mixing rates to offer a thorough knowledge of the halide transfer processes. On the pace and scope of the halide exchange processes, the impacts of ligand content and the origin of the halogen salt are demonstrated.

Omar Abu Arqub et al. (2014) detailed to enable to efficiently solve systems of second-order boundary value problems, that work introduces the continuous Genetic Algorithm (GA), which relies on smooth solution curves throughout its evolutionary process in order to get the necessary nodal values of the unknown variables [28]. Nodal values provided by genetic operators are used to transform the challenge of solving the system of differential equations into one of minimizing the global residue or optimizing the fitness function. In degree to solve systems of second-order boundary value problems, the suggested approach is shown to be a reliable and precise technique by the numerical results.

Zaer Abo-Hammour, et al. (2014) introduced the optimization approach, the continuous genetic algorithm, for numerically approximating the solutions to Troesch's and Bratu's problems [20]. To begin with, it should not need more complex mathematical tools; that is, the algorithm should be easy to comprehend and apply, and therefore readily accepted in the mathematical and physical application sectors. Second, in terms of the answers found and its capacity to handle other mathematical and physical issues, the algorithm is of global character. Third, the suggested approach has an implied parallel aspect, implying that it would be implemented on parallel computers.

Emad H. M. Zahran et al. (2023) examined the major goal of this research was to generate a large number of novel forms of soliton solutions for the Radhakrishnan-Kundu-Lakshmanan equation, that depicts unstable optical solitons that originate from optical propagations using birefringent fibers [148]. These novel forms were discovered using four separate techniques: the extended simple equation method, the Paul-Painlevé approach method, the Riccati-Bernoulli-sub ODE method, and the solitary wave ansatz method. The novel solitons can be assembled to produce a soliton catalogue with new amazing characteristics, and can contribute to future research not just for this model but also for optical propagations via birefringent fiber.

According to the analysis of the literature, microfluidics research has temperature measurements. However, many lack short of expectations of performance and precision. In an effort to facilitate drug injection, a better method is created to account for and monitor the temperatures in microfluidics.

4.2 Proposed Microfluidics Temperature Compensation and Tracking Method

This section deals with the working principle, material selection process, fabrication process, thermal flow meter characterization setup for analysis, and parameters for numerical analysis are discussed in this section.

4.2.1 Working principle and design

Steady Power and Steady Temperatures are the two separate sensing methods used by the current flow meter. The heating temperature is measured using the Continuous Power (CP) method, while the heating power is kept constant. The amount of liquid or gas that passes through a pipeline in a certain amount of time is measured by a flow meter. Flow meters, measuring flow rates, provide essential insight into material is flowing across pipes, drainage systems, and other forms of infrastructure. Due to the

increasing heat exchange, the heating temperature drops as the flow rate rises. Equation (4.2.1) shows a description of a one-dimensional concept of the heating temperatures.

$$T_h = \frac{h_p}{k_t w_h \left(\frac{l_t}{\alpha} + \sqrt{4k + \frac{v\sigma^2}{4b^2}} \right)} \quad (4.2.1)$$

where T_h denotes the temperature of the heating element, h_p denotes the heat output, k_t denotes the heat capacity of the liquid, w_h denotes the heater's thickness, and l_t denotes its length, α denotes the width of the boundary surface, v denotes the average flow rate, b denotes the fluid's diffusion coefficient, and k denotes the incompressible component, the thermoelectric undertake Even though the heater's impedance changes a little bit according to the flow speed, it is safe to presume that the overall power stays constant. The right-hand side of Equation (4.2.1) is therefore constant, except v , \sqrt{v} has an inverse relationship with T_h .

In Continuous Temperature (CT) mode, the exterior electrical circuit modifies the current to maintain a consistent resistance (heat) of the heat source [28]. To account for heat transfer and sustain the temperatures, the warming power must rise as the flow rate does. Equation (4.2.1) is used to represent a one-dimensional model of heat load, where T_h is steady and P is proportionate to \sqrt{v} . The little membrane that surrounds the heater reduces the k component, lowering the amount of P and T_h needed to retain responsiveness. Additionally, the tiny heat capability has the benefit of shortening the time it takes to attain a steady state, producing a quick response time.

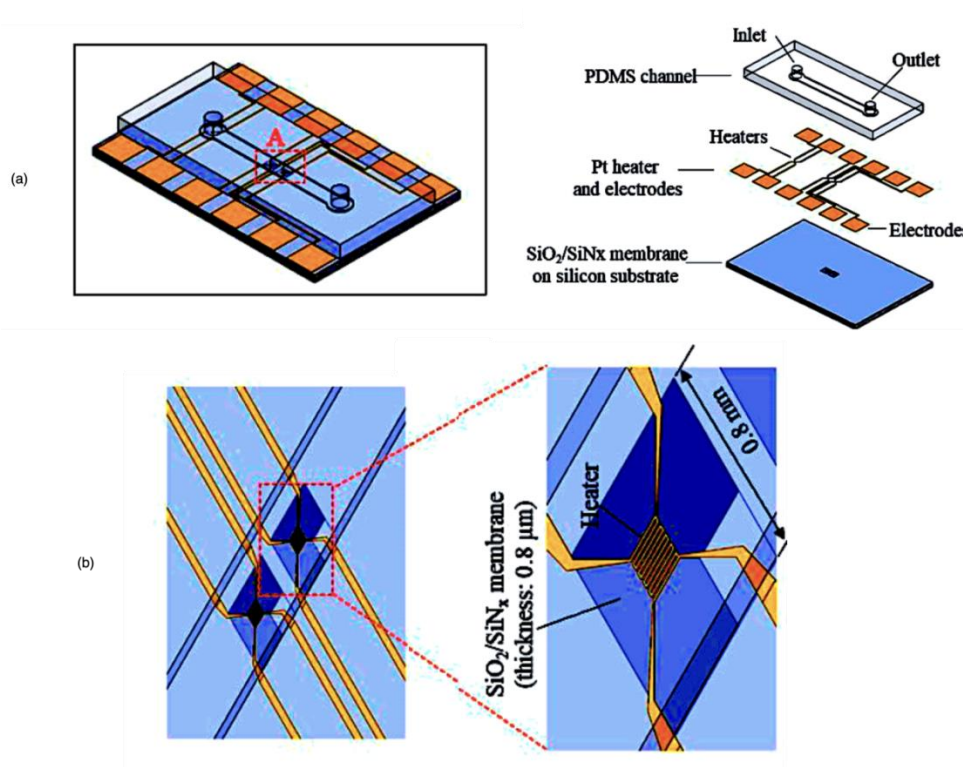


Figure. 4.2.1. The design and working process of the flow meter

The design and working process of the flow meter is denoted in Fig. 4.2.1. The basic architecture is shown in Fig. 4.2.1(a), and the substrate view is shown in Fig. 4.2.1(b), respectively. A platinum (Pt) covering with warmers and poles, a Polydimethylsiloxane (PDMS) channels layer, and silicon substrates with a silicate dioxide/silicon nitrogen (SiO₂/SiN_x) membrane make up the flow rate. Each radiator is situated on the 800x800x0.8 mm silicone SiO₂/SiN_x membranes. Due to its great sensibility for flow monitoring, the membranes only permit the transmission of heat to the liquid and not to the substrates. To have a rapid reaction period and great responsiveness, membranes that are smaller and wider are preferable. To reduce heat circulation through the platform and increase heat convection via the liquid, the researchers chose a membrane width of 0.8 mm, which is more than 500 times narrower than the silicon substrates. Additionally, this concept's ultralow thermal capability allows for a substantial reduction in the reaction period. The research created films that were 600 μm, 800 μm, and 1000 μm broad to find the ideal membrane thickness (data not shown). The research discovered that an 800-μm-widemembrane was the best flow meter foundation because a 1000-μm-widemembrane had poor manufacturing yield and inconsistent physical endurance during the flow assessment.

This configuration can complement the stress concentration (compressive pressure for the SiO₂ and compressive strength pressure for the SiN_x) for the robust physical features and flat morphological attributes of the tissue. The structure of the membrane phase included 150 nm-thick SiN_x wedged by 300 nm and 350 nm-thick SiO₂ tiers. A Mechanically Pulsating Heat Exchanger on either side act as a benchmark sensor for fluid temperature measurement upstream and downstream. To function in constant energy or fixed temperature mode, the burner in the centre acts as a flow-sensing component. The heater is made up of serpentine electrical wiring with a width of 10 μm and a total dimension of 0.19 mm by 0.20 mm. The heating may function as both a warmer and a temperature probe since it is linked to four electrical wires for 4-wire remotely sensed. The PDMS channel has a width of 0.5 mm or 1.5 mm and a height of 100 μm. The 0.5 mm-wide thin stream was chosen because it would completely cover the heating surface with 190 μm-widths. Then, to study the impact of bandwidth, a 1.5 mm wide channel was selected, making it three times broader than the narrow strait [20]. Due to the simplicity of production while utilizing SU-8 2050, 0.1 mm for the channel height was ultimately chosen. A critical design consideration, too-low fluid flow lowers flow meter accuracy and a 0.1 mm canal height demonstrated a velocity distribution of at least 10 mm/h at a 0.5 g/h flow rate. The microchannel has inlet/outlet apertures on both sides and is 10 mm long overall. The platform has an overall dimension of 11.5 mm in width, 17.5 mm in height, and 1.5 mm in depth.

4.2.2 Material selection

The best material to use to create adaptable fluidic and heat flux devices is thermoplastics. Their benefits over say different metals include their physical strength-to-mass ratio, corrosion immunity, stretchability, the simplicity with which an almost infinite range of complicated forms and shapes may be created, and their complete recyclability. Their employment in heat exchange and thermal managing systems, nonetheless, may be compromised by their comparatively poor heat capacity and melting temperatures.

The following parameters were used to determine which synthetic polymers would be best for creating fluidic gadgets: The following requirements must be met: (i) physical flexibility; (ii) chemical compliance with a variety of fluids, including freshwater, silicone lubricants, acidic and alkaline solutions, and coolants; (iii) maximum continual service temperatures of 120°C; and (iv) abrasive resistance [23]. Polyethylene was chosen as a suitable material for the aforementioned requirements. Black polymer strips with the

channels of the microfluidic devices cut out of them were then placed between two translucent polypropylene sheets, which were joined to the black sheet by selective transfer welding processes.

4.2.3 Laser cutting

The polypropylene strips were cut into the forms necessary to construct the different "fluid and heat flux devices" using an LS1290 PRO CO₂ laser engraver with a maximal output of 80 W. Numerous factors, including cutting force, cutting edge hardness, slag, and the breadth of the heat impacted zone, influence cutting quality. The kerf breadth, which must be as tiny as feasible, is the most important variable.

Trial and error were used to find the cutting settings. Specifically, the chopping head velocity was 20 mm/s, the stand-off range was 0.5 mm, and the laser energy was kept at 90% of the maximum output (72 W). Machining was done repeatedly during engraving, eliminating around 0.1 mm of substance each time, to increase the cutting-edge polish. After slicing, abrasive material was employed to polish the surface and clean out any dust, slag, or debris from the edge of the plastic that might have impacted the quality of the weld.

4.2.4 Fabrication process

A silicon wafer with a diameter of 6 inches and a thickness of 500 μm was used to begin manufacturing. The P-type, (100)-oriented, 6-inch silicon wafer had 500 μm of thickness and was 500 μm wide. Firstly, silicon chip sheets of SiO₂ and SiN_x (300 nm of SiO₂ and 150 nm of SiN) were created by Low-Pressure Chemistry Vapor Deposits (LPCVD) at temperatures of 600 °C for SiO and >700 °C for SiN_x, correspondingly [24]. After that, 20 nm/200 nm thick films of titanium (Ti)/Pt were formed (by hydrothermal method) and shaped using lift-off and standard photolithography. To provide galvanic isolation for the warmers, a second SiO₂ film (350 nm thick) was formed by Plasma-Enhanced Chemistry Vapour Device (PECVD) and structured. To prevent damaging impacts on the metallic surface at warm altitudes (750 °C) during the LPCVD procedure, the SiO₂ layers were formed during the PECVD procedure at a low heat (150 °C).

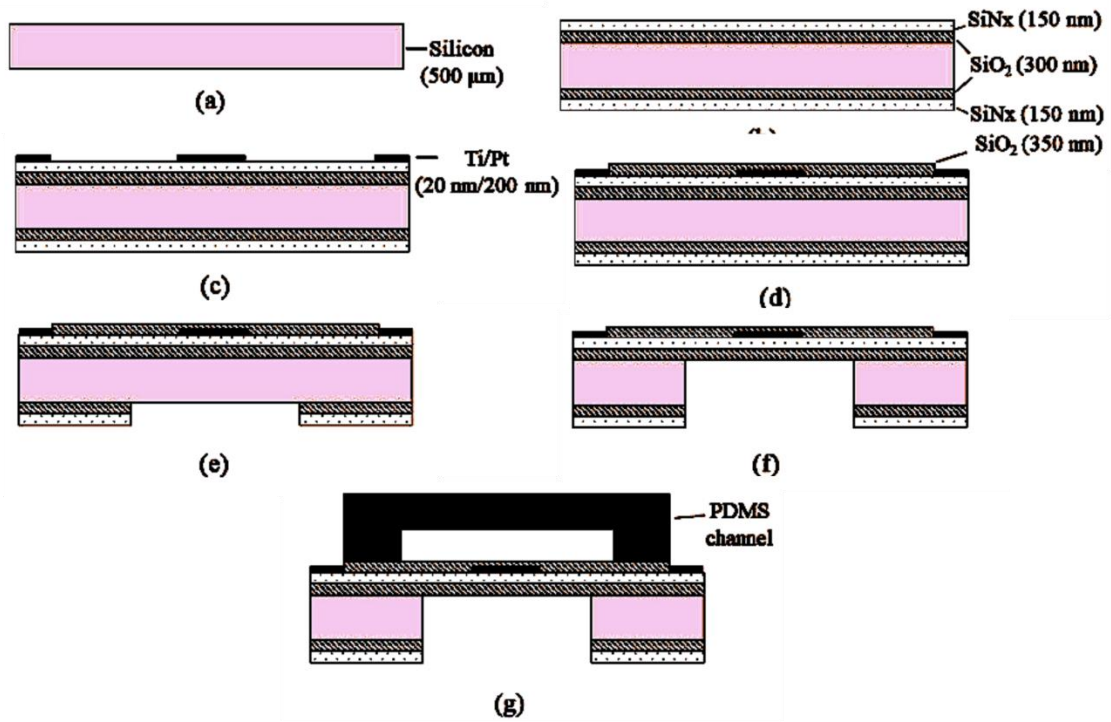


Figure. 4.2.2 The fabrication process of the flowmeter

The fabrication process of the flow meter is denoted in Fig. 4.2.2. The silicon metal (a), the SiO₂/SiN₂ layer (b), Ti/Pt layer (c), PECVD layer (d), etched wafer (e), coated wafer (f) and final flow meter (g) are shown in different figures. Then, to provide a channel for the extensive etching procedure of the silicon wafer, the reverse SiO₂/SiN_x was etched. Shallow Reactive-Ion Etching was used after a silicon profound etching to produce a mucosal coating. Using a slicing saw, the completed wafers were then cut into unit components.

The conduit was created using SU-8 negative lithography and a PDMS micro-moulding process. In a nutshell, using a traditional photoresist, SU-8 with a 100 μm thickness was printed onto the 4-inch silicon chip and utilized as a mould. The next step was to create PDMS by combining a base and hardener in 10:1 weight ratios. PDMS was put into the mould and dried on the hot plate (100 °C for 15 min.) after refluxing the solution in a vacuum chamber for 10 min. Following oxygen laser irradiation, the PDMS down a part was subsequently attached to the unit gadget.

4.2.5 Thermal flow meter characterization setup

The water flow was produced by external air density acting on the water tank. The flow rate was managed with a Mass Flow Controller (MFC) called a Bronkhorst micro Cori-flow M120. Water is flowing evenly from the MFC via the flow meter and

onto the scale mechanism. To prevent liquid from evaporating while the measurements were being taken, an evaporating trap was put on the collection glasses. Fluorinated Ethylene Polypropylene (FEP) tubing was used to link every component of the system. At the scales, the piping was attached to the needles. To prevent droplet development and enable a continuous measuring of the flow rate as time passed, the tip of the needles was submerged in the liquid in the gathering glass container.

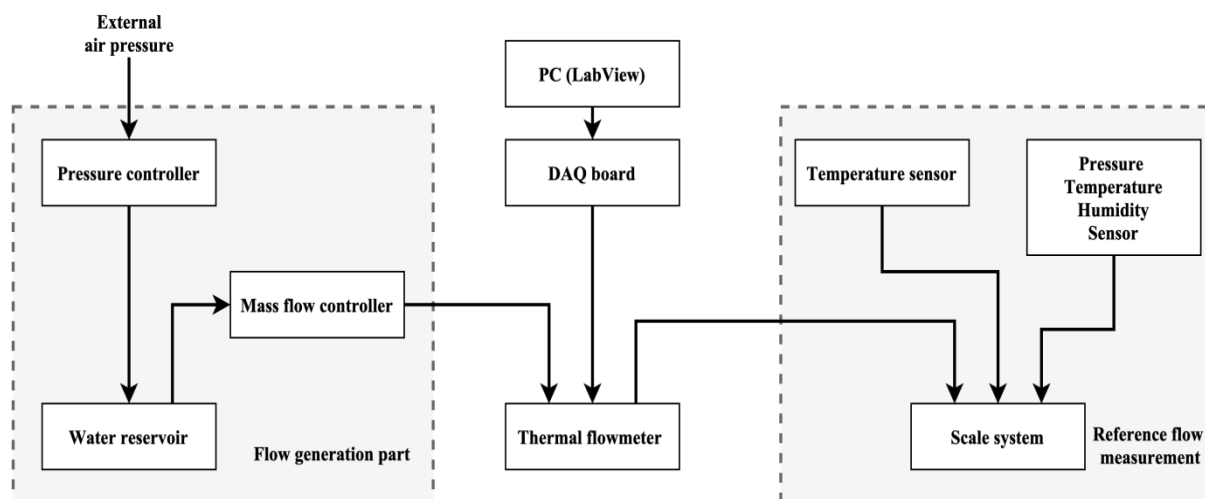


Figure. 4.2.3 The setup connection for flow meter-based temperature compensation and measurement

The setup connection for flow meter-based temperature compensation and measurement of the microfluidics is shown in Fig. 3. The block has a flow generation part and reference flow measurement modules are used to measure and compensate the temperature of microfluidics. For the flow measuring characterisation, four heater terminals on the flow meter were electronically linked to a Source Measurement Device. The supplied current was managed by a customised Lab VIEW application, which also kept track of the flow meter's electrical output. The temperature across the radiator was taken to determine heater impedance, and the electrical flow for CP mode was set at 3 mA. While the current flowing was beneficial for getting good sensitivity, there was a higher chance of bubble production owing to warming, particularly at a lower flow rate. Nevertheless, in CT mode, incoming power was detected and a closed-loop feedback mechanism regulated the flow to keep the impedance 3 greater than the impedance at room temperature.

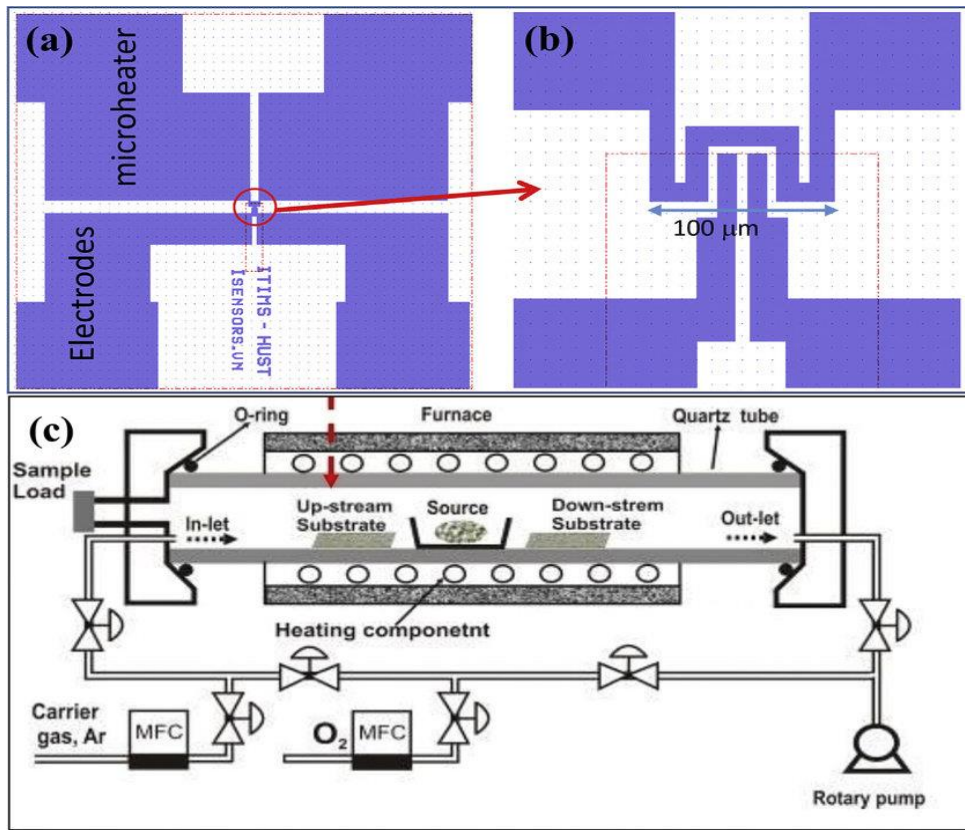


Figure 4.2.4 chips and design

The temperature-dependent PCR chip is used to validate the physical structure before carrying out the numerical optimizing research. Here, the research describes a design for an S-shaped micro-channel that includes two inlets for two flows of reagent introduction. The micro channel is made up of a 100 m wide by 30 m deep rectangle-shaped cross-section tube with an S-shaped unit in the middle that helps the reagent mix more uniformly. Well before exit, there is a circle observation area on the linear micro channel, and there is just one outflow upstream for subsequent processing.

The glass slide is given a 20-minute soak in acetone, followed by 15-second rinses in rubbing alcohol and DI freshwater and final air-drying. After being plasma treated by a plasma generator, the previously described PDMS block adheres to a glass plate. Four phases make up the plasma therapy and bonding process:

- a. Insert a glass slide that has been polished and a PDMS block with the side of the channel visible into the plasma binding device.
- b. Vacuum the apparatus to a value of roughly 100 Kpa of tension.
- c. Start a 40-second plasma live electrical explosion.

d. Remove the PDMS blocks and quickly bind them to the microscope slide to prevent surface conformational changes or contamination.

4.2.6 Temperature calibration and solution delivery

The microfluidic device is heated using a translucent toughened glass warmer and has a temperature inaccuracy of 0.1 °C. The impedance temperature heat controller is glued into the through-hole of the PDMS block and contains molten material to monitor the heat of the glassy slide's top part and store the information. To monitor and store the temperature readings of the convection cells, a high-precision thermostatic thermal sensor is placed inside the micro channels. The thermal link between the two discussed above is then taken into account when creating a compensating function. The functional computation indicates that it is possible to describe the temperatures of the micro fluid without using precision heating sensors by measuring the heat of the glass plate.

A PCR amplification research that was extremely temperature-sensitive is provided to evaluate the effectiveness of measuring temperature. Thus, a flow pattern is created at the very start of the chip by pumping two streams of water solution via the inlets with distinct, separately regulated programmed flow controllers. The S-shaped tube is then filled with laminar fluids to provide better reagent interaction. The heater is precisely calibrated to a predetermined heat and runs for 20 minutes once the fluid has filled the platform. Then use a microscope to study the fluorescence impact in the region upstream of the micro-channels.

4.3 Numerical analyses

The numerical analysis setup and the parameters are discussed in the following subsection.

4.3.1 Control Equation and Boundary Condition Settings

For modelling, the mechanical field components of the occurrences and solids and liquids heat exchange are employed. Assuming that all heat transmission between solids and liquids occurs in this way, the [energy-saving expression is shown in Equation 4.3.1](#).

$$\rho \times V \times C_p \times \frac{dT}{dt} + \nabla(-V \times k \times \nabla T) = Q_o \quad (4.3.1)$$

where k is the thermal conductance, V is the area of the warmed item, C_p is the capacitor evaluated at steady pressures, and Q_o is the rate at which energy is produced across the whole system. Material intensity is denoted ρ .

A steady energy P_o and a status indication State Heater (specified in the Event interfaces) are chosen as thermal power sources to replicate the heater's heat regulation, and the electricity creation rate is adjusted using Equation (4.3.2).

$$Q_o = P_o \times S_h \quad (4.3.2)$$

S_h denoted the state heater, and the steady energy is indicated P_o . Given that thermal protection is expected to cover the heater's bottom, the boundary requirement is specified using Equation (4.3.3).

$$n(-k \times \nabla T) = h_c(T - T_o) \quad (4.3.3)$$

T_o is the outside temperatures and h_c is the heat flow ratio for natural circulation. The plank/s constant is denoted k , the present temperature is denoted T , and the temperature deviation is denoted ∇T . The system's radiative heat flow to the environment can be adjusted using Equation (4.3.4).

$$n(-k \times \nabla T) = \tau \rho (T^k - T_o^k); \text{ where } k = 4 \quad (4.3.4)$$

The temperature of the microfluidics is denoted T , the channel length is denoted n , and the deviation is denoted ∇T . τ denotes the material's transmittance, $0 < \rho < 1$, and σ denotes the Stefan-Boltzmann constants. Among the heating mantle and the glass slides, there is interface heat loss that mostly consists of contacting and spacing heat capacity, which is represented in Equation (4.3.5).

$$n(-k \times \nabla T) = h(T_d - T_u) + \frac{rQ_o}{A_d} \quad (4.3.5)$$

The temperature capacity is denoted T_d , the compensated temperature is denoted T_u , and r is the heat partition coefficient. The generated energy is denoted Q_o , the gain is denoted A_d , and the heat coefficient is denoted h . The heat coefficient is indicated in Equation (4.3.6).

$$h = h_c + h_g \quad (4.3.6)$$

The contact and gap heat are expressed h_c and h_g . The surface smoothness, micro-hardness, and contacting pressure of the substance are all strongly correlated with

the heat transport ratio of heat transfer impedance. The contact heat of the flowmeter is denoted in Equation (4.3.7).

$$h_c = 1.25k \times \frac{m_a}{\alpha_a} (P/H_c)^{0.85} \quad (4.3.7)$$

where the asperities mean slopes and elevation surface smoothness are, correspondingly, m_a and α_a is the heat conductance of the substances in interaction. P is the contact force between the glass sliding and the burner. The glass's hardness value is H_c . The gap heat is constant and the value is fixed for the experimental analysis.

The kind of gas and contact temperature among two touching objects affect the separation heat impedance. Although the value range may be tested, there is currently no dedicated expression method.

4.3.2 Parameter settings in the simulation

Here, the research did not suggest a real 3D model to compute the heat transfer procedure because the 3D model's architecture is quite regular and has comparable abutments. The research has provided a 2D numerical model of a transverse cross contour for clarity. COMSOL Multiphysics 5.4, a piece of finite element technology, is used to run the thermal transfer simulation. A discontinuous grid for the simulation study, several domains and border elements in various element widths, and grid-independent testing are all provided in the Supplementary Materials along with convergence solution techniques.

This section discusses the design and working principle of the flow meter to compensate for and measure the temperature of microfluidics in drug injection applications. The mathematical model helps to produce results with higher accuracy.

4.4 Result and discussion:

Platinum (Pt) impedance sensors use contact conductivity and energy to monitor temperature signals. The ability of ambient materials put close to the detector to transmit heat has a big impact on how response signals are picked up. The Pt sensor is first placed directly into the hole, brought as near to making touch with the surface of the glassy slides as feasible, and then sealed with gel. For example, setting the goal temperatures to 60 C and having the hole's diameter twice as large as the sensor's. The 2D microfluidic microchip heat exchange system's thermal variation is depicted numerically.

The glass surface temperature analysis of the proposed MFTCTM is shown in Fig. 5. The simulation analysis is done by varying the test temperature from 30°C to 100°C, and the respective glass surface temperature of the flow meter is then analysed and measured. The microfluidic temperature and the glass surface temperature are directly related to each other. The glass surface temperature increases when the microfluidic temperature rises above some threshold value. The mechanically pulsating heat exchanger compensates for the heat and thus helps in drug injection applications to reduce body heat using microfluidics.

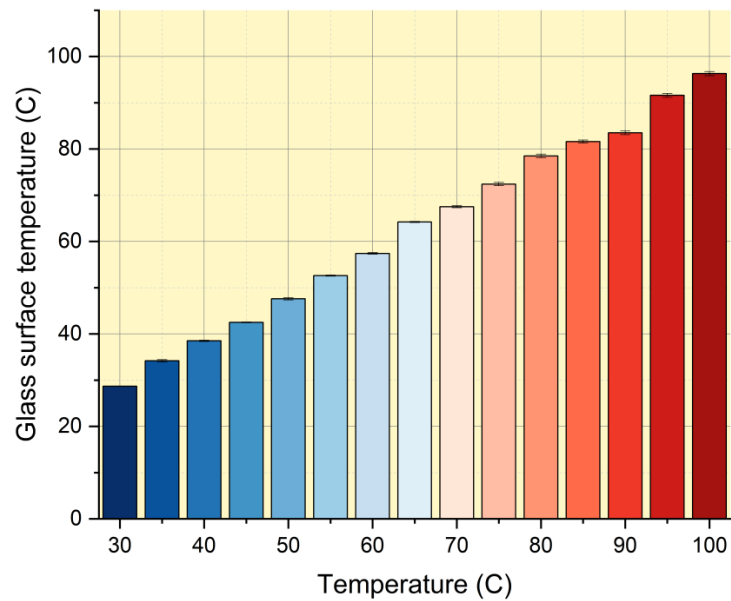


Figure. 4.4.1 Glass surface temperature analysis

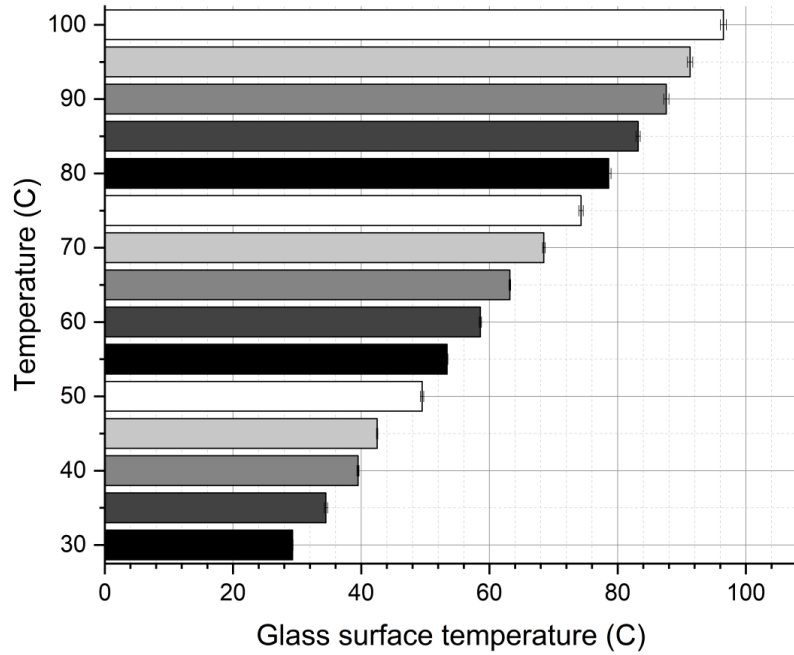


Figure. 4.4.2 Glass surface temperature analysis under the microfluidics condition

The glass surface temperature analysis under the microfluidics condition is analysed, and the results are plotted in Fig. 6. The variation in the temperature of the microfluidics concerning the body temperature is computed, and the results show a linear relationship between those temperatures. The designed mechanically pulsating heat exchanger compensates for body temperature and helps reduce the microfluidics temperature in drug injection applications. The results show that the MFTCTM is the most accurate way to measure and adjust the temperatures in microfluidic systems.

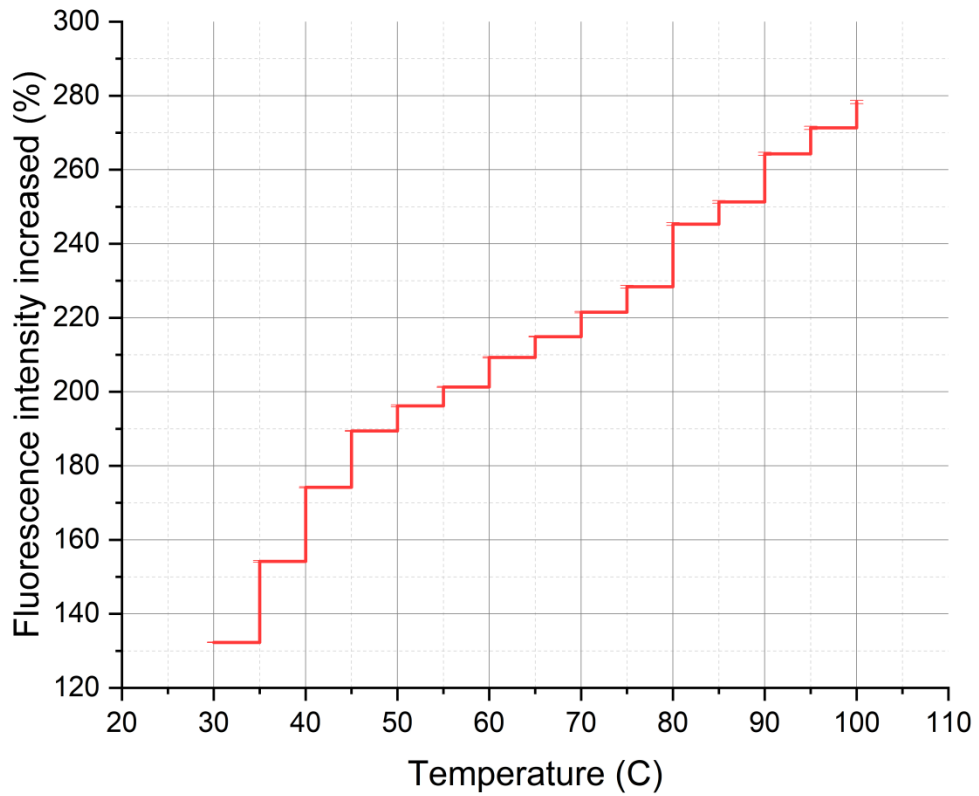


Figure.4.4.3. The increased fluorescence intensity analysis

In Fig. 4.4.3, the increased fluorescence intensity analysis of microfluidics concerning temperature is analysed and plotted. As the microfluidics temperature increases, the fluorescence intensity in the flow meter increases, which results in the highest compensation. The MFTCTM shows the highest detection because of the optimum structure of the flow meter and the materials used for its construction. The intensity results are analysed from 30°C to 100°C with a step count of 10°C, which ensures the performance of the mechanically pulsating heat exchanger in all the temperature variations.

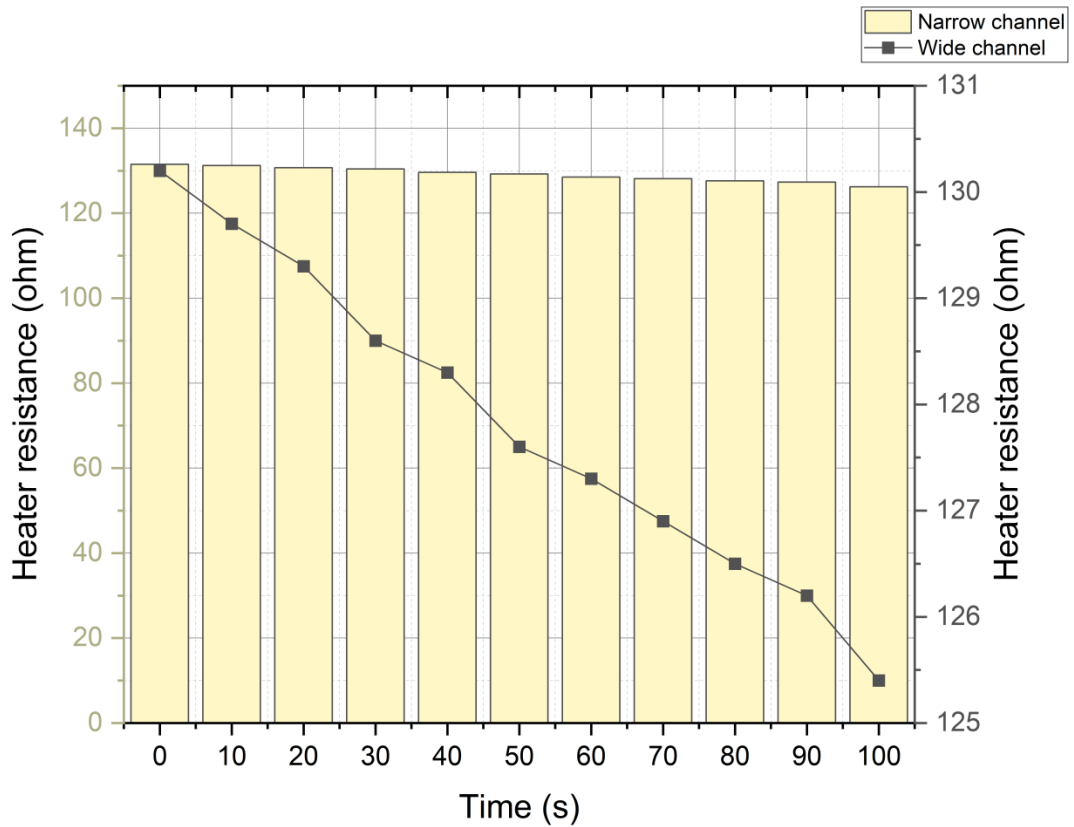


Figure. 4.4.4 Heater resistance analysis of the proposed system

The mechanically pulsating heat exchanger performance is analysed in microfluidics, and the results are plotted in Fig. 4.4.4. The analysis is done by varying the channel width in two conditions, such as a narrow channel and a wide channel. The heater's resistance to temperature is directly related to the channel width. The narrow channel has lower resistance, whereas the wider channel has higher resistance. The heater resistance is analysed concerning the timing variations. As time goes on, the resistance of both narrow and wide channels also reduces.

The heater power is calculated for the mechanically pulsating heat exchanger, and Fig. 9 displays the findings about time variation. The respective power provided by the mechanically pulsating heat exchanger grows as time passes. In the study, both the narrow channel and the large channel are evaluated. The findings indicate that the narrow channel functions effectively and generates more energy than the broad channel. The outcomes are further improved by the choice of materials and production methods.

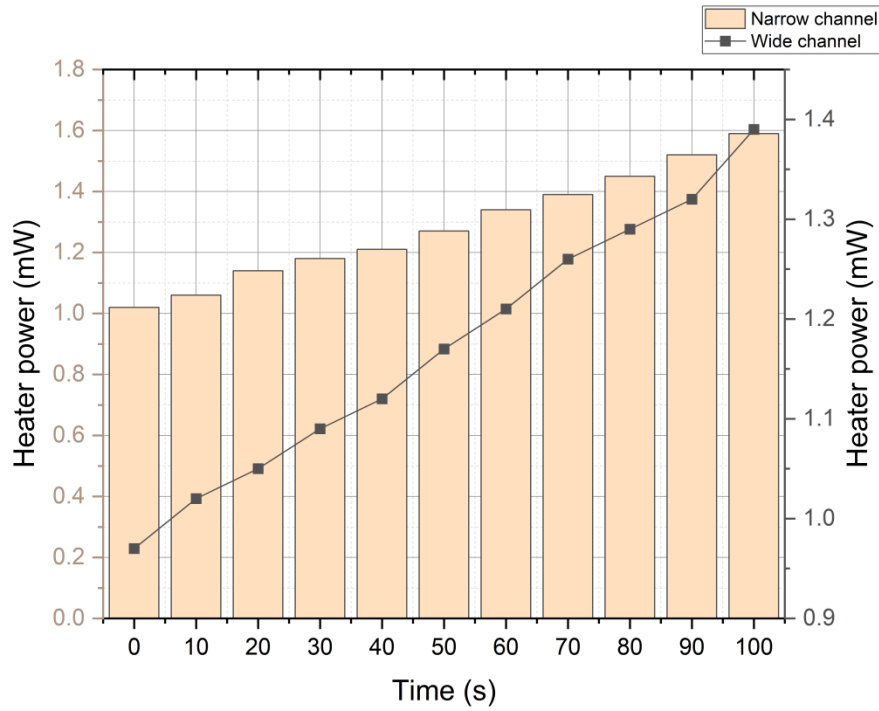


Figure. 4.4.5 Heater power analysis of the Mechanically Pulsating Heat Exchanger

The results of the flow rate analysis of the mechanically pulsating heat exchanger-based flow meter to detect and correct the microfluidics temperature are displayed in Table 4.4.1 for various conditions. The heat resistance and heater power for various flow rates are analysed, and the results are summarized. The findings guarantee the rise in terms of heater resistance and heater power about the increase in flow rate. Utilizing a mechanically pulsating heat exchanger, the suggested system achieves more accurate temperature monitoring and adjustment in microfluidics.

Table 4.4.1 Flow rate analysis of the Mechanically Pulsating Heat Exchanger based flowmeter

Flow rate (g/h)	Heater resistance (ohm)		Heater power (mW)	
	Narrow channel	Wide channel	Narrow channel	Wide channel
0.5	131.5	131.1	1.1	0.7
1	130.4	130.4	1.6	1.2
1.5	130.1	129.7	2.1	1.4
2	129.8	129.2	2.4	1.6
2.5	129.7	128.2	2.7	1.8
3	129.3	127.5	3.1	1.9

4.5 Conclusion:

Micro-machining is used to develop and construct a MEMS flow meter with a microfluidic tunnel to monitor low flow rates for infusion-pump validation. A silicon substrate, a Pt heating film atop a SiO/SiN small membrane, and a PDMS mould with dimensions of 11.5 mm (widths) and 17.5 mm (lengths) 3 mm made up the MEMS flow meter (heights). The flow meter's efficiency is assessed using the conventional GM in two distinct modes (the CP and CT variants) and 2 distinct channel lengths (0.5 mm and 1.5 mm). In the 0.5-2.5 g/h range, the measurement system in CT function with a 0.5 mm-wide channel exhibits the best efficiency, with an inaccuracy that is five times lower than that of conventional portable infusing pumps. To examine the interaction between the glass substrates of a conventional microfluidic system and the microfluidics, a heat exchange simulation was provided using a Mechanically Pulsating Heat Exchanger. The millimetre-scale commercial heating element might be used for temperature detection of micro-scale liquids thanks to an intelligent building system and fluid metals. The technique gets over the problems with thermal monitoring for microfluidics. From 30 °C to 100 °C, the linear trend spectrum of observed temperature is shown, and the uncertainty error is less than 0.5 °C. The thermal precision of this technique has also been clarified by temperature-sensitive amplification tests using nucleic acids. Consequently, it can be inferred that this technique has great promise for micro-macro interaction detection and is useful for purposes beyond microfluidic ones. Microfluidic devices offer an appropriate regulated environment for cell cultivation and drug testing on a broad range of cells, like cancer, liver, and microbial. The regulated atmosphere permits the observation of cell cultures over lengthy periods of time. Thermal resistance is a measure of heat flow resistance across a certain thickness of material. Thermal resistance is calculated by dividing a sample's thickness by its thermal conductivity. Electrical resistance, or resistance to electricity, is a force that opposes the passage of current. In this manner, it indicates the challenge it is for current to flow. Resistance values are measured in ohms.

MICROFLUIDIC SYSTEMS WITH A PULSATING HEAT PIPE

In this chapter, a detailed analysis of numerous new theoretical and practical investigations on the thermal and flow properties of pulsating heat pipes constructed of flat plates and two-phase flows in rectangular mini- and micro channels is presented.

The main significant contributions in this chapter are as follows:

- 1) For better separation and performance, we developed a novel PHP called Temperature Regulation in a Pulsating Heat Pipe Using Microfluidics [TRPHP-MF] that uses dividing barriers built into the channel itself.
- 2) A change in the flow pattern of the liquid and vapor plugs may lead to enhanced thermal performance in the heat pipe.
- 3) The heat transport model is validated by a comparison of theoretical and experimental results, which demonstrates its efficacy in enhancing separation while reducing energy use.

The chapter is laid out as shown. Section 5.1 provides context for the Temperature Control in a Pulsating Heat Pipe Using Microfluidics [TRPHP-MF] system. In Section 5.2, we develop and analyse the proposed procedure. The simulation analysis and the study's conclusions are illustrated in Section 5.3. Last section 5.4 presents the study's findings and conclusion.

5.1 Temperature Regulation in a Pulsating Heat Pipe Using Microfluidics [TRPHP-MF]:

One intriguing alternative to traditional heat pipes is the pulsating heat pipe (PHP; sometimes named oscillating heat pipe by some writers), which was designed in the early 1990s. A simple capillary tube describes PHP. Figure 5.1.1 illustrates this where the bubbles are regions of vapor that are separated by liquid plugs due to capillarity. When the evaporator and condenser surface temperature is large enough, the bubbles and plugs will migrate back and forth on their own, penetrating both the cooled and heated sections of the tubes (evaporator). Liquid plugs in PHP's evaporator and condenser facilitate convective heat transmission, which works in tandem with latent heat transfer.

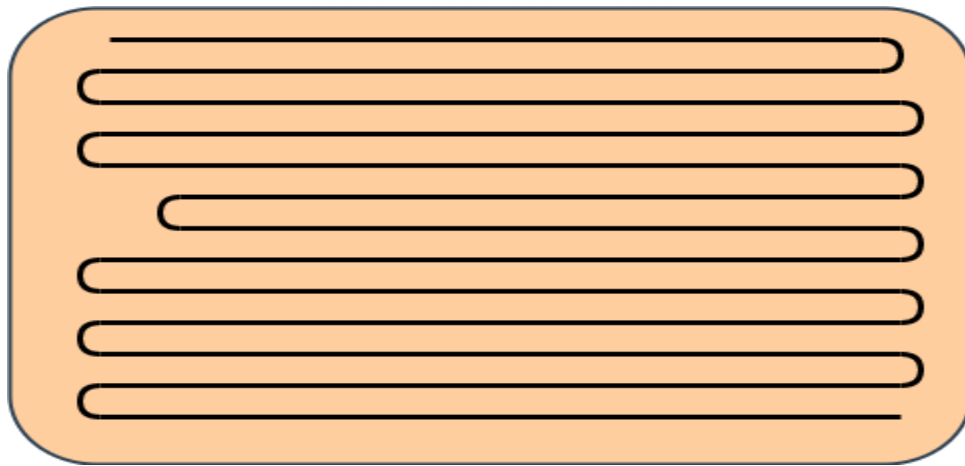


Figure 5.1.1: Creating U-turns on a copper plate via a machine-engraved square channel of the PHP

This characteristic, together with rigorous requirements like compactness, lightweight, and low energy use in the aerospace, transportation, and energy industries has created challenging heat management issues. When it comes to passive heat transfer systems, electronic equipment has benefited greatly from the development of pulsating heat pipes (PHP). PHPs are two-phase passive devices driven by temperature changes, and they function by utilizing the capillary forces and liquid motion brought about by a phase shift. A capillary is a thin, narrow tube or channel. They have one main tube with several branches. Saturated liquid/vapor mixture is pumped into the tube and dispersed as liquid slugs and vapor plugs due to surface tension effects. Flow disturbances in the condensate and evaporation zones, which may take the form of bubble flow, slug/plug flow, or annular flow, all have an impact on the total thermal gradient conveyed by the PHP from the heated to the chilled areas. Making a U-turn on a copper plate using the PHP" technique, which involves engraving a square channel. To ensure that readers can easily recognize and relate to the components depicted in the picture, a comprehensive inventory of all pertinent parts should be provided.

Provides a brief description of the components' duties inside the system next to the list of those components. This explanation ought to clarify the role of each component in the depicted process of creating U-turns on the copper plate through the machine-engraved square channel of the PHP.

If these changes are made, the image will become a thorough visual guide, fulfilling the author's original goal of providing a simple yet useful picture of the system. In turn, this will help readers recognize the significance of the exhibited process's various elements. In intricate scientific or technical situations, the diagram is a visual aid

that helps with comprehension, communication, and provides an understandable overview of a specific area in Creating U-turns on a copper plate via a machine-engraved square channel of the PHP.

Due to this effect, PHPs are far more efficient than other heat pipe designs. One other perk of PHP is that the difference between the pool's CHF and convective boiling suggests a larger dry out limit. PHPs are simple and therefore more reliable and affordable than other cooling options. It's important to note that there are three primary PHP setups. The iterative PHP depicted in figure 1 which stands out as an example of the most effective design, as acknowledged by numerous publications. Finishing with a Cap in the Figure 1 orientation, PHP has a channel closure at both its top and bottom right ends, and no feedback node. There is some study done on the open end PHP, in which either end can be exposed to a reservoir that exerts the mean pressure.

In this chapter, we will examine a subset of PHP called "Flat Plate Pulsating Heat Pipes" (FPPHP), which can be defined as follows: a flat plate having a single, usually rectangular or square channel etched or machined (or generated through additive/etching manufacturing) to create a circuit among one or more hot inputs and one or even more cold sources.

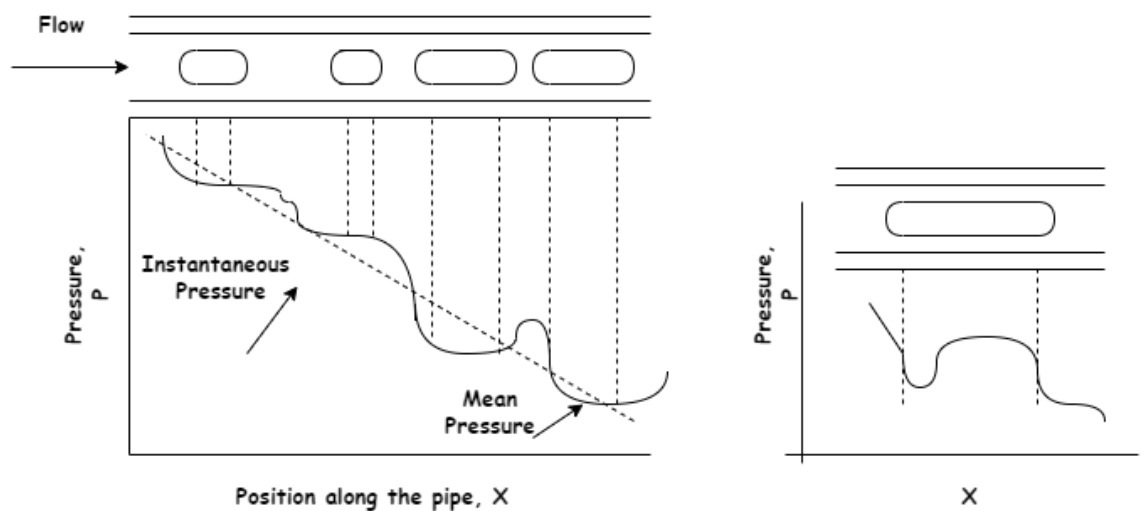


Figure 5.1.2: Reduced pressure

This means that the phase transition between liquid and gas is spread out along the channel's sides and corners. Microtubule heat transfer fluid mode, as used by the FPPHP, is successful even for modest heat energy inputs when operating at a more favourable vertical inclination, unlike circular-shaped channels. Second, the geometric continuity between channels means that heat spreads and tends to greatly reduce heat gradients. Figure 5.1.2 is commonly used in technical and scientific writing to

graphically depict data, concepts, processes, or relationships. Figure 5.1.2: Reduced Pressure in Microfluidic Systems with a Pulsating Heat Pipe show how the implementation of a pulsating heat pipe reduces the pressure within a microfluidic system. This diagram may show how a pulsating heat pipe's heat transfer processes might cause alterations in the microfluidic environment's pressure dynamics, which in turn may affect the behaviour of fluids or particles.

As a result, pressure differences in the channels, a primary cause of oscillations in the phase of slug movement, and especially at a horizontal angle are smoothed out. Nevertheless of their flat surfaces, heat sources with high surface-to-volume ratios are optimal because they can be brought into good thermal contact. The design is significantly more intricate than a tubular PHP, necessitating sometimes intricate or costly production methods.

We have a good understanding of the physical principles behind pulsating heat pipes at this point. However, modelling methodologies are made more difficult by the complexity of the processes and the prevalence of intensive transfer places along the pipes. This section's goal is to introduce the fundamental physical phenomena that underpin heat and mass movement within PHPs, with an eye toward facilitating comprehension of the subsequent analyses and concerns. It is commonly believed that slug flow is the fluid flow pattern in the capillary tube/channels of pulsating heat pipes due to the fact that liquid slugs and vapor plugs are first spread in the half full tube, moving according to the various drivers of change between them.

5.2 PHP implementation of liquid film dynamics:

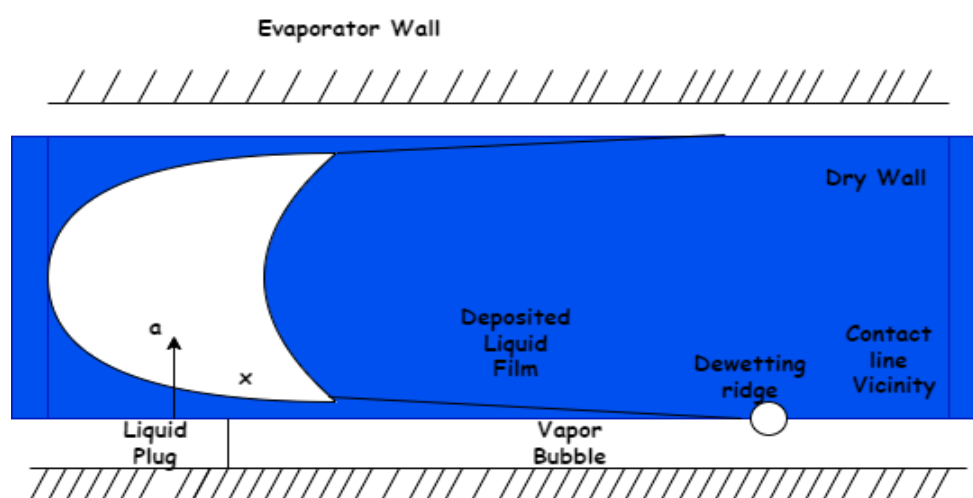


Figure 5.2.1 PHP evaporator liquid film form

Heat and mass transport through liquid films constitute a significant fraction of both processes as it does in other types of heat pipes. For this reason, it is crucial that liquid films be accurately modelled. Passive heat exchange via the films was formerly

assumed to be much weaker, recent simulations using actual film data have revealed otherwise. Further localized calculations and measurement models verified these results. Considering that PHP's oscillation dynamics are governed by mass transfer, this problem takes on utmost significance there.

Oscillations are produced by the principal flow regime inside the PHP, which is analogous to secondary flow in convective boiling. As an alternative, we employ the "bubble" and "plug" terminology of the earliest PHP documentation. It is known as "squeezed bubble flow" or "Taylor bubble flow" is a common term in hydrodynamics (and more specifically microfluidics). When the gravitational forces that tend to form different layers of fluid moving past one another in a horizontal channel segments are outweighed by the capillary forces, a pulsating flow pattern results. As a result of this situation, there is a well-known lower bound on the width of the channels themselves.

$$c < c_{dr} = 2 * \sqrt{\left(\frac{\phi}{f(\partial_1 - \partial_v)}\right)} \quad (5.2.1)$$

In the above equation (5.2.1), this need is required not sufficient for PHP oscillation to work. Since the liquid plugs are moving so quickly, their menisci can be torn apart by inertial forces, because of this, PHPs with only one turn (called a single loop) exhibit annular flow in the gravity-assisted domain. This is comparable to the thermosyphon operation.

$$FT = -\beta d\theta L * \frac{\partial u}{\partial q} = 2\theta\mu L\rho C(Wo) \quad (5.2.2)$$

$$C(Wo) = Wo * \sqrt{i} \left(\frac{T_o(Wo\sqrt{i})}{T_1(Wo\sqrt{i})} - \frac{2}{Wo\sqrt{i}} \right)^{-1} \quad (5.2.3)$$

$$= 4 + \frac{i}{6} Wo^2 + \epsilon(Wo^4)$$

In the above equation (5.2.2 & 5.2.3), where u the fluid's axial velocity, and the small-eddy approximation Wo .

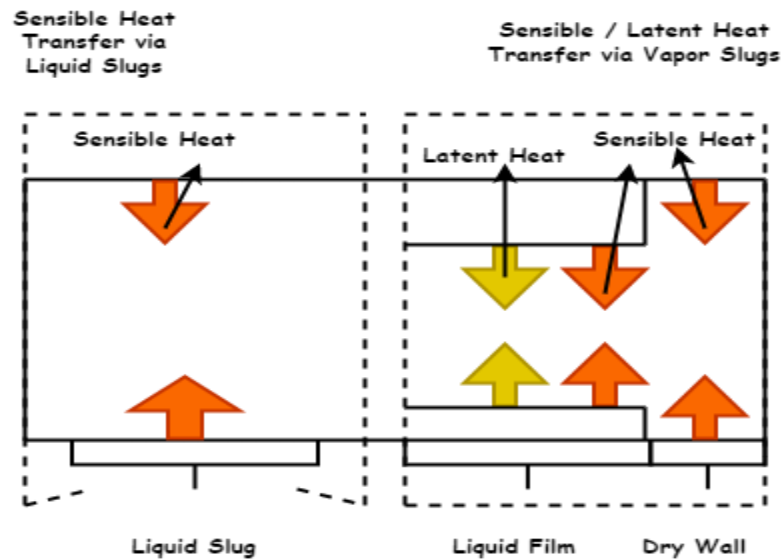


Figure 5.2.2 Correlating heat exchange between zones

Modeling the transmission of momentum and energy inside PHPs requires an accurate assessment of the vapor's thermodynamic condition, which adds another level of complexity. This analysis relies in part on the work of, who compiled, from the existing literature on PHPs, an in-depth and comprehensive examination of the modeling approaches of the vapor thermal phase, especially with respect to the spring that causes oscillations.

$$FT = 8 \pi \mu LV + \frac{mV}{3} \quad (5.2.4)$$

$$\Delta p = \frac{16 * \rho V^2}{D_e * r} L + 5.45 * D_e^{\frac{1}{3}} * C * a^{\frac{2}{3}} * \frac{\phi}{d} \quad (5.2.5)$$

In the above equation (5.2.4 & 5.2.5), Let liquid plug length be L , the numerical coefficient, D_e be the dependence offer the greatest approximation to numerical data and experimental data involving air bubbles in a variety of liquids. PHP flows typically go below this threshold, allowing just the laminar scenario to be considered. The Richardson annular effect describes the situation in which the velocity is greatest at a distance of C from the wall.

Other authors, however, showed that vapor can be superheated by measuring fluid temperature at different micro-FPPHP locations, and they highlighted, with a long enough vapor plugs, both an overheated region in the exchanger zone and a concentrated thermal region inside the adiabatic zone within a single bubble. As a result, a vapor plug's temperature can fluctuate widely, and small superheated regions can form.

Furthermore, they have conducted microgravity testing of their hybrid thermosiphon / tubular PHP.

$$F = C * \emptyset * r * \beta_1 * V^2 * L \quad (5.2.6)$$

$$C = \begin{cases} \frac{16}{D_e} & 0 < D_e < 1180 \\ 0.07945 * D_e^{0.25} & \end{cases} \quad (5.2.7)$$

Consideration of global turbulence's effect is now possible using D_e .

$$\frac{d}{dt}(mV) = (p - p_{nxt})S - F - F_{turn} + G \quad (5.2.8)$$

where G is the gravity force. The pressure $p - p_{nxt}$ corresponds to the end of the plug.

$$F_{turn} = 0.105 * S * p * V^2 * A_{turn}(\emptyset) \quad (5.2.9)$$

$A_{turn}(\emptyset)$ is the nonlinear in the above equation (5.2.9).

From the above equation (5.2.6), (5.2.7), (5.2.8) & (5.2.9) It is important to remember that the liquid temperature has no bearing on the vapor bubbles state or the PHP dynamics as a whole when there are enforced values in both the evaporator and condenser sections. When a thermal fluid-solid connection is introduced, both the fluid dynamics and the thermal transfer between both the liquid and the solid must be addressed at each time step. This clearly compounds the difficulty of the situation.

$$\frac{\partial T}{\partial t} = D_w * \frac{\partial^2 T}{\partial t^2} + \frac{j}{\partial c} \quad (5.2.10)$$

The equation (5.2.10) describes the temperature profile along the inner tube wall.

They demonstrated that with a certain amount of heat input, the subcooling level would increase in the condenser and decrease in the evaporator, revealing a predominant superheating pattern in both regions. The authors claim that at temperatures above saturation, the fluid is a supercooled liquid, whereas at temperatures below saturation, it is a subcooled vapor. When calculating the net energy gain or loss of a pulsing heat pipe, when describing the thermodynamic state of a fluid at a saturated equilibrium, it is important to take into account the transmission of sensible heat (or latent heat in the metastable condition).

$$\Delta pd = \Delta pd_0 - \frac{\partial \emptyset}{\partial t} * pd - e^{i\emptyset t^{-1}} \quad (5.2.11)$$

From the equation (5.2.11), the mathematical expression for flow in a microchannel that is being propelled by a pulsatile differential pressure is pd where pd_0 is the pressure at zero time, is the amplitude of the pressure fluctuations, is the frequency of the pressure changes, and t is the time elapsed. Several different flow fields can be defined by using this equation.

When a lump of liquid moves through a capillary tube, divided by two (advancing and retreating) menisci, a slug flow pattern is formed when liquid forms a thin coating on the wall from around vapor bubbles. The liquid film appears to be the outcome of a competition between viscosity and capillaries forces at a transition region adjacent to the liquid meniscus. The meniscus's thickness is affected by both viscous friction and surface tension forces; the former tends to keep the fluid stationary close to the wall, while the latter reduces the meniscus's size. The capillary count is used to depict this rivalry.

However, it was repeatedly established in the earliest studies of PHP that this study demonstrates that sensible heat of liquid bodies moving in both the warm and cool PHP sections accounts for a considerable amount of the heat exchanged, and that vapor evaporation/condensation mostly leads to slug/plug flow motion as a controller for PHP oscillations. Heat exchanges in pulsating heat pipes (in which it appears that latent heat transfers in both the evaporator and the condenser account for 55%-80% of the total heat transfer) have recently been experimentally proved to be dominated by latent heat.

Droplet Generation:

Over the past two decades, many papers report on both basic and applied research in droplet microfluidics, and some businesses, such Dolomite Bio, have caught up with the progress made in this area. Because the carrier fluid separates each droplet from the others and from the channel walls, Chemical or biological processes can be carried out within the confines of the droplets, which can serve as micro reactors by enclosing cells, particles, or molecules (DNA, proteins). The formation of droplets is dominated by the conflict between interfacial tension and viscous forces at low flow rates (shear force is insignificant), making interfacial tension management, along with flow and geometric condition control, one of the most effective techniques to generate droplets on demand. The interfacial tension between two fluid phases can be adjusted by changing the temperature or by adding surfactants to one or both phases.

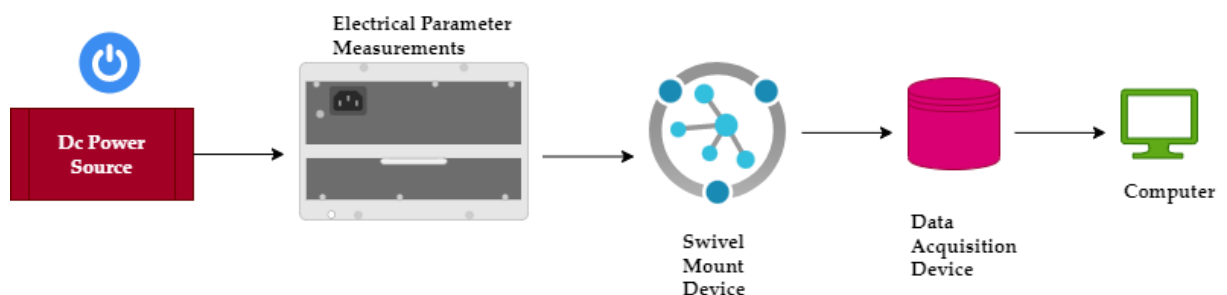


Figure 5.2.3 Schematic Diagram

Figure 5.2.3 shows the schematic diagram. A flat-plate OHP's thermal performance differs between its left and right sides due to inefficient heating. Therefore, the exchanger difference in temperature, heat capacity, and non-homogeneous heat transfer ratio are embraced and determined by calculating from the quasi-steady temperature data to assess the thermal efficiency of the left half, the right half, and the entire flat-plate OHP subjected to non-uniform heating. Thermal resistance was used to determine the temperature gap between the left and right portions of the evaporator.

In most cases, the creation of droplets is the first and most crucial stage, and its results should be reliable and repeatable. Droplet production must be precisely regulated for applications such as biochemical screening, click chemistry, and DNA polymerase chain reaction if they are to produce consistent results. By adjusting the pressures and channel geometries, droplets can be passively generated at kHz rates in micro-channel networks, although precise control of individual droplets is challenging due to design mistakes, manufacturing faults, and pressure changes. The creation of droplets or bubbles through thermal mediation was a breeze with the help of embedded heaters.

Droplet mixing and nanoparticle formation are both aided by microwave heating, as shown by several experimental studies. Droplets with specific dielectric characteristics are ideal for depositing thermal energy generated by microwave heating. Based on the dissimilar dielectric characteristics of the droplets and the surrounding carrier fluid, it can heat the droplets alone. Pulse heating is possible with microwaves because the heating stops as soon as the power is switched off. This note demonstrates how to generate droplets on demand by using an external microwave source and a controlled heating pulse. Droplet generation efficiency as a function of microwave power is studied, and the mechanism of generation is briefly explained.

Table 5.2.1 Comparison Analysis on Performance:

No. of Dataset	SLPHP	DF-MF	T-FB	FP-OHP	T-PHP	TRPHP-MF
10	31.01	38.33	35.14	36.56	32.76	49.22
20	35.21	39.45	41.24	20.6	43.65	50.01
30	41.36	34.15	34.19	46.99	54.11	69.1
40	20.21	29.47	43.76	62.62	71.65	52.43
50	42.56	56.33	69.33	69.34	12.98	57.34
60	33.98	47.14	36.54	41.98	47.26	68.44
70	51.54	21.89	56.39	36.41	53.61	75.65
80	67.22	65.25	65.25	59.89	57.98	86.98
90	72.36	82.66	66.15	83.57	79.1	95.09

PHP, in comparison, is not a static procedure rather is dependent on numerous material and physical factors. Thus, empirical correlations are frequently useless. Here, we suggest a PHP called Temperature Regulation in a Pulsating Heat Pipe Using Microfluidics [TRPHP-MF] that uses separating barriers built into the channel to enhance separation and efficiency. Droplet creation can alter the flow pattern of the liquid and vapor plugs, which may improve the heat pipe's thermal performance. We validate the heat transport model by comparing it to both theoretical and experimental results. The current research contrasts conventional analytical approaches with new ones for achieving effective heat transfer via Pulsating Heat Pipes (PHPs) embedded in microfluidic devices. Among the proposed methods is Temperature Regulation in a Pulsating Heat Pipe Using Microfluidics [TRPHP-MF], which takes full advantage of passive heat transfer and structural alterations. The proposed approaches for heat transfer via PHPs in microfluidic systems present a dynamic approach that is well-aligned with the intricate interplay of passive mechanisms and fluid dynamics. This method differs from the more common analytical approaches, which may not be able to fully capture the complexities of such interconnected systems. The proposed approaches need to be tested and researched further before they can be considered viable or have any real-world impact.

5.3 Results & Discussion:

There is a brief discussion of the shortcomings of the literature review. Model-based conclusions were analyzed for accuracy analysis, efficiency, volume flow rate, performance, and thermal analysis in simulations. It is important to remember that the fluid temperature inside a PHP cannot be directly replaced by the wall temperature as measured by thermocouples, as the wall's thermal resistance and the exterior thermocouple attachment method make them less accurate.

Table 5.3.1 Material Properties and Setup Dimensions

Material	Thermal Conductivity (W/m·K)	Density (kg/m ³)	Specific Heat (J/kg·K)
Material A	250	2000	800
Material B	150	1800	600
Material C	300	2200	750

Fluid motion can be either pulsatile or constant, with both having their own unique properties and systemic implications. The fluid is moving in a uniform and consistent manner, as in a steady flow. Regardless of where you measure the fluid's speed, it stays the same throughout time. The steady flow of water through a pipe is one example of a commonplace situation involving this type of flow. On the other hand, pulsatile flow is defined by the presence of periodic changes in both the fluid's velocity and pressure. This pattern of increased and decreased blood flow is reminiscent of the regular beating of a heart. Blood vessels are naturally prone to pulsatile flow, it is possible to create such flow with medical equipment or hydraulic systems. Research into the effects of pulsatile flows, with their oscillations and variations, on heat transfer, fluid dynamics, or other relevant elements, in the context of microfluidic systems containing a pulsating heat pipe, is one possible direction of investigation. In order to maximize heat transfer efficiency or other system features in microfluidic setups, it is helpful to have a firm grasp of the ways in which pulsatile flows provide advantages over steady flows.

5.3.1 Accuracy Analysis:

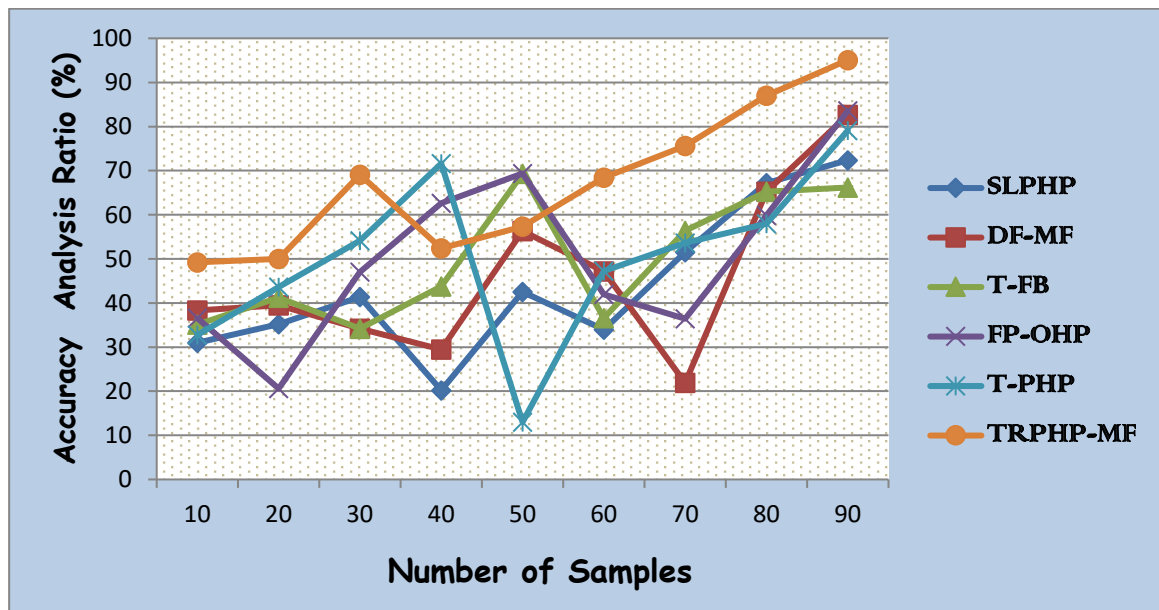


Figure 5.3.1 Accuracy Analysis

Figure 5.3.1 shows the precision test results. The x-axis and y-axis of this graph were used to tally up the samples and calculate the precision with which the analysis was performed. The method may be more accurate over the long run than any other currently used approach.

5.3.2 Evaluation of Thermal Insulation:

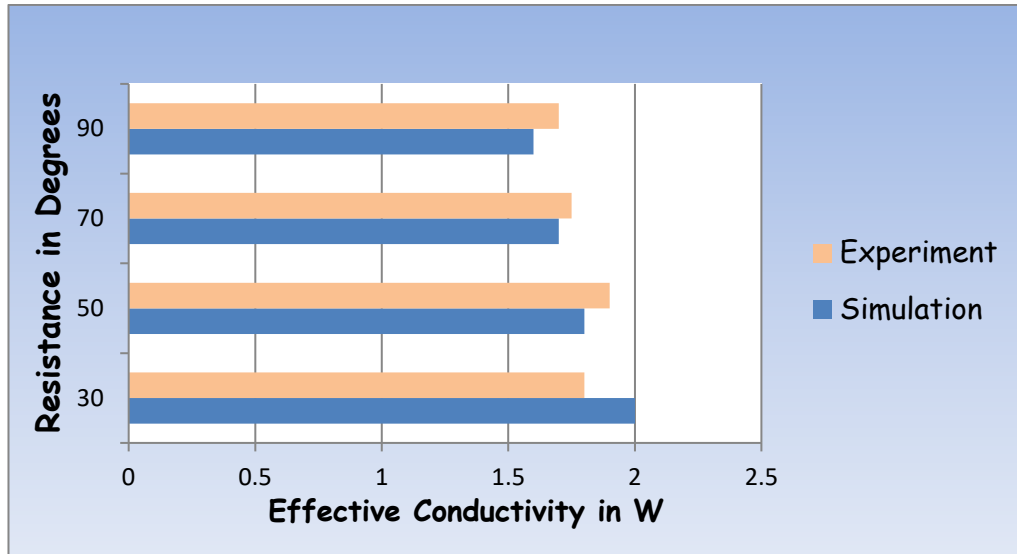


Figure 5.3.2 Thermal Insulation

The process for measuring the thermal insulation analysis ratio is shown in Figure 5.3.7. To better comprehend the relationship between the inclination angle variation (Y-axis) and conductivity (X-axis), a comparison is drawn between the two. Above, we saw how their similarities can be predicted. Insulating two spaces from one another with a material or method can keep the temperature differences between them and save on energy costs.

5.3.3 Examination of Volume Flow rate:

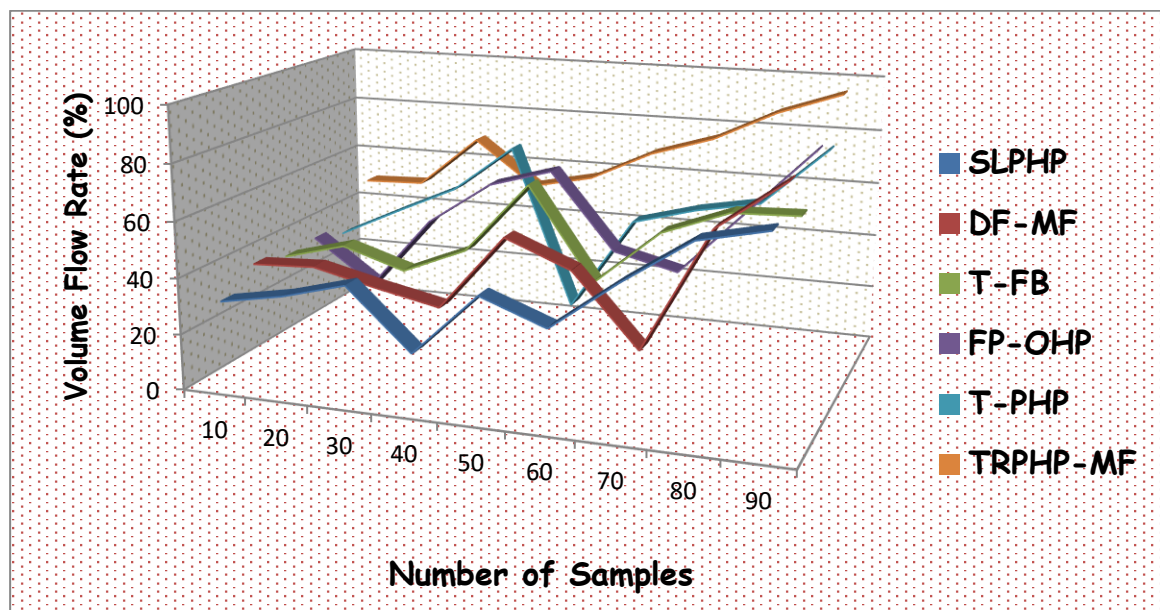


Figure 5.3.3 Volume Flow rate

The results of a volume flow ratio test for analyzing flow rates are shown in Figure 5.3.3. It is possible to gain insight into both the (X-axis) and the flow rate (Y-axis) by comparing and contrasting them. As mentioned previously, a comparison can be drawn between the two. The volume flow rate is the quantity of fluid moving across a particular area per unit time, typically expressed in cubic meters per second (m³/s) or liters per minute (L/min).

5.3.4 Performance Analysis:

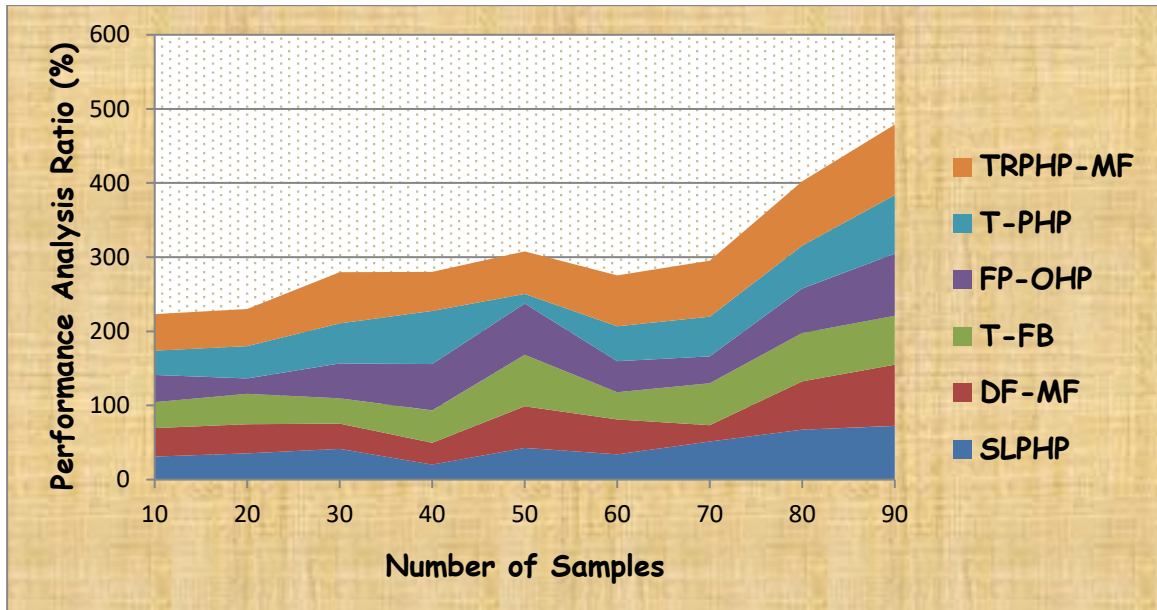


Figure 5.3.4 Performance Analysis

The benefits of performance evaluation are shown in Figure 5.3.4. The y-axis represents the total number of observations, while the x-axis displays the various ratios produced through performance analysis. Therefore, in order to put each hypothesis to the test, a variety of samples were collected at varying ratios. The TRPHP-MF used in this model is a significant improvement over the state of the art.

5.3.5 Efficiency Analysis:

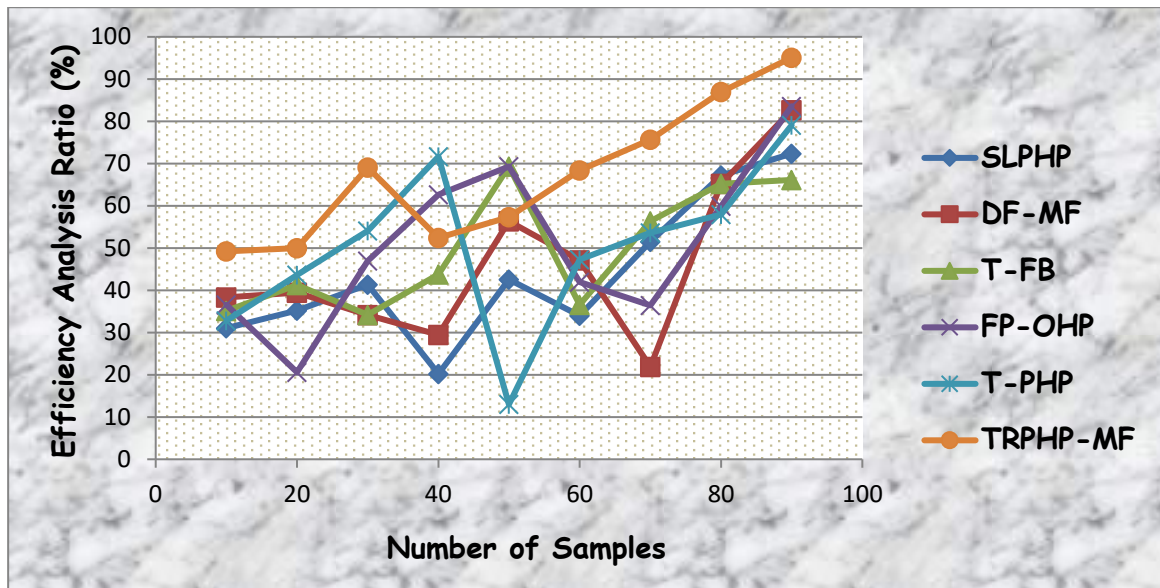


Figure 5.3.5 Efficiency Analysis

Figure 5.3.5 depicts the gains from efficiency analysis. On the x-axis are the various ratios obtained through efficiency analysis, and on the y-axis is the number of observations. Consequently, a number of samples were collected at varying percentages to test each hypothesis. This model's TRPPHP-MF is a major step forward from previous methods.

Our findings show that the TRPPHP-MF model is superior to its contemporaries in every one of these respects. Reportedly developed in response to the competitive pressure discussed in the preceding section and aided by the proposed model, this new feature.

5.4 Conclusion:

The many advantages of miniaturization have led to an uptick in the use of microfluidic devices over the past two decades. Their small form factor and extensive feature set make them perfect for use on the go with little in the way of a learning curve. Since their widths are typically on the order of millimeters, low-Re flows are often the result. These influxes have the potential to start and stop suddenly and dependably. Features on the micrometer scale permit the precise manipulation of particles such as red blood cells, tumors, bacteria, viruses, and micro and Nano particles. The use of pulsating or oscillating flows in microfluidic devices could solve a number of problems. A combination of an intelligent building system and fluid metals could allow the millimeter-scale commercial heating element to be used for temperature detection of micro-scale liquids. Temperature-sensitive amplification tests with nucleic acids have

further elucidated the thermal accuracy of this method. Therefore, this method shows great potential for detecting micro-macro interactions and has applications beyond microfluidics.

Our work here proposes a TRPHP-MF that makes use of microfluidics. This is achieved by erecting walls within the flow channel. There are minimum, maximum, and median values for blood flow represented in each vascular waveform. No significant differences were found in flow or pulsatility between patients with cortical and lacunar stroke. Heat transfer correlations appear to have limited predictive power for the PHP case due to their non-stationary behavior. It appears that this method of accurate modeling is the PHP dynamic simulation. Tools for predictive simulation that can aid in the development of optimized industrial prototypes are needed. For better comprehension of the thermofluidic working principles of rectangular-channel TRPHP-MF, this paper presents a comprehensive analysis of many new theoretical and experimental investigations on the thermal and flow characteristics of pulsing heat pipes made of flat plates and two-phase flows in rectangular mini- and micro channels and gains better accuracy and efficiency of 90.9% and the performance is achieved as 97.8%. For effective heat transmission in today's electronics, the incorporation of Pulsating Heat Pipes (PHPs) in microfluidic systems is an exciting new development. PHPs have the ability to handle temperature control difficulties because to their distinctive characteristics, which are driven by passive mechanisms and strengthened by the suggested Temperature Regulation in a Pulsating Heat Pipe Using Microfluidics [TRPHP-MF]. This investigation highlights the need of having a thorough understanding of PHP-based thermal solutions and continuing to commit time and energy to their discovery as we negotiate the complexity of pulsatile flows and expands our horizons.

ENHANCING PULSATING HEAT PIPE PERFORMANCE USING NANOFLUIDS AND DEEP LEARNING METHODS: AN EXPERIMENTAL ANALYSIS

Pulsating Heat Pipes (PHP) have emerged as a novel and space-efficient heat transfer mechanisms that have garnered considerable interest in contemporary times [89]. They provide effective thermal management solutions for diverse applications requiring heat dissipation. PHPs can effectively manage thermal energy in small-scale systems and electronics by utilizing capillary action and phase change phenomena.

The origins of PHPs can be traced to the early 1990s when the initial concept was introduced. Subsequently, considerable research and development endeavors have been aimed at refining their configuration and augmenting their efficacy. PHPs refer to closed-loop networks comprising interconnected channels filled with a working fluid [103]. The fluid oscillates between its liquid and vapor phases due to the pressure differential resulting from the temperature gradients present along the tracks.

PHPs provide numerous essential characteristics and benefits. Primarily, they demonstrate elevated heat transfer coefficients, facilitating effective heat dissipation [75,142]. Due to their diminutive dimensions and flexible arrangement, they are well-suited for implementation in scenarios where spatial limitations are a factor. PHPs can function across various orientations and demonstrate exceptional thermal stability, even amidst transient circumstances. In addition, their power demands are minimal due to their reliance on passive capillary action instead of mechanical pumps [149].

The utilization of nanofluids in experimental analysis has emerged as a promising approach to enhance the performance of PHPs. Colloidal suspensions of nanoparticles in a base fluid, commonly known as nanofluids, have demonstrated enhanced thermal conductivity compared to traditional fluids [112,137]. Integrating nanofluids into the working fluid of PHP can result in a noteworthy improvement in heat transfer efficiency. Prior research has indicated that nanofluids benefit PHP, resulting in increased heat transfer coefficients, decreased thermal resistance, and improved thermal stability [113]. Nevertheless, additional empirical investigation is necessary to gain a deeper comprehension of the intricate heat transfer mechanisms and enhance the nanofluid configuration to attain the most favorable performance of the pulsating heat pipe.

The complexities associated with improving the performance of PHPs through nanofluid analysis and deep learning-based prediction are multifaceted. These challenges include the intricate nature of heat transfer in PHPs, the necessity for precise performance prediction, and the optimization of nanomaterial composition to achieve optimal heat transfer enhancement [122]. The method under consideration aims to tackle the challenges by offering a methodical strategy to scrutinize and enhance the characteristics of nanofluids. It employs advanced deep learning techniques to ensure precise performance prediction, thereby facilitating effective and dependable thermal management in PHP applications.

The main contributions are outlined as follows:

- The present study proposes the integration of TiO_2 nanomaterials into the working fluid of PHP to augment thermal conductivity and enhance heat transfer performance.
- The proposed methodology involves conducting a thorough experimental analysis to assess the efficacy of PHPs when utilizing nanofluids. This analysis will encompass temperature profile measurements and the determination of heat transfer characteristics.
- The study aims to create an Artificial Neural Network (ANN) model utilizing deep learning techniques to predict the performance of PHP based on empirical data. The proposed model is expected to provide reliable and efficient performance estimation.
- The present study aims to optimize the composition of nanofluids by investigating their thermal properties to achieve optimal heat transfer enhancement in PHP.

The subsequent sections are organized in the prescribed order: this section presents a comprehensive background and literature survey of PHP analysis. This includes an overview of the technology, its underlying principles, and a review of prior research in this area. Section 6.1 presents the proposed methodology, Deep Learning-Based Prediction and Enhancing Performance (DL-PEP). This approach employs advanced deep learning techniques to forecast the performance of PHP and optimize its overall efficiency. Section 6.2 presents the experimental results and values, showcasing the outcomes of extensive experiments on PHPs utilizing nanofluids. The conclusion and findings section summarizes the study's key outcomes. It emphasizes the efficacy of the

DL-PEP methodology in augmenting PHP performance and its potential for enhancing thermal management in diverse applications.

6.1 Proposed Deep Learning-Based Prediction and Enhancing Performance

This section presents the DL-PEP methodology, which is based on deep learning, to predict and enhance the performance of PHP. The research elucidates the implementation of deep learning methodologies, focusing on constructing an ANN framework for the precise prognostication of PHP efficacy [138]. The section highlights the potential of DL-PEP in enhancing the overall efficiency and thermal management capabilities of PHPs.

6.2 Material preparation

6.2.1. Preparation and characterization of TiO₂ nanomaterials

The preparation of TiO₂ nanofluid samples was carried out through a two-step process. Anatase TiO₂ nanoparticles below 10 nm were synthesized through a sol-gel technique utilizing butyl titanate and anhydrous ethanol at ambient temperature (25C). Figure 6.2.1 displays the Transmission Electron Microscopy (TEM) image of TiO₂ nanoparticles [86].

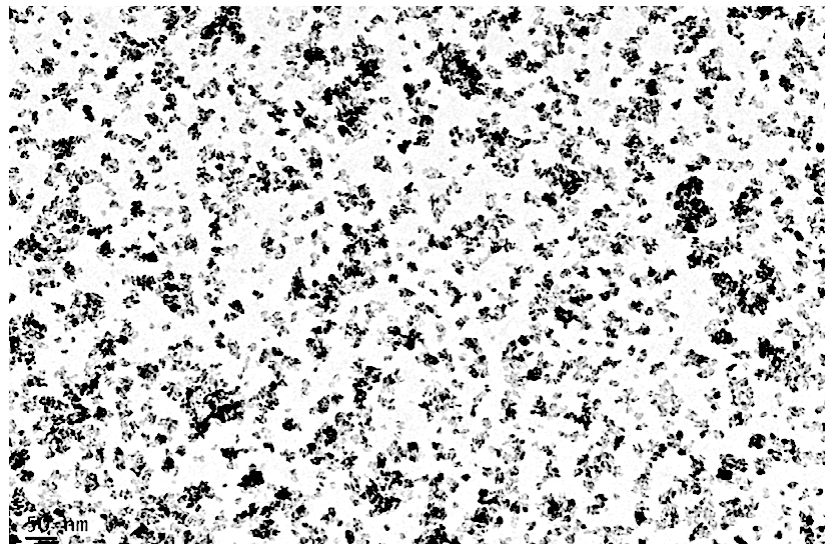


Figure 6.2.1 TEM image of TiO₂ nanoparticles

The dispersion of nanoparticles was carried out in deionized water, serving as the foundational medium for the nanofluid. The suspension underwent magnetic stirring and ultrasonic fluctuations for 30 minutes each. For this study, the nanofluids were created at a volume concentration of 2%.

6.2.2. PHP preparation

The experiments were conducted with a closed-loop type PHP. It was manufactured with copper, with an inner diameter of 3 mm and an external diameter of 3 mm, with five turns, a total length of 280 mm, and a total width of 120 mm. According to the design requirements of the battery module of national standard size and the actual battery size in a pure electric vehicle (136 mm wide, 181 mm long), the length of the evaporator and condenser sections were 170 mm and 120 mm, respectively. Rectangular fins were installed at the condensation end to increase the area of heat dissipation. A total of 90 fins were installed; each was 45 mm long, 25 mm wide, and 0.5 mm thick, with a 2 mm spacing between adjacent fins.

Before injecting the working fluid (TiO_2 nanofluid), the PHP was evacuated up to 10^{-4} m-bar by a vacuum pump. Moreover, non-condensable gasses in the working fluid were removed by the degassing process in which the working fluid in the vacuum chamber was heated and then cooled to obtain a purified fluid. After the degassing process, the working fluid was precisely charged into the PHP using a mass pipette to get the target filling ratio of 50%. The investigations utilized a PHP of the closed-loop variety. The object in question was produced using copper material and possessed an internal diameter of 3 mm and an external diameter of 3 mm. It consisted of 5 turns, measured a total length of 280 mm, and had a full width of 120 mm. Based on the design specifications for the battery module of a standard size as per national regulations and the dimensions of the actual battery in a pure electric vehicle (136 mm in width and 181 mm in length), the evaporator and condenser sections were determined to have measurements of 170 mm and 120 mm, respectively. Rectangular fins were affixed to the condensation end to augment the surface area available for heat dissipation. Ninety fins were attached, each measuring 45 mm in length, 25 mm in width, and 0.5 mm in thickness. The fins were spaced 2 mm apart from one another.

Before introducing the operational medium, specifically the TiO_2 nanofluid, the PHP underwent evacuation to a pressure of 10^{-4} m-bar through a vacuum pump. Furthermore, the elimination of non-condensable gases from the working fluid was achieved through a degassing procedure, whereby the working fluid was subjected to heating and subsequent cooling within a vacuum chamber to yield a refined fluid. Following the degassing procedure, the working fluid was accurately introduced into the PHP using a mass pipette, achieving a desired filling ratio of 50% and a concentration of 2% by volume.

6.3 Experimental setup

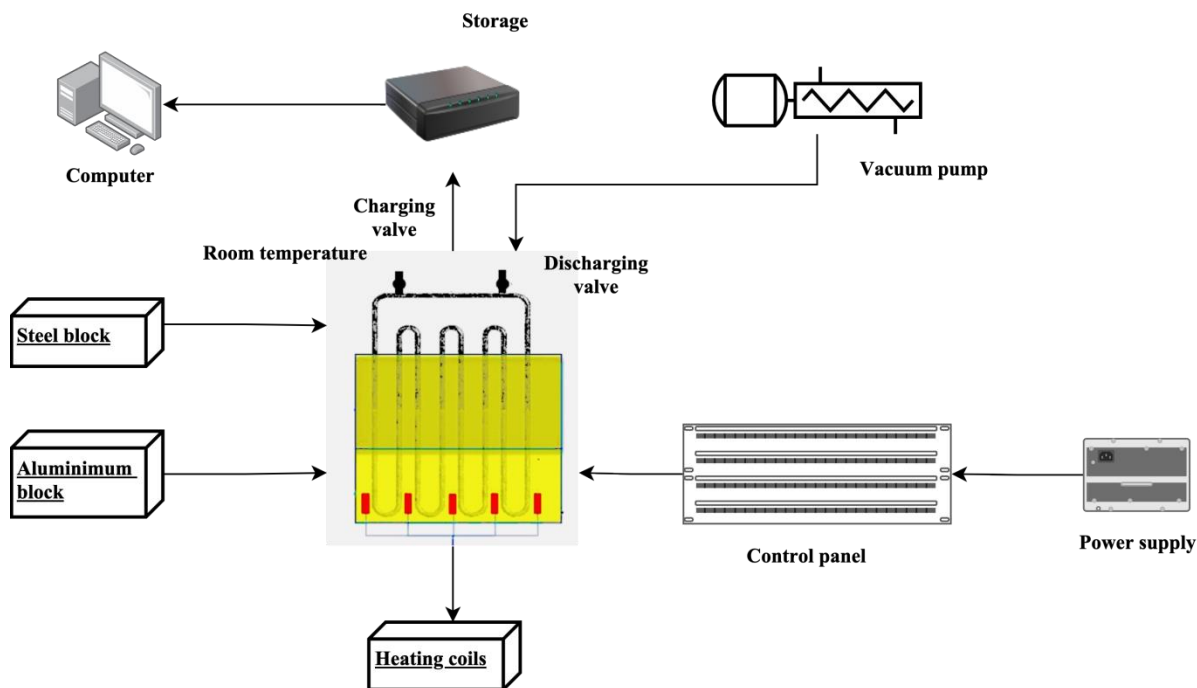


Figure 6.3.1 Experimental setup for PHP

Figure 6.3.1 depicts the schematic representation of the testing arrangement for PHP. The system comprised a vacuum pump, a pulse height analyzer, a device for recording data, a panel for controlling the system, and a source of electrical power. A copper-based PHP consisting of four turns was enveloped by an aluminum block measuring 155 mm X 55 mm X 25 mm at the evaporator segment. The aluminum block was fitted with five cartridge heaters that were circular in shape, measuring 6 mm in diameter and 45 mm in dimensions. The heat sources were positioned alternately amidst the copper pipe with four turns, which were situated within the aluminum blocks, to ensure adequate and uniform heating. The adiabatic portion was covered with a steel block. The steel block was filled with densely packed glass wool to insulate against heat. The condenser component comprised three pipe roles, and a tube of copper measuring 55 mm in length was intentionally exposed to ambient temperature to facilitate heat dissipation. The manipulation of the heating supply to the evaporator was achieved by utilizing a dimmer stat, which reduced the variation of voltage and current within the range of 0-65 V and 0-5 A, accordingly, to the cartridge heating systems. The current and voltage were measured with a digital ammeter and voltmeter, respectively, with an accuracy of $\pm 0.2\%$. The experimental setup involved employing an oil rotary vacuum pump to establish a vacuum pressure of up to 0.02 m-bar within the PHP.

6.3.1 Experimental procedure

The experiment is conducted according to the following method:

- The Closed Loop PHP (CLPHP) system initially undergoes evacuation and subsequent charging with a specific quantity of working fluid [23].
- A consistent airflow velocity is implemented to cool the condenser section.
- The amperage of the provided energy is adjusted by hand to the desired rate employing an ammeter.
- Under steady-state circumstances, the heat input is systematically incremented by 44 W while concurrently recording the corresponding evaporator ambient temperatures.
- The procedure, comprising Steps 1 through 4, is reiterated with a modified quantity of working fluid. The filling ratio in this scenario consists of the values 0.2, 0.4, 0.6, and 0.8.

The CLPHP underwent an initial evacuation process to establish distinct stages until reaching a pressure of 0.2 bars. Subsequently, the desired stresses were found using a controlling valve and a pressure gauge.

The assessment of the thermal efficiency of PHPs necessitates the consideration of crucial data points, including but not limited to heat demand, heat transfer, average evaporator temperatures, and thermal resistance. Thermal resistance is a concept that profits from multiple definitions. One possible definition of ∇H is the thermal gradient between the evaporator and condensation chamber or the disparity between the surrounding temperature and the cooling system. In this study, the utilization of an external fan as the condenser unit and the absence of input-output fluid cooling formation have led to the adoption of the second definition of the term. By subtracting the ambient temperature from the evaporator's temperatures, the influence of the former on the efficiency of a PHP has been mitigated. The decreased temperature of the evaporators serves as evidence of the enhanced efficacy of the condenser component, which encompasses the active substance and an extrinsic fan operating at a consistent velocity. **The thermal resistance and the thermal gradient are expressed in Equations (6.3.1) and (6.3.2).**

$$R = \frac{\nabla H_e}{K} \quad (6.3.1)$$

$$\nabla H_e = H_e - H_a \quad (6.3.2)$$

The computational constant is denoted K . The experimental temperature is denoted as H_a , while H_e represents the mean temperature of the evaporator blocks, which is determined using Equation (6.3.3):

$$H_e = \frac{1}{3} \sum_{i=0}^2 H_{e,i} \quad (6.3.3)$$

A minimal thermal resistance ($H_{e,i}$) shows greater heat transfer effectiveness, corresponding to a lower H_e value and, thus, a more significant amount of heat transmitted from the evaporator blocks. The process of evaluating and quantifying the potential errors and variability in measurements, data, and models is called uncertainty evaluation.

The inclusion of uncertainty evaluation is a fundamental component in the process of conducting experimental analysis. The present study identifies the source of error in the test information as arising from the temperature detector and heat pipe heating devices. The correlation between indirect and direct mistakes can be mathematically represented using Equation (6.3.5), and the given scenario is computed using Equation (6.3.6):

$$V = f(w_1, w_2, w_3, \dots, w_k) \quad (6.3.4)$$

$$Er_v = \sqrt{\sum_{x=0}^{k-1} \left(\frac{dV}{dw_x} \right)^2 Er_{w_x}^2} \quad (6.3.5)$$

The present study considers a scenario where variable V is determined indirectly, while variable w_x is measured immediately. The errors associated with the indirect measurement of V and the direct measurement of w_x are denoted by Er_v and Er_{w_x} , accordingly. The estimation of the general heat resistance uncertainty can be conducted using Equation (6.3.6).

$$\frac{\nabla R}{R} = \sqrt{\left(\frac{\nabla(H_e - H_a)}{Q_{dc}} \right)^2} \quad (6.3.6)$$

The equation provided relates the change in the heating resistance (∇R) of a PHP to its heating resistance (R) in units of $C \cdot W^{-1}$. The temperatures (C) of the condensing ends of the PHP are denoted as H_e , while the temperatures (C) of its evaporation concludes characterized as H_a . Additionally, the heating power (W) is represented by Q_{dc} . The computations are performed by utilizing the variables' uncertainties to mitigate potential sources of error.

6.3.2 The building of the ANN model for prediction

The heating transfer procedure of the PHP was simulated using a fully connected feed-forward ANN system based on the data gathered. The back propagation learning method, renowned for its exceptional adaptability, has been widely employed in developing ANNs. In line with this trend, the present study also utilized this algorithm. The transfer function chosen for the concealed layer was sigmoidal functioning. The gathered data was partitioned into three distinct sets through a random process. The training set comprised 70% of the data, while the validation and evaluation sets contained 15% each. Optimizing the number of neurons in the concealed layer was crucial to balancing computation speed and precision. Trial-and-error was utilized to determine the best neuron nodes for the concealed layer. The present study employed the Mean Square Error (MSE) and correlation coefficient (r) to evaluate predictive performance. These metrics are expressed as follows:

$$MSE = \frac{1}{M} \sum_{x=0}^{M-1} (Y_{e,x} - Y_{a,x})^2 \quad (6.3.7)$$

$$r = \frac{K_v(e,a)}{\sqrt{K_v(e,e)}\sqrt{K_v(a,a)}} \quad (6.3.8)$$

The symbols $Y_{e,x}$, $Y_{a,x}$, and K_v denote the anticipated outcomes generated by the ANN model, the empirical data, and the covariance, correspondingly. Consequently, an ANN system was constructed, comprising seven nodes in the input layer, the concealed layer, and one in the output layer. Figure 3 illustrates the construction of the ANN model.

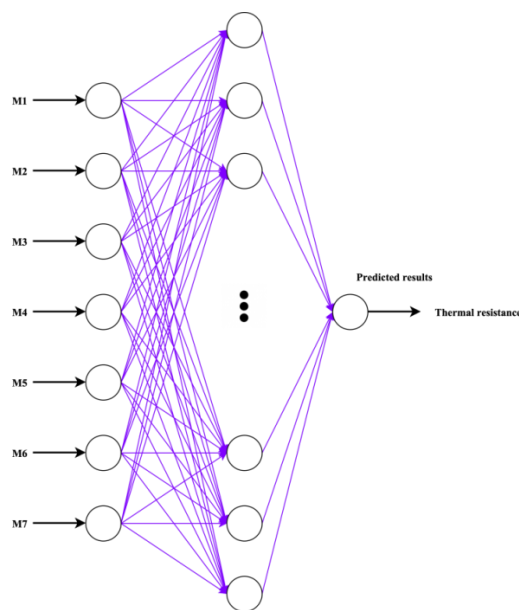


Figure 6.3.2 ANN architecture

The authors suggested a novel artificial neural network model for directly predicting thermal resistance in PHP, considering various fluids used for work and a wide range of operational circumstances. In addition, the ANN model was utilized to propose a parameterized approach for assessing the temperatures of the evaporation and condensation segments. The primary findings of this study indicate that an ANN model was developed to forecast the PHP thermal resistance utilizing the gathered empirical data. The present study investigated the impact of geometric, property, and operational variables on the system performance. The Kutateladze quantity (Ku or M1), Bond quantity (Bo or M2), Morton quantity (Mo or M3), Prandtl quantity (Pr or M4), Jacob quantity (Ja or M5), the amount of turns (N or M6), and the proportion of the evaporation part dimension to the diameter (Led or M7) were utilized as the input variables for the analysis. The dimensionless numbers' thermo-physical characteristics were computed based on the known coolant temperature during the initial phase.

The ANN architecture comprises three layers: the input, concealed, and output layers. The optimization of the number of nodes in the hidden layer was achieved through the utilization of the trial-and-error approach, resulting in a value of 11. The findings indicate that the outcomes projected by the ANN model exhibited high concurrence with the empirical data gathered. The MSE and the correlation coefficient were calculated to be 0.014 and 0.97. The working fluid significantly impacted the accuracy of the ANN model's predictions. The discrepancies observed in the performance of PHP when operated with water were comparatively higher than those analyzed when used with other working fluids. It is possible to assess the temperatures of both the evaporation and condensation sections by integrating heat transfer correlations. The proposed approach employs a lumbered variable methodology to predict the PhP's flow path and heating network.

The section outlines the DL-PEP technique, which integrates deep learning and PHP analysis methods to improve performance prediction. An ANN model facilitates the precise evaluation of PHP functionality through empirical data. This section underscores the potential of DL-PEP in enhancing the design of PHP and enabling effective thermal management across diverse applications.

6.4 Experimental Analysis and Outcomes

A novel fully-connected ANN system was suggested to establish a dependable method for predicting the thermal performance of PHP under various operating circumstances, utilizing different working fluids.

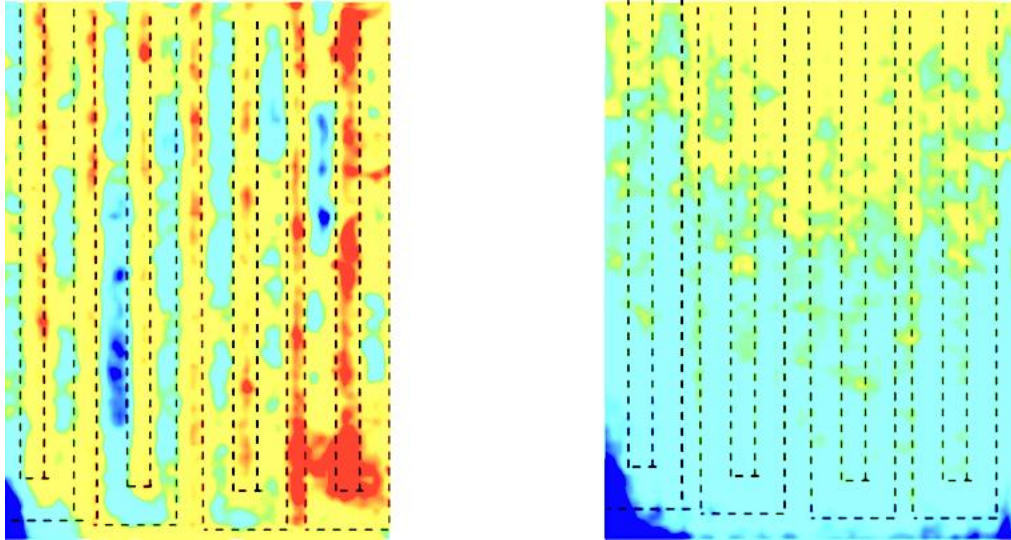


Figure 6.4.1 Image of Temperature distribution analysis of different time

Temperature distribution analysis at different times is shown in Figure 6.4.1. The temperature of the liquid and wall in the evaporator part of PHP was comparatively higher than that in the condenser and adiabatic area. According to observations, the wall temperature was greater than that of the working fluid within the PHP. Furthermore, it was observed that the temperatures within various sections and turns of the PHP exhibited irregularities and temporal fluctuations. The hybrid nanofluids showed a comparatively lower fluid temperature at the evaporator region than PHP when subjected to water charging. This phenomenon increased the temperature differential between the evaporator and condenser regions, leading to an elevation in thermal resistance during water utilization as the operating fluid. The study revealed that using nanofluid with PHP reduced the temperature differential between the evaporator and condenser regions, comparable to that observed in water. The observed phenomenon can be attributed to the thermal conductivity improvement of the nanofluids in the simulations, which has resulted in a higher heat transfer capacity. This allows for more excellent absorption and dissipation of heat at a faster rate than water. The current numerical findings about temperature contours provide a means of visualizing and elucidating the behavior of fluid temperature in PHP. These results corresponded with

the thermal properties demonstrated in the current experimental outcomes. Furthermore, similar temperature patterns were noted in PHP across multiple simulation trials conducted at a 60% filling ratio, utilizing hybrid nanofluids and water as coolants and subject to varying levels of thermal energy input.

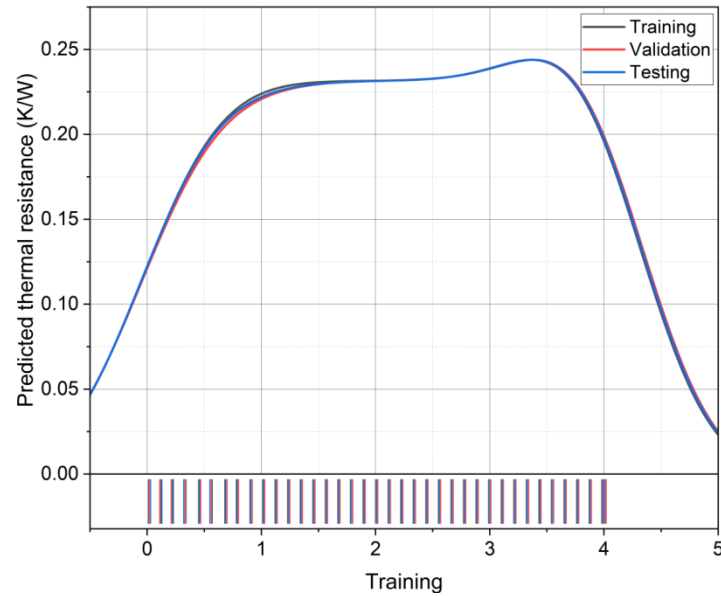


Figure 6.4.2. Predicted thermal resistance analysis

Figure 6.4.2 illustrates a comparative analysis of the suggested concept's anticipated heating resistance (K/W) and the observed thermal resistance (K/W) for training, validation, and testing condition. The information provided encompasses the mean outcomes of the deep learning algorithm's training, verification, and testing stages. The close alignment between the anticipated thermal resistance and the testing values suggests that the deep learning-based forecasting conduct is successful. The model's forecasting ability has been consistent and accurate across various temperature resistance values, evidenced by an average variance of 0.02 K/W between the anticipated and measured values. The results underscore the suggested framework's dependability and accuracy in forecasting the vibrating PHP's thermal resistance.

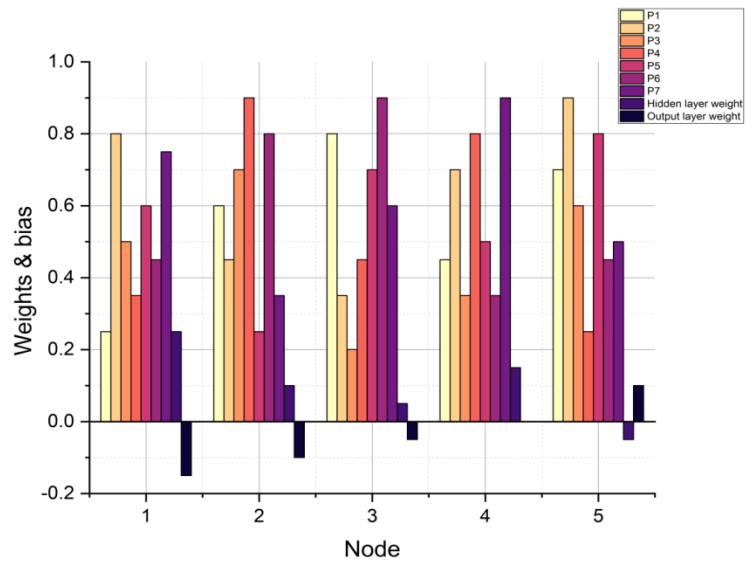


Figure 6.4.3 Weights & bias analysis of the ANN system

Figure 6.4.3 displays the weights and biases of the ANN model employed in the suggested concept. The numerical values assigned to the relationships between the nodes in the hidden and resultant layers are called weights, indicating these connections' relative strength. Biases are utilized as variables that offset and modify the input signals. The provided data discloses the precise numerical values of the weights and biases assigned to every node in both the hidden and output layers. The impact of the input features on the ultimate production of the model is determined by these values. Higher weights indicate a more significant effect of the equivalent input feature on the estimation, whereas lower weights suggest a comparatively lower influence. Biases are helpful in the process of refining forecasts. Through the manipulation of weights and preferences, the model can acquire the ability to learn and generate precise estimations based on the input data provided, thereby enhancing the efficacy of the proposed concept.

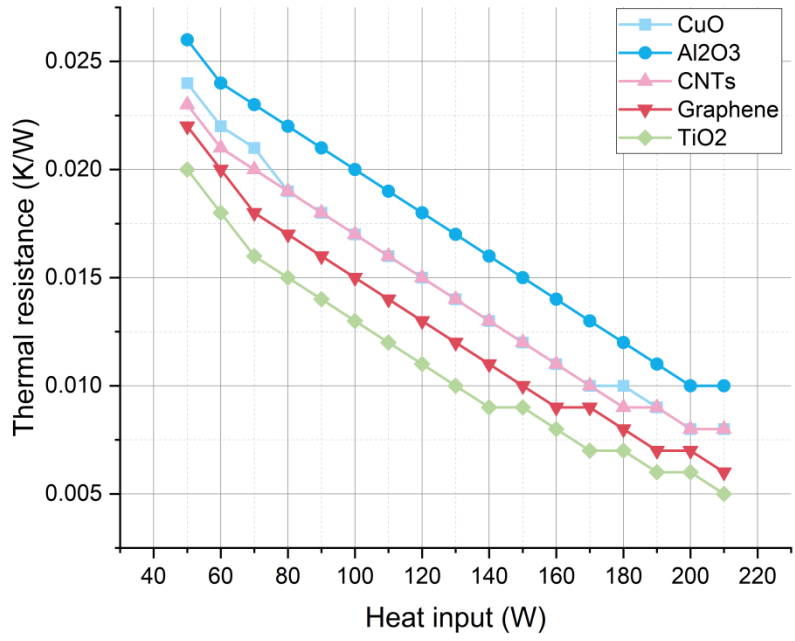


Figure 6.4.4 Thermal resistance analysis vs. heat input analysis of different nanomaterials

The thermal resistance values (in K/W) for various nanofluids, such as CuO, Al₂O₃, CNTs, Graphene, and TiO₂, at different heat input levels are depicted in Figure 6.4.4. Thermal resistance pertains to the degree of hindrance to heat transmission. It evaluates the efficacy of heat transfer in a system that has been improved with nanofluids. The empirical evidence indicates that an increase in heat input reduces thermal resistance, which suggests a corresponding enhancement in heat dissipation. Furthermore, the findings indicate that all types of nanofluids exhibit a decrease in heating resistance compared to the underlying fluid. TiO₂ displays the least heating resistance among the various types of nanofluids, with Graphene, CNTs, Al₂O₃, and CuO following in order of increasing thermal resistance. The mean outcomes suggest that integrating these nanofluids into the PHP amplifies its comprehensive thermal efficacy, resulting in heightened heating transfer and dissipation efficiency. This study's results support the suggested method of using nanofluids to augment the efficiency of PHP and confirm the potential of these particular nanofluids in attaining enhanced thermal management techniques.

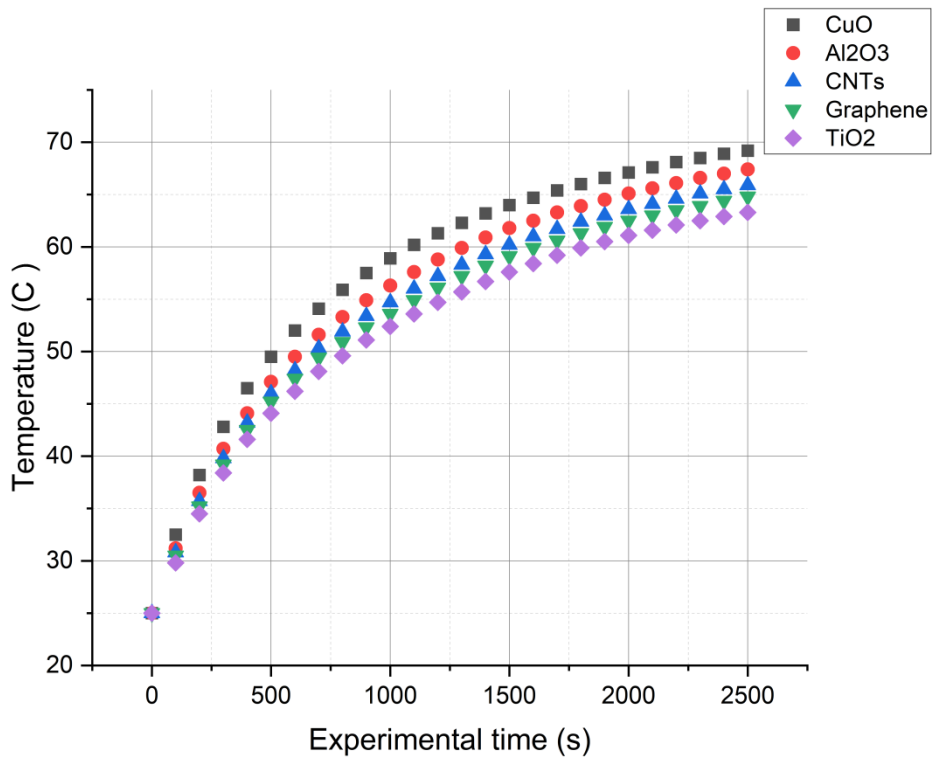


Figure 6.4.5 Temperature analysis of PHP with different experimental time

The profiles (in degrees Celsius) for various nanofluids, namely CuO, Al₂O₃, CNTs, Graphene, and TiO₂, during a simulated time interval, are plotted in Figure 6.4.5. The temperature profiles exhibit the nanofluids' impact on the system's thermal characteristics. At the outset, all nanofluids commence at ambient temperature, typically 25°C. As the simulation progresses, all nanofluids' temperatures gradually increase, albeit with varying rates of temperature rise. Based on the average outcomes, it can be inferred that the TiO₂ nanofluid displays the minimum temperature, succeeded by Graphene, CNTs, Al₂O₃, and CuO. The results validate the efficacy of integrating nanofluids into the PHP to augment heat transfer and optimize thermal regulation. The proposition is by the discoveries since the application of nanofluids facilitates the attainment of effective heat dissipation and the preservation of reduced temperatures in various thermal regulation systems.

During a simulated time interval, the results display temperature profiles for various nanofluids, namely CuO, Al₂O₃, CNTs, Graphene, and TiO₂. The temperature profiles exhibit the nanofluids' impact on the system's thermal characteristics. At the outset, all nanofluids commence at ambient temperature, typically 25°C. As the simulation continues, all nanofluids' temperatures gradually grow, albeit with varying rates of temperature rise. Based on the average outcomes, it can be inferred that the TiO₂

nanofluid displays the minimum temperature, succeeded by Graphene, CNTs, Al₂O₃, and CuO. The results validate the efficacy of integrating nanofluids into the PHP to augment heat transfer and optimize thermal regulation. The proposition is by the discoveries since the application of nanofluids facilitates the attainment of effective heat dissipation and the preservation of reduced temperatures in various thermal regulation systems.

6.5 Conclusion and future scope

The present study aimed to improve the operational efficiency of PHP by integrating nanofluids and deep learning-based forecasting techniques. Using PHPs as a heat transfer mechanism has surfaced as a promising prospect with diverse applications across diverse industries. The DL-PEP method was proposed to augment the thermal conductivity of PHPs by integrating TiO₂ nanomaterials into their working fluid. The experiment's findings indicate a significant enhancement in the thermal resistance of PHP upon incorporating nanofluids.

The accurate prediction of heat transfer properties in PHPs was facilitated using deep learning techniques, specifically an ANN model. The artificial neural network model that was created demonstrated significant correlation coefficients, thereby confirming its dependability in predicting the performance of PHP. The study's findings suggest that the TiO₂ nanofluid demonstrates the least thermal resistance (2.76 K/W) compared to the other nanofluids tested, namely Graphene, CNTs, Al₂O₃, and CuO. The nanofluids of CuO, Al₂O₃, CNTs, Graphene, and TiO₂ exhibit average temperature values of 60.1°C, 57.9°C, 56.7°C, 55.8°C, and 54.9°C, respectively. The results indicate that nanofluids, specifically TiO₂, can enhance thermal management and facilitate heat dissipation within the system.

The findings of this study provide novel insights into the potential applications of nanofluids and deep learning-based prediction techniques in enhancing the overall efficiency of PHPs. The results emphasize the feasibility of integrating nanomaterials, specifically TiO₂ nanoparticles, into the design of PHP to improve their thermal conductivity. In addition, incorporating deep learning methodologies presents a potentially advantageous pathway for precise forecasting of PHP functionality, thereby facilitating the implementation of more effective thermal regulation systems. Future investigations may delve into the refinement of nanofluid composition and concentration to attain superior outcomes in augmenting the performance of pulsating heat pipes. Furthermore, a thorough examination of the impact of various nanomaterials and their

amalgamations on the heat transfer characteristics of PHP could yield significant findings. Moreover, future investigating the practical implementation of DL-PEP in real-life situations and assessing its efficacy in thermal management systems on a large scale would be of considerable significance.

CONCLUSIONS AND FUTURE SCOPE

7.1 Conclusions

The entire research work is carried out to study the microfluidics flow through the heated pulsating heat pipe. Various application oriented physical phenomena are used to model and analyse the microfluidics through the pulsating heat pipe. The salient conclusions are given below:

The present study is one of the first to shed light on how non-Newtonian fluids' heat and mass transfer characteristics are affected by external magnetic fields and variations in liquid properties. A stepper motor drives the pump's mechanical system, separated from the electrical system by a power supply and a microprocessor. In this work, we propose a Mechanically Pulsating Heat Exchanger (MPHE-MT) that uses microfluidic technology. Hence to accomplish this, walls are constructed inside the flow channel. Each vascular waveform includes its minimum, maximum, and median flow rate. Patients with cortical and lacunar stroke did not differ significantly on any measure of flow or pulsatility.

According to the findings, the filling ratio had no effect on PHP speed. But when the condenser temperature and this parameter were both optimized, the PRS model showed that they work together to decrease the THR value. Both the concentration and the amount of heat supplied were critical operational parameters that determined the PHP's efficacy. While increasing the concentration of graphene Nano platelets did not improve the thermal performance of the PHP, adding more heat to the evaporator had a multiplicative effect. The pipes are not at a right angle, the heat is evenly distributed, the oscillation mode is marked by abrupt changes, and the PHP shows very little resistance to heat. Further, the shape of the heat distribution is unaffected by the inclination angle during gravity-assisted circulation of the working fluid, but the way in which temperatures oscillate is. When subjected to gravity-inhibited circulation at angles larger than 90 degrees, a single tube exhibits small-amplitude oscillations and a homogenous temperature distribution. By filling them with water, we assessed the heat exchangers' performance. Here, we introduce HP-PRS, a method for calculating heat exchanger efficiency by means of heat pipes equipped with pulsing response surfaces. The outcome is a strong thermal resistance for this mode. A symmetrical distribution of heat exists

even when the angle is one degree. But it seems like the way things are done doesn't change too often. At this very moment, the PHP has the lowest heat transmission resistance. We can find out how different materials with different wettability behave thermally by doing numerical simulations. When surfaces are wet or dry, the advancing and retreating angles change, which in turn affects the capillary resistance. Since the resistance increases as the number of liquid plugs increases, more hydrophobic plugs, as opposed to more hydrophilic ones, will result in a higher capillary resistance.

Thermal resistance is a measure of heat flow resistance across a certain thickness of material. Thermal resistance is calculated by dividing a sample's thickness by its thermal conductivity. From 30°C to 100 °C, the linear trend spectrum of observed temperature is shown, and the uncertainty error is less than 0.5°C. The thermal precision of this technique has also been clarified by temperature-sensitive amplification tests using nucleic acids. Consequently, it can be inferred that this technique has great promise for micro-macro interaction detection and is useful for purposes beyond microfluidic ones. Microfluidic devices offer an appropriate regulated environment for cell cultivation and drug testing on a broad range of cells, like cancer, liver, and microbial.

Our work here proposes a TRPHP-MF that makes use of microfluidics. This is achieved by erecting walls within the flow channel. There are minimum, maximum, and median values for blood flow represented in each vascular waveform. No significant differences were found in flow or pulsatility between patients with cortical and lacunar stroke. Heat transfer correlations appear to have limited predictive power for the PHP case due to their non-stationary behavior. It appears that this method of accurate modeling is the PHP dynamic simulation. Tools for predictive simulation that can aid in the development of optimized industrial prototypes are needed. For better comprehension of the thermofluidic working principles of rectangular-channel TRPHP-MF, this paper presents a comprehensive analysis of many new theoretical and experimental investigations on the thermal and flow characteristics of pulsing heat pipes made of flat plates and two-phase flows in rectangular mini- and micro channels and gains better accuracy and efficiency of 90.9% and the performance is achieved as 97.8%. For effective heat transmission in today's electronics, the incorporation of Pulsating Heat Pipes (PHPs) in microfluidic systems is an exciting new development. PHPs have the ability to handle temperature control difficulties because to their distinctive characteristics, which are driven by passive mechanisms and strengthened by

the suggested Temperature Regulation in a Pulsating Heat Pipe Using Microfluidics [TRPHP-MF]. This investigation highlights the need of having a thorough understanding of PHP-based thermal solutions and continuing to commit time and energy to their discovery as we negotiate the complexity of pulsatile flows and expands our horizons.

The findings of this study provide novel insights into the potential applications of nanofluids and deep learning-based prediction techniques in enhancing the overall efficiency of PHPs. The results emphasize the feasibility of integrating nanomaterials, specifically TiO₂ nanoparticles, into the design of PHP to improve their thermal conductivity. In addition, incorporating deep learning methodologies presents a potentially advantageous pathway for precise forecasting of PHP functionality, thereby facilitating the implementation of more effective thermal regulation systems. Future investigations may delve into the refinement of nanofluid composition and concentration to attain superior outcomes in augmenting the performance of pulsating heat pipes. Furthermore, a thorough examination of the impact of various nanomaterials and their amalgamations on the heat transfer characteristics of PHP could yield significant findings.

7.2 Future Scope

The study of flow through oscillatory micro channels has the vast applications in MEMS, medical and automobile and many other industries. So the present study can be extended with different materials and correlating the numerical results with the experimental values is having high demand in designing the devices in the above said industries. Moreover, future investigating the practical implementation of DL-PEP in real-life situations and assessing its efficacy in thermal management systems on a large scale would be of considerable significance.

REFERENCES

- 1 Ali, A., Si, Q., Yuan, J., Shen, C., Cao, R., SaadAlGarni, T., ...& Aslam, B. (2022). Investigation of energy performance, internal flow and noise characteristics of miniature drainage pump under water–air multiphase flow: Design and part load conditions. *International Journal of Environmental Science and Technology*, 19(8), 7661-7678.
- 2 Chen, X., Chen, S., Zhang, Z., Sun, D., & Liu, X. (2021). Heat transfer investigation of a flat-plate oscillating heat pipe with tandem dual channels under nonuniform heating. *International Journal of Heat and Mass Transfer*, 180, 121830.
- 3 Cornejo, I., Nikrityuk, P., Lange, C., & Hayes, R. E. (2020). Influence of upstream turbulence on the pressure drop inside a monolith. *Chemical Engineering and Processing-Process Intensification*, 147, 107735.
- 4 Eidan, A. A., Alshukri, M. J., Al-fahham, M., AlSahlani, A., & Abdulridha, D. M. (2021). Optimizing the performance of the air conditioning system using an innovative heat pipe heat exchanger. *Case Studies in Thermal Engineering*, 26, 101075.
- 5 Grimstein, M., Yang, Y., Zhang, X., Grillo, J., Huang, S. M., Zineh, I., & Wang, Y. (2019). Physiologically based pharmacokinetic modelling in regulatory science: an update from the US Food and Drug Administration's Office of Clinical Pharmacology. *Journal of pharmaceutical sciences*, 108(1), 21-25.
- 6 Jo, J., Kim, J., & Kim, S. J. (2019). Experimental investigations of heat transfer mechanisms of a pulsating heat pipe. *Energy Conversion and Management*, 181, 331-341.
- 7 Jouhara, H., Almahmoud, S., Brough, D., Guichet, V., Delpech, B., Chauhan, A., ...& Serey, N. (2021). Experimental and theoretical investigation of the performance of an air to water multi-pass heat pipe-based heat exchanger. *Energy*, 219, 119624.
- 8 Jouhara, H., Bertrand, D., Axcell, B., Montorsi, L., Venturelli, M., Almahmoud, S., ...& Chauhan, A. (2021). Investigation on a full-scale heat pipe heat exchanger in the ceramics industry for waste heat recovery. *Energy*, 223, 120037.

- 9 Meng, J., Yu, C., Li, S., Wei, C., Dai, S., Li, H., & Li, J. (2022). Microfluidics Temperature Compensating and Monitoring Based on Liquid Metal Heat Transfer. *Micromachines*, 13(5), 792.
- 10 Pries, A.R., Albrecht, K.H. and Gachtgens, P. “Model studies on phase separation at a capillary orifice”. *Biorheology*, 18; pp. 355-367, 1981.
- 11 Santhosh Nallapu and Radhakrishnamacharya, G. “Effect of Slip in a Two-Fluid Model of Couple-Stress Fluid flow through a Porous Medium in a Narrow Channel”. Vol.113, No.11, 55-64, 2017.
- 12 Shang, F., Fan, S., Yang, Q., & Liu, J. (2020). An experimental investigation on heat transfer performance of pulsating heat pipe. *Journal of Mechanical Science and Technology*, 34, 425-433.
- 13 Sun, H., Duan, M., Wu, Y., Lin, B., Yang, Z., & Zhao, H. (2021). Thermal performance investigation of a novel heating terminal integrated with flat heat pipe and heat transfer enhancement. *Energy*, 236, 121411.
- 14 Wang, C. S., Wei, T. C., Shen, P. Y., & Liou, T. M. (2020). Lattice Boltzmann study of flow pulsation on heat transfer augmentation in a louvered microchannel heat sink. *International Journal of Heat and Mass Transfer*, 148, 119139.
- 15 Xu, Y., Xue, Y., Qi, H., & Cai, W. (2020). Experimental study on heat transfer performance of pulsating heat pipes with hybrid working fluids. *International Journal of Heat and Mass Transfer*, 157, 119727.
- 16 Yin, S., Yu, R., Sheng, D., Mao, W., & Zhao, Y. (2023). Research on the Dynamic Characteristics Analysis and Power Control Method of Heat Pipe Reactors. *Applied Sciences*, 13(20), 11284.
- 17 Zhang, Y., Ji, J., Song, Z., Ke, W., & Xie, H. (2023). Performance prediction on a novel dual-mode heat pump with a hybrid photovoltaic/micro-channel heat pipe/fin heat exchanger. *Energy Conversion and Management*, 293, 117505.

- 18 Zhao, J., Jian, Q., & Huang, Z. (2020). Visualization study on enhancing water transport of proton exchange membrane fuel cells with a dead-ended anode by generating fluctuating flow at anode compartment. *Energy Conversion and Management*, 206, 112477.
- 19 Abdel-Latif, K., Epps, R. W., Kerr, C. B., Papa, C. M., Castellano, F. N., & Abolhasani, M. (2019). Facile Room-Temperature Anion Exchange Reactions of Inorganic Perovskite Quantum Dots Enabled by a Modular Microfluidic Platform. *Advanced functional materials*, 29(23), 1900712.
- 20 Abo-Hammour, Z., Abu Arqub, O., Momani, S., & Shawagfeh, N. (2014). Optimization solution of Troesch's and Bratu's problems of ordinary type using novel continuous genetic algorithm. *Discrete Dynamics in Nature and Society*, 2014 <https://doi.org/10.1155/2014/401696>.
- 21 Abu-Hamdeh, N. H., Bantan, R. A., Aalizadeh, F., & Alimoradi, A. (2020). Controlled drug delivery using the magnetic nanoparticles in non-Newtonian blood vessels. *Alexandria Engineering Journal*, 59(6), 4049-4062.
- 22 Ahmed, S., Nashine, C., & Pandey, M. (2022). Thermal management at microscale level: Detailed study on the development of a micro loop heat pipe. *Micro and Nano Engineering*, 16, 100150.
- 23 Al Jubori, A. M., & Jawad, Q. A. (2020). Computational evaluation of thermal behavior of a wickless heat pipe under various conditions. *Case Studies in Thermal Engineering*, 22, 100767.
- 24 Alhajaj, Z., Bayomy, A. M., Saghir, M. Z., & Rahman, M. M. (2020). Flow of nanofluid and hybrid fluid in porous channels: Experimental and numerical approach. *International Journal of Thermofluids*, 1, 100016.
- 25 Alizadeh, A., Ghadamian, H., Aminy, M., Hoseinzadeh, S., Sahebi, H. K., & Sohani, A. (2022). An experimental investigation on using heat pipe heat exchanger to improve energy performance in gas city gate station. *Energy*, 252, 123959.

- 26 Alizadeh, A., Movahedi, P., Mirzahosseini, S., &Ekhtiari, S. (2022). Investigating different types of fluids in pulsating heat pipes for improving heat transfer in an air-cooled heat exchanger. *Proceedings of the Institution of Mechanical Engineers, Part A: Journal of Power and Energy*, 09576509221076689.
- 27 Alqahtani, A. A., Edwardson, S., Marengo, M., &Bertola, V. (2022). Performance of flat-plate, flexible polymeric pulsating heat pipes at different bending angles. *Applied Thermal Engineering*, 216, 118948.
- 28 Arqub, O. A., & Abo-Hammour, Z. (2014). Numerical solution of systems of second-order boundary value problems using continuous genetic algorithm. *Information sciences*, 279, 396-415.
- 29 Attinger, E. O. (Ed.) (1964), *Pulsatile blood flow*. In *Proc. Int. Symp. Pulsatile Blood Flow*, April 11-13, 1963, McGraw-Hill, New York.
- 30 Ayel, V., Slobodeniuk, M., Bertossi, R., Karmakar, A., Martineau, F., Romestant, C., ... &Khandekar, S. (2022). Thermal performances of a flat-plate pulsating heat pipe tested with water, aqueous mixtures, and surfactants. *International Journal of Thermal Sciences*, 178, 107599.
- 31 Ayel, V., Slobodeniuk, M., Bertossi, R., Romestant, C., &Bertin, Y. (2021). Flat plate pulsating heat pipes: A review on the thermohydraulic principles, thermal performances and open issues. *Applied Thermal Engineering*, 197, 117200.
- 32 Bai, W., Chen, W., Zeng, C., Wu, G., & Chai, X. (2022). Thermo-hydraulic performance investigation of heat pipe used annular heat exchanger with densely longitudinal fins. *Applied Thermal Engineering*, 211, 118451.
- 33 Barrak, A. S., Saleh, A. A., &Naji, Z. H. (2020). An experimental study of using water, methanol, and binary fluids in oscillating heat pipe heat exchanger. *Engineering Science and Technology, an International Journal*, 23(2), 357-364.

- 34 Bhatt, A. A., Jain, S. V., & Patel, R. N. (2022). Experimental Investigations on performance analysis of a wickless thermosiphon heat pipe with two heat sources and multiple branches. *Journal of Thermal Science and Engineering Applications*, 14(10), 101006.
- 35 Bhavana, H. T., Sunil, M. A., Sanjana, T., & Harshitha, B. (2023). Recent Advances in Drug Delivery Systems: MEMS Perspective. *Disruptive Developments in Biomedical Applications*, 299-309, eBook ISBN : 9781003272694.
- 36 Błasiak, P., Opalski, M., Parmar, P., Czajkowski, C., & Pietrowicz, S. (2021). The thermal—Flow processes and flow pattern in a pulsating heat pipe—Numerical modelling and experimental validation. *Energies*, 14(18), 5952.
- 37 Brough, D., Ramos, J., Delpech, B., & Jouhara, H. (2021). Development and validation of a TRNSYS type to simulate heat pipe heat exchangers in transient applications of waste heat recovery. *International Journal of Thermofluids*, 9, 100056.
- 38 Bunge, F., van den Driesche, S., Waespy, M., Radtke, A., Belge, G., Kelm, S., ... & Vellekoop, M. J. (2019). The microfluidic oxygen sensor system is a tool to monitor the metabolism of mammalian cells. *Sensors and Actuators B: Chemical*, 289, 24-31.
- 39 Buonomo, B., di Pasqua, A., Manca, O., & Nardini, S. (2020). Evaluation of thermal and fluid dynamic performance parameters in aluminum foam compact heat exchangers. *Applied Thermal Engineering*, 176, 115456.
- 40 Cao, Y., Wang, T., & Sepúlveda, N. (2023). Microfluidic thermal flow sensor based on phase-change material with ultra-high thermal sensitivity. *Journal of Materials Chemistry C, J. Mater. Chem. C*, 2023, 11, 1278-1284.
- 41 Cavaniol, C., Cesar, W., Descroix, S., & Viovy, J. L. (2022). Flowmetering for microfluidics. *Lab on a Chip*, 22(19), 3603-3617.
- 42 Chakravarty, S. and Datta, A., “Effects of Stenosis on Arterial Rheology through Mathematical Model”, *Math. Comput. Model*, Vol. 12, No.12, (1989), 1601 – 1612.

- 43 Chaturani, P. and Upadhya, V.S. "A Two – Fluid Model for Blood Flow through Small diameter Tubes," *Bio rheology*, Vol.18, pp.245-253, 1981.
- 44 Chaturani, P. and Upadhya, V.S. "On Micro polar Fluid Model for Blood Flow through Narrow Tubes," *Bio rheology*, Vol.16, pp. 419-428, 1979.
- 45 Chen, G., Zheng, J., Liu, L., & Xu, L. (2019). Application of microfluidics in wearable devices. *Small Methods*, 3(12), 1900688.
- 46 Chien, S. Usami, S. and Skalak, R. "Blood flow in small tubes", in: *Handbook of Physiology, Section 2: "The Cardiovascular System IV", Part I:Microcirculation*, Renkin, E.M. and Michel, C. C.eds, American Physiological Society, Bethesda, MD, 1984, pp. 217-249.
- 47 Chirag, D. A. V. E., Dandale, P., Shrivastava, K., Dhaygude, D., Rahangdale, K., & Nilesh, M. O. R. E. (2021). A review on pulsating heat pipes: Latest research, applications and future scope. *Journal of Thermal Engineering*, 7(3), 387-408.
- 48 Chopra, K., Pathak, A. K., Tyagi, V. V., Pandey, A. K., Anand, S., & Sari, A. (2020). Thermal performance of phase change material integrated heat pipe evacuated tube solar collector system: An experimental assessment. *Energy Conversion and Management*, 203, 112205.
- 49 Coluccio, M. L., Perozziello, G., Malara, N., Parrotta, E., Zhang, P., Gentile, F., ... & Di Fabrizio, E. (2019). Microfluidic platforms for cell cultures and investigations. *Microelectronic Engineering*, 208, 14-28.
- 50 Cooksey, G. A., Patrone, P. N., Hands, J. R., Meek, S. E., & Kearsley, A. J. (2019). Dynamic measurement of nanoflows: realization of an optofluidic flow meter to the nanoliter-per-minute scale. *Analytical chemistry*, 91(16), 10713-10722.
- 51 Cui, W., Yesiloz, G., & Ren, C. L. (2020). Microwave heating induced on-demand droplet generation in microfluidic systems. *Analytical Chemistry*, 93(3), 1266-1270.
- 52 Dincau, B., Dressaire, E., & Sauret, A. (2020). Pulsatile flow in microfluidic systems. *Small*, 16(9), 1904032.

- 53 Doh, I., Sim, D., & Kim, S. S. (2022). Microfluidic Thermal Flowmeters for Drug Injection Monitoring. *Sensors*, 22(9), 3151.
- 54 Edwardson, S., & Bertola, V. (2020). Manufacturing low-cost fluidic and heat transfer devices by selective transmission laser welding, 11th CIRP conference on photonic technologies, 2020.
- 55 Esfe, M. H., Bahiraei, M., Torabi, A., & Valadkhani, M. (2021). A critical review on pulsating flow in conventional fluids and nanofluids: Thermo-hydraulic characteristics. *International Communications in Heat and Mass Transfer*, 120, 104859.
- 56 Fahraeus, R. and Lindqvist, T. "Viscosity of Blood in Narrow Capillary Tubes". *Am J Physiol.* 96 (1931) 562 – 568.
- 57 Firdous, H., Husnine, S. M., Hussain, F., & Nazeer, M. (2020). Velocity and thermal slip effects on two-phase flow of MHD Jeffrey fluid with the suspension of tiny metallic particles. *Physica Scripta*, 96(2), 025803.
- 58 Fonseca, L. D., Pfothenauer, J., & Miller, F. (2018). Results of a three evaporator cryogenic helium pulsating heat pipe. *International Journal of Heat and Mass Transfer*, 120, 1275-1286.
- 59 Gaehtgens, P.A. (1970). Pulsatile pressure and flow in the mesenteric vascular bed of the cat, *Pflügers Arch.* 316, 14-151.
- 60 Gan, J. S., Yu, H., Tan, M. K., Soh, A. K., Wu, H. A., & Hung, Y. M. (2020). Performance enhancement of graphene-coated micro heat pipes for light-emitting diode cooling. *International Journal of Heat and Mass Transfer*, 154, 119687.
- 61 Hao, T., Jiang, Z., Cui, W., Wen, R., Ma, X., & Ma, H. Heat Transfer Enhancement in an Oscillating Heat Pipe with Self-Dispersion Liquid Metal Micro-Droplets, *SSRN 3989560, 2022.*
- 62 Intaglietta, M. (1971). Pulsatile velocity components in the cat mesenteric microvasculature. "Proc. VI Conference on Microcirculation." Karger, Basel, 1971.

- 63 Iwata, N., Bozzoli, F., Pagliarini, L., Cattani, L., Vocale, P., Malavasi, M., & Rainieri, S. (2022). Characterization of thermal behavior of a micro pulsating heat pipe by local heat transfer investigation. *International Journal of Heat and Mass Transfer*, 196, 123203.
- 64 Jderu, A., Soto, M. A., Enachescu, M., & Ziegler, D. (2021). Liquid flow meter by fibre-optic sensing of heat propagation. *Sensors*, 21(2), 355.
- 65 Jung, C., Lim, J., & Kim, S. J. (2020). Fabrication and evaluation of a high-performance flexible pulsating heat pipe hermetically sealed with metal. *International Journal of Heat and Mass Transfer*, 149, 119180.
- 66 Kang, Z., Shou, D., & Fan, J. (2021). Numerical study of a novel Single-loop pulsating heat pipe with separating walls within the flow channel. *Applied Thermal Engineering*, 196, 117246.
- 67 Kelly, B., Hayashi, Y., & Kim, Y. J. (2018). Novel radial pulsating heat-pipe for high heat-flux thermal spreading. *International Journal of Heat and Mass Transfer*, 121, 97-106.
- 68 Khalilmoghadam, P., Rajabi-Ghahnavieh, A., & Shafii, M. B. (2021). A novel energy storage system for latent heat recovery in solar still using phase change material and pulsating heat pipe. *Renewable Energy*, 163, 2115-2127.
- 69 Kim, J., & Kim, S. J. (2020). Experimental investigation on working fluid selection in a micro pulsating heat pipe. *Energy Conversion and Management*, 205, 112462.
- 70 [Kim, W., & Kim, S. J. \(2021\). Fundamental issues and technical problems about pulsating heat pipes. *Journal of Heat Transfer*, Oct 2021, 143\(10\): 100803 \(10 pages\) Paper No: HT-21-1192.](#)
- 71 Kingston, T. A., Weibel, J. A., & Garimella, S. V. (2020). Time-resolved characterization of microchannel flow boiling during transient heating: Part 1—Dynamic response to a single heat flux pulse. *International Journal of Heat and Mass Transfer*, 154, 119643.

- 72 Kong, M., Li, Z., Wu, J., Hu, J., Sheng, Y., Wu, D., ... & Wang, S. (2019). A wearable microfluidic device for rapid detection of HIV-1 DNA using recombinase polymerase amplification. *Talanta*, 205, 120155.
- 73 Krishnaraj, S., Kumar, A., Murali, B., &Subathra, T. (2021). Optimization of One Way Tesla Valve (No. 2021-28-0250). SAE Technical Paper.
- 74 Li, C., & Li, J. (2023). Thermal characteristics of a flat plate pulsating heat pipe module for onsite cooling of high power server CPUs. *Thermal Science and Engineering Progress*, 37, 101542.
- 75 Li, C., & Li, J. (2023). Thermal characteristics of a flat plate pulsating heat pipe module for onsite cooling of high-power server CPUs. *Thermal Science and Engineering Progress*, 37, 101542.
- 76 Li, J., Hu, Z., Jiang, H., Guo, Y., Li, Z., Zhuge, W., ...& Ouyang, M. (2023). Coupled characteristics and performance of heat pipe cooled reactor with closed Brayton cycle. *Energy*, 280, 128166.
- 77 Li, Q., Wang, C., Wang, Y., Wang, Z., Li, H., &Lian, C. (2020). Study on the effect of the adiabatic section parameters on the performance of pulsating heat pipes. *Applied Thermal Engineering*, 180, 115813.
- 78 Li, Z., Sarafraz, M. M., Mazinani, A., Moria, H., Tlili, I., Alkanhal, T. A., ... &Safaei, M. R. (2020). Operation analysis, response, and performance evaluation of a pulsating heat pipe for low-temperature heat recovery. *Energy Conversion and Management*, 222, 113230.
- 79 Li, Z., Sarafraz, M. M., Mazinani, A., Moria, H., Tlili, I., Alkanhal, T. A., ...&Safaei, M. R. (2020). Operation analysis, response and performance evaluation of a pulsating heat pipe for low temperature heat recovery. *Energy Conversion and Management*, 222, 113230.
- 80 Liu, S., Fan, Y., Gao, K., & Zhang, Y. (2018). Fabrication of Cyclo-olefin polymer-based microfluidic devices using CO₂ laser ablation. *Materials Research Express*, 5(9), 095305.

- 81 Liu, X., Chen, X., Zhang, Z., & Chen, Y. (2020). Thermal performance of a novel dual-serpentine-channel flat-plate oscillating heat pipe used for multiple heat sources and sinks. *International Journal of Heat and Mass Transfer*, 161, 120293.
- 82 Liu, X., Xu, L., Wang, C., & Han, X. (2019). Experimental study on thermo-hydrodynamic characteristics in a micro oscillating heat pipe. *Experimental Thermal and Fluid Science*, 109, 109871.
- 83 Liu, Z., Quan, Z., Zhao, Y., Zhang, W., Yang, M., Shi, J., & Bai, Z. (2023). Dynamic modelling and performance prediction of a novel direct-expansion ice thermal storage system based multichannel flat tube evaporator plus micro heat pipe arrays storage module. *Renewable Energy*, 217, 119153.
- 84 Lohse, D. (2022). Fundamental fluid dynamics challenges in inkjet printing. *Annual review of fluid mechanics*, 54, 349-382.
- 85 Luo, X., Su, P., Zhang, W., & Raston, C. L. (2019). Microfluidic devices in fabricating nano or micromaterials for biomedical applications. *Advanced Materials Technologies*, 4(12), 1900488.
- 86 Lv, W., Li, J., & Chen, M. (2023). Experimental study on the thermal management performance of a power battery module with a pulsating heat pipe under different thermal management strategies. *Applied Thermal Engineering*, 227, 120402.
- 87 MacDonald, D.A.(1960), "Blood Flow in Arteries," Arnold, London.
- 88 Maithili Sharan., Alexander S. Popel. "A two-phase model for flow of blood in narrow tubes with increased effective viscosity near the wall". *Biorheology*, 415-428, 2001.
- 89 Mameli, M., Besagni, G., Bansal, P. K., & Markides, C. N. (2022). Innovations in pulsating heat pipes: From origins to future perspectives. *Applied Thermal Engineering*, 203, 117921.
- 90 Mangini, D., Pozzoni, M., Mameli, M., Pietrasanta, L., Bernagozzi, M., Fioriti, D., ... & Marengo, M. (2018). Infrared analysis and pressure measurements on a single loop pulsating heat pipe at different gravity levels. In *Proceedings of the Joint 19th*

IHPC and 13th IHPS, Pisa, Italy, June 10-14, 2018. (pp. 1-10). ITA.

- 91 Mapelli, A. (2020). Microfabricated silicon substrates for pixel detectors assembly and thermal management aka Silicon Microchannel Cooling Plates. Nuclear Instruments and Methods in Physics Research Section A: Accelerators, Spectrometers, Detectors and Associated Equipment, 958, 162142.
- 92 Markal, B., &Varol, R. (2020). Thermal investigation and flow pattern analysis of a closed-loop pulsating heat pipe with binary mixtures. Journal of the Brazilian Society of Mechanical Sciences and Engineering, 42(10), 1-18.
- 93 Markal, B., &Varol, R. (2021). Experimental investigation and force analysis of flat-plate type pulsating heat pipes having ternary mixtures. International Communications in Heat and Mass Transfer, 121, 105084.
- 94 Maruthi Prasad, K. and Radhkrishnamacharya, G., “Flow of Herschel-Bulkley Fluid through an Inclined tube of Non-uniform Cross-section with Multiple Stenosis,” Arch. Mech., Vol. 60, No. 2, pp. 161-172, 2008.
- 95 Matellan, C., & del Río Hernández, A. E. (2018). Cost-effective rapid prototyping and assembly of poly (methyl methacrylate) microfluidic devices. Scientific reports, 8(1), 1-13.
- 96 Misra, J.C. and Chakravarthy, S., “Flow in Arteries in the Presence of Stenosis”, J. Biomech., Vol.19, No. 11, (1986), 907-918.
- 97 Nair, P.K. Hellums, J.D. and Olson, J.S. “Prediction of oxygen transport rates in blood flowing in large capillaries”, Microvasc. Res.38 (1989), 269-285.
- 98 Narayan, S., Moravec, D. B., Dallas, A. J., & Dutcher, C. S. (2020). Droplet shape relaxation in a four-channel microfluidic hydrodynamic trap. Physical Review Fluids, 5(11), 113603.
- 99 Nikolayev, V. S. (2021). Physical principles and state-of-the-art of modeling of the pulsating heat pipe: A review. Applied Thermal Engineering, 195, 117111.

- 100 Noh, H. Y., & Kim, S. J. (2020). Numerical simulation of pulsating heat pipes: Parametric investigation and thermal optimization. *Energy conversion and management*, 203, 112237.
- 101 Ordu, M., & Der, O. (2023). Polymeric Materials Selection for Flexible Pulsating Heat Pipe Manufacturing Using a Comparative Hybrid MCDM Approach. *Polymers*, 15(13), 2933.
- 102 Pagliarini, L., Cattani, L., Bozzoli, F., Mameli, M., Filippeschi, S., Rainieri, S., & Marengo, M. (2021). Thermal characterization of a multi-turn pulsating heat pipe in microgravity conditions: Statistical approach to the local wall-to-fluid heat flux. *International Journal of Heat and Mass Transfer*, 169, 120930.
- 103 Palanivel, V., Govindasamy, K., & Arunachalam, G. K. (2022). Optimization and prediction of pulsating heat pipe compound parabolic solar collector performances by hybrid deep belief network-based bald eagle search optimizer. *Environmental Progress & Sustainable Energy*, 41(2), e13740.
- 104 Parot, J., Caputo, F., Mehn, D., Hackley, V. A., & Calzolari, L. (2020). Physical characterization of liposomal drug formulations using multi-detector asymmetrical-flow field flow fractionation. *Journal of Controlled Release*, 320, 495-510.
- 105 Pavan, C. A., & Guerra-Garcia, C. (2022). Nanosecond pulsed discharge dynamics during passage of a transient laminar flame. *Plasma Sources Science and Technology*, Colin A Pavan and Carmen Guerra-Garcia 2022 **31** 115016.
- 106 Peng, J., Fang, C., Ren, S., Pan, J., Jia, Y., Shu, Z., & Gao, D. (2019). Development of a microfluidic device with precise on-chip temperature control by integrated cooling and heating components for single cell-based analysis. *International Journal of Heat and Mass Transfer*, 130, 660-667.
- 107 Phan, N., & Nagano, H. (2022). Novel hybrid structures to improve performance of miniature flat evaporator loop heat pipes for electronics cooling. *International Journal of Heat and Mass Transfer*, 195, 123187.

- 108 Pietrasanta, L., Mameli, M., Mangini, D., Georgoulas, A., Michè, N., Filippeschi, S., & Marengo, M. (2020). Developing flow pattern maps for accelerated two-phase capillary flows. *Experimental Thermal and Fluid Science*, 112, 109981.
- 109 Pries, A.R. Secomb, T.W. and Gaehtgens, P. “Biophysical aspects of blood flow in the microvasculature”, *Cardiovasc. Res.* 32 (1996), 654-667.
- 110 Rajale, M. J., Prasad, P. I., & Rao, B. N. (2023). A review on the heat transfer performance of pulsating heat pipes. *Australian Journal of Mechanical Engineering*, 21(5), 1658-1702.
- 111 Rappaport, M.B.Bloch, E.H., And Irwin, J.W. (1959), A manometer for measuring dynamic pressure in the microvascular system, *J. Appl. Physiol.* 14, 651-655.
- 112 Riehl, R. R., &Murshed, S. S. (2022). Performance evaluation of nanofluids in loop heat pipes and oscillating heat pipes. *International Journal of Thermofluids*, 14, 100147.
- 113 Rudresha, S., Babu, E. R., &Thejaraju, R. (2023). Experimental Investigation and Influence of Filling Ratio on Heat Transfer Performance of a Pulsating Heat Pipe. *Thermal Science and Engineering Progress*, 101649.
- 114 Rudresha, S., Babu, E. R., &Thejaraju, R. (2023). Experimental investigation and influence of filling ratio on heat transfer performance of a pulsating heat pipe. *Thermal Science and Engineering Progress*, 38, 101649.
- 115 Saad, M. G., Selahi, A., Zoromba, M. S., Mekki, L., El-Bana, M., Dosoky, N. S., ... &Shafik, H. M. (2019). A droplet-based gradient is microfluidic to monitor and evaluate the growth of *Chlorella Vulgaris* under different levels of nitrogen and temperatures. *Algal Research*, 44, 101657.
- 116 Sankar, D.S. and Lee, U., “Two-fluid Herschel-Bulkley Model for Blood Flow in Catheterized Arteries,” *J. Mech. Sci. Tech.* Vol.22, pp. 1008-1018, 2008.
- 117 Santhosh Nallapu and Radhakrishnamacharya, G. “Flow of Jeffrey Fluid through Narrow tubes”. Vol. 4, Issue 11, 2013.

- 118 Santhosh Nallapu., Radhakrishnamacharya G. “Jeffrey Fluid Flow through A Narrow Tube In The Presence Of a Magnetic Field”. 127, (2015), 185 – 192.
- 119 Sharan, M. and Popel, A.S. “ A Two-Phase Model for Flow of Blood in Narrow Tubes with increased Effective Viscosity near the Wall,” Bio rheology, Vol.38, pp.415-428, 2001.
- 120 Sharan, M. and Popel, A.S. “A Two-phase Model for Flow of Blood in Narrow Tubes with increased Effective Viscosity near the Wall” Bio rheology 38 (2001) 415-428.
- 121 Somasundaram, R., &Subramanyam Reddy, A. (2021). Pulsating flow of electrically conducting couple stress nanofluid in a channel with ohmic dissipation and thermal radiation–Dynamics of blood. Proceedings of the Institution of Mechanical Engineers, Part E: Journal of Process Mechanical Engineering, 235(6), 1895-1909.
- 122 Sonawane, C. R., Tolia, K., Pandey, A., Kulkarni, A., Punchal, H., Sadasivuni, K. K., ... & Khalid, M. (2023). Experimental and numerical analysis of heat transfer and fluid flow characteristics inside pulsating heat pipe. Chemical Engineering Communications, 210(4), 549-565.
- 123 Stevens, K. A., Smith, S. M., & Taft, B. S. (2019). Variation in oscillating heat pipe performance. Applied Thermal Engineering, 149, 987-995.
- 124 Sukarno, R., Putra, N., & Hakim, I. I. (2021). Non-dimensional analysis for heat pipe characteristics in the heat pipe heat exchanger as energy recovery device in the HVAC systems. Thermal Science and Engineering Progress, 26, 101122.
- 125 Sun, H., Wu, Y., Lin, B., Duan, M., Lin, Z., & Li, H. (2020). Experimental investigation on the thermal performance of a novel radiant heating and cooling terminal integrated with a flat heat pipe. Energy and Buildings, 208, 109646.
- 126 Tang, D., “An Axisymmetric Model for Viscous flow in Tapered Collapsible Stenotic Elastic Tubes”, Adv. Bioengi., Vol. 33, (1996), 87-88.

- 127 Tharayil, T., Asirvatham, L. G., Manova, S., Vivek, V. M., Senthil Saravanan, M. S., Sajin, J. B., & Wongwises, S. (2022). An experimental investigation on the heat transfer characteristics of closed-loop pulsating heat pipe with graphene–water nanofluid. *Journal of Thermal Analysis and Calorimetry*, 147(22), 12721-12737.
- 128 Thurgood, P., Suarez, S. A., Pirogova, E., Jex, A. R., Peter, K., Baratchi, S., & Khoshmanesh, K. (2020). Tunable harmonic flow patterns in microfluidic systems through simple tube oscillation. *Small*, 16(43), 2003612.
- 129 Vajravelu, K., Sreenadh, S, and Devaki, P. and Prasad K.V., “Mathematical Model for a Herschel-Bulkley Fluid Flow in an Elastic Tube,” *Cent. Eur. J. Phys.*, Vol. 9, No. 5, pp. 1357-1365, 2011.
- 130 Van Erp, R., Soleimanzadeh, R., Nela, L., Kampitsis, G., & Matioli, E. (2020). Co-designing electronics with microfluidics for more sustainable cooling. *Nature*, 585(7824), 211-216.
- 131 Verma, S.R. and Anuj Srivastava. “Analytical study of A Two-Phase Model for Steady Flow of Blood in A Circular Tube”. Vol. 4, pp. 01-10, 2014.
- 132 VK, N. Opportunities, challenges, and state of the art of flexible heat-pipe heat exchangers: A comprehensive review. *Heat Transfer*, 2023.
<https://doi.org/10.1002/htj.22978>
- 133 Wang, H. (2020). Analytical and computational modeling of multiphase flow in ferrofluid charged oscillating heat pipes, 2020. <https://hdl.handle.net/11244/324967>.
- 134 Wang, H., Bao, Y., Liu, M., Zhu, S., Du, X., & Hou, Y. (2022). Experimental study on dynamic characteristics of cylindrical horizontal axially rotating heat pipe. *Applied Thermal Engineering*, 209, 118248.
- 135 Wang, J., Xie, J., & Liu, X. (2020). Investigation of wettability on performance of pulsating heat pipe. *International Journal of Heat and Mass Transfer*, 150, 119354.
- 136 Wang, P., He, L., & Liu, Y. (2020). Acoustics-driven vortex dynamics in channel branches with round intersections: Flow mode transition and three-

dimensionality. *Physics of Fluids*, 32(2), 025101.

- 137 Wang, W. W., Song, Y. J., Zhang, C. Y., Zhang, H. L., Cai, Y., Zhao, F. Y., & Guo, J. H. (2023). Fluid hydrodynamics and thermal transports in nanofluids pulsating heat pipes applied for building energy Exploitations: Experimental investigations and full numerical simulations. *Energy and Buildings*, 290, 113067.
- 138 Wang, W. W., Zhang, H. L., Song, Y. J., Song, J. W., Shi, D. K., Zhao, F. Y., & Cai, Y. (2022). Fluid flow and thermal performance of the pulsating heat pipes facilitated with solar collectors: Experiments, theories, and GABPNN machine learning. *Renewable Energy*, 200, 1533-1547.
- 139 Winkler, M., Rapp, D., Mahlke, A., Zunftmeister, F., Vergez, M., Wischerhoff, E., ...& Schäfer-Welsen, O. (2020). Small-sized pulsating heat pipes/oscillating heat pipes with low thermal resistance and high heat transport capability. *Energies*, 13(7), 1736.
- 140 Womersley, J.R. (1957). "An Elastic Tube Theory of Pulse Transmission and Oscillatory Flow in Mammalian Arteries." WADC Tech. Rep. TR-56-514.
- 141 Wu, T., Shen, J., Li, Z., Xing, F., Xin, W., Wang, Z., ... & Fu, S. (2021). Microfluidic-integrated graphene optical sensors for real-time and ultra-low flow velocity detection. *Applied Surface Science*, 539, 148232.
- 142 Wu, Z., Bao, H., Xing, Y., & Liu, L. (2022). Heat transfer performance and prediction of open pulsating heat pipe for self-cooling cutting tool. *The International Journal of Advanced Manufacturing Technology*, 121(9-10), 6951-6972.
- 143 Xu, Y., Xue, Y., Qi, H., & Cai, W. (2020). Experimental study on heat transfer performance of pulsating heat pipes with hybrid working fluids. *International Journal of Heat and Mass Transfer*, 157, 119727.
- 144 Xu, Y., Xue, Y., Qi, H., & Cai, W. (2021). An updated review on working fluids, operation mechanisms, and applications of pulsating heat pipes. *Renewable and*

- 145 Yang, K. S., Jiang, M. Y., Tseng, C. Y., Wu, S. K., & Shyu, J. C. (2020). Experimental investigation on the thermal performance of pulsating heat pipe heat exchangers. *Energies*, 13(1), 269.
- 146 Yang, M., Gao, Y., Liu, Y., Yang, G., Zhao, C. X., & Wu, K. J. (2021). Integration of microfluidic systems with external fields for multiphase process intensification. *Chemical Engineering Science*, 234, 116450.
- 147 Yang, Y., Zhou, L., Shi, W., He, Z., Han, Y., & Xiao, Y. (2021). Interstage difference of pressure pulsation in a three-stage electrical submersible pump. *Journal of Petroleum Science and Engineering*, 196, 107653.
- 148 Zahran, E. H., Arqub, O. A., Bekir, A., & Abukhaled, M. (2023). New diverse types of soliton solutions to the Radhakrishnan-Kundu-Lakshmanan equation. *AIMS Math*, 8, 8985-9008.
- 149 Zhang, D., He, Z., Guan, J., Tang, S., & Shen, C. (2022). Heat transfer and flow visualization of pulsating heat pipe with silica nanofluid: An experimental study. *International Journal of Heat and Mass Transfer*, 183, 122100.
- 150 Zhao, P. J., Gan, R., & Huang, L. (2020). A microfluidic flow meter with micromachined thermal sensing elements. *Review of Scientific Instruments*, 91(10), 105006.
- 151 Zhao, W., Yu, H., Wen, Y., Luo, H., Jia, B., Wang, X., ... & Li, W. J. (2021). Real-time red blood cell counting and osmolarity analysis using a photoacoustic-based microfluidic system. *Lab on a Chip*, 21(13), 2586-2593.
- 152 Zhao, X., Gao, W., Yin, J., Fan, W., Wang, Z., Hu, K., ... & Jin, Q. (2021). A high-precision thermometry microfluidic chip for real-time monitoring of the physiological process of live tumour cells. *Talanta*, 226, 122101.

- 153 Zhu, J. Y., Nguyen, N., Baratchi, S., Thurgood, P., Ghorbani, K., & Khoshmanesh, K. (2018). Temperature-controlled microfluidic system incorporating polymer tubes. *Analytical chemistry*, 91(3), 2498-2505.
- 154 Zhu, J. Y., Suarez, S. A., Thurgood, P., Nguyen, N., Mohammed, M., Abdelwahab, H., ... & Khoshmanesh, K. (2019). Reconfigurable, self-sufficient convective heat exchanger for temperature control of microfluidic systems. *Analytical chemistry*, 91(24), 15784-15790.
- 155 Zohdi, T.I., "A simple Model for Shear Stress Mediated Lumen Reduction in Blood Vessels", *Biomech. Model Mechanobio.*, Vol.4, No. 1, (2005), 57-61.

LIST OF PAPERS

Published/Communicated

List of published papers

1. G.C. Sankad., **G. Durga Priyadarsini.**, Magda Abd El-Rahman., M. R. Gorji Nizar., Abdallah Alsufi., **Microfluidics temperature compensation and tracking for drug injection based on mechanically pulsating heat exchanger.**, Journal of Thermal Analysis and Calorimetry, <https://doi.org/10.1007/s10973-023-12520-7> September 13, 2023.
2. **Gampala Durga Priyadarsini.**, Gurunath Sankad., **Microfluidic systems with a pulsating heat pipe.** Physics of Fluids 35, 112001 (2023) Vol. 35, Issue 11 <https://doi.org/10.1063/5.0170426> November 01, 2023.

List of papers communicated

1. **G. Durga Priyadarsini.**, G.C. Sankad., **Enhancing Pulsating Heat Pipe Performance Using Nano Fluids and Deep Learning Methods: An Experimental Analysis** Communicated to Journal of Nano Fluids.
2. **G. Durga Priyadarsini.**, G.C. Sankad., **Dynamic Heat Pipe & Heat Exchanger** Performance Communicated to Journal of Applied Fluid Mechanics.